Regulatory Toxicology and Pharmacology 81 (2016) S59–S81

Contents lists available at ScienceDirect

Regulatory Toxicology and Pharmacology

journal homepage: www.elsevier.com/locate/yrtph

Evaluation of the Tobacco Heating System 2.2. Part 4: 90-day OECD 413 rat inhalation study with systems toxicology endpoints demonstrates reduced exposure effects compared with cigarette smoke

Ee Tsin Wong [a], Ulrike Kogel [b], Emilija Veljkovic [a], Florian Martin [b], Yang Xiang [b], Stephanie Boue [b], Gregory Vuillaume [b], Patrice Leroy [b], Emmanuel Guedj [b], Gregory Rodrigo [c], Nikolai V. Ivanov [b], Julia Hoeng [b], Manuel C. Peitsch [b], Patrick Vanscheeuwijck [b, *]

[a] Philip Morris International Research Laboratories Pte Ltd, 50 Science Park Road, The Kendall #02-07 Science Park II, 117406, Singapore[1]
[b] Philip Morris International R&D, Philip Morris Products S.A., Quai Jeanrenaud 5, 2000, Neuchâtel, Switzerland[1]
[c] Former employee of Philip Morris International R&D, Philip Morris Products S.A., Switzerland

ARTICLE INFO

Article history:
Received 4 July 2016
Received in revised form
4 October 2016
Accepted 24 October 2016
Available online 26 October 2016

Keywords:
Heat-not-burn
Modified risk tobacco product
Pulmonary inflammation
Inhalation toxicology study
Inhalation systems toxicology

ABSTRACT

The objective of the study was to characterize the toxicity from sub-chronic inhalation of test atmospheres from the candidate modified risk tobacco product (MRTP), Tobacco Heating System version 2.2 (THS2.2), and to compare it with that of the 3R4F reference cigarette. A 90-day nose-only inhalation study on Sprague-Dawley rats was performed, combining classical and systems toxicology approaches. Reduction in respiratory minute volume, degree of lung inflammation, and histopathological findings in the respiratory tract organs were significantly less pronounced in THS2.2-exposed groups compared with 3R4F-exposed groups. Transcriptomics data obtained from nasal epithelium and lung parenchyma showed concentration-dependent differential gene expression following 3R4F exposure that was less pronounced in the THS2.2-exposed groups. Molecular network analysis showed that inflammatory processes were the most affected by 3R4F, while the extent of THS2.2 impact was much lower. Most other toxicological endpoints evaluated did not show exposure-related effects. Where findings were observed, the effects were similar in 3R4F- and THS2.2-exposed animals. In summary, toxicological changes observed in the respiratory tract organs of THS2.2 aerosol-exposed rats were much less pronounced than in 3R4F-exposed rats while other toxicological endpoints either showed no exposure-related effects or were comparable to what was observed in the 3R4F-exposed rats.
© 2016 The Author(s). Published by Elsevier Inc. This is an open access article under the CC BY-NC-ND license (http://creativecommons.org/licenses/by-nc-nd/4.0/).

1. Introduction

The U.S. Family Smoking Prevention and Tobacco Control Act (FSPTCA) defines a MRTP as “any tobacco product that is sold or distributed for use to reduce harm or the risk of tobacco related disease associated with commercially marketed tobacco products” (Family Smoking Prevention and Tobacco Control Act). This publication is part of a series of nine publications describing the nonclinical and part of the clinical assessment of a candidate MRTP, THS2.2 regular and a mentholated version (THS2.2M). The series of publications provides part of the overall scientific program to assess the potential for THS2.2 to be a reduced risk product. The first publication in this series describes THS2.2 and the assessment program for MRTPs (Smith et al., submitted (this issue)). This is followed by six publications, including this one, that describe the nonclinical assessment of THS2.2 regular and THS2.2M (Kogel et al., submitted (this issue); Oviedo et al., submitted (this issue); Schaller et al., submitted (this issue)-a; Schaller et al., submitted (this issue)-b; Sewer et al., submitted (this issue); Wong et al., submitted (this issue)). The eighth publication in the series describes a clinical

* Corresponding author.
E-mail address: Patrick.Vanscheeuwijck@pmi.com (P. Vanscheeuwijck).
[1] part of Philip Morris International group of companies.

http://dx.doi.org/10.1016/j.yrtph.2016.10.015
0273-2300/© 2016 The Author(s). Published by Elsevier Inc. This is an open access article under the CC BY-NC-ND license (http://creativecommons.org/licenses/by-nc-nd/4.0/).

Abbreviations

THS2.2	Tobacco Heating System version 2.2
HPHCs	Harmful and potentially harmful components
MRTP	Modified risk tobacco product
OECD	Organization for Economic Co-operation and Development
CO	Carbon monoxide
MA	Mainstream aerosol
MS	Mainstream smoke
GLP	Good Laboratory Practice
AAALAC	American Association for the Accreditation of Laboratory Animal Care
AVA	Agri-Food & Veterinary Authority of Singapore
PMI	Philip Morris International
PDSP	Programmable Dual-port Syringe Pump
COHb	Carboxyhemoglobin
HOCOT	*Trans*-3'-hydroxycotinine
NCOT	Norcotinine
COT	Cotinine
NNO	Nicotine-N'-oxide
NNIC	Nornicotine
HPLC	High-performance liquid chromatography
ABF	Analytisch-biologisches Forschungslabor GmbH
HPMA	3-hydroxypropylmercapturic acid
NNAL	4-(methylnitrosamino)-1-(3-pyridyl)-1-butanol
SPMA	S-phenylmercapturic acid
CEMA	2-cyanoethylmercapturic acid
LC-MS	Liquid chromatography-tandem mass spectrometry
PT	Prothrombin time
APTT	Activated partial thromboplastin time
BALF	Bronchoalveolar lavage fluid
PBS	Phosphate-buffered saline
MyriadRBM	Myriad Rules-Based Medicine
EGAFS	Ethanol glycerol acetic acid formaldehyde saline
H&E	Hematoxylin andeosin
AB-PAS	Alcian blue/periodic acid-Schiff's reagent
LPT	Laboratory of Pharmacology and Toxicology GmbH & Co. KG
HBSS	Hepes-buffered saline solution
TPM	Total particulate matter
RNE	Respiratory nasal epithelium
fRMA	Frozen-Robust Microarray Analysis
FDR	False discovery rate
RBC	Red blood cells/erythrocytes
Hb	Hemoglobin concentration
MCV	Mean corpuscular volume
MCHC	Mean cell hemoglobin content
MCH	Mean corpuscular hemoglobin
HCT	Hematocrit
ALP	Alkaline phosphatase
AST	Aspartate aminotransferase
ALT	Alanine aminotransferase
MMAD	Mass median aerodynamic diameter
GSD	Geometric standard deviation
LOQ	Lower limit of quantification
PIF	Peak inspiratory flow
TV	Tidal volume
RF	Respiratory frequency

study to assess whether the reduced formation of Harmful and Potentially Harmful Constituents (HPHCs) for THS2.2 regular also leads to reduced exposure to HPHCs when the product is used in a clinical setting (Haziza, submitted (this issue)). A final publication utilizes data gathered from the reduced exposure clinical study on THS2.2 regular to determine if a systems pharmacology approach can identify exposure response markers in peripheral blood of smokers switching to THS2.2 (Martin et al., submitted (this issue)).

Here we report the results of a 90-day inhalation study that was conducted to identify and characterize potentially adverse toxicological effects and underlining molecular changes following repeated daily inhalation exposure to test atmosphere from THS2.2 and 3R4F in Sprague Dawley rats. The recommendations from the Organization for Economic Co-operation and Development (OECD) Test Guideline 413 (OECD, 2009) were followed during the conceptualization and the conduct of this study, with special emphasis on histopathology of the respiratory tract, lung inflammation, and additional molecular endpoints using transcriptomics analysis – the latter being a part of a systems toxicology assessment to enable a multi-level systems evaluation of the effects of aerosol inhalation, and to provide insights into the mechanistic drivers behind the changes observed (Kogel et al., submitted (this issue)).

2. Materials and methods

2.1. Experimental design

Ninety two male and 92 female Sprague Dawley rats were allocated into 7 groups (named the 'OECD groups'). Rats were exposed to filtered fresh air (sham), diluted mainstream aerosol (MA) from THS2.2 at 3 target concentrations of nicotine (15, 23 and 50 μg nicotine/l aerosol, designated as THS2.2_15, THS2.2_23, and THS2.2_50), or diluted mainstream smoke (MS) from 3R4F at 3 target test atmosphere concentrations of nicotine (8, 15 and 23 μg nicotine/l aerosol, designated as 3R4F_8, 3R4F_15, and 3R4F_23). Groups of 10 male and 10 female rats were exposed for a period of 90–96 days (90d) at an exposure regimen of 6 h a day, 5 days per week (no exposure on weekend), and were subsequently euthanized and necropsied. Additional cohorts of 6–10 rats per sex, concomitantly exposed with the 90-day animals, were kept for approximately additional 42 days (90 + 42d) to assess reversibility or persistence of findings, and consisted of a sham, a 3R4F_23 group, and a THS2.2_50 group, named 'recovery groups'. These rats were euthanized and necropsied 44–45 days after the completion of the 90-day exposure period (Supplementary Table 1). In addition to the OECD groups, Sprague Dawley rats were also allocated to 7 'OECD Plus' groups, and exposed to the same aerosols in the same inhalation chambers, concomitantly with the OECD groups. In the OECD Plus groups, 6 male and 6 female rats per group were allocated for 90d (actual 93–96 days) exposure, and 5 to 6 rats per sex per group (with the exception of the THS2.2_50 group) were allocated for 90 + 42d exposure (actual 42–44 days) (Supplementary Table 1).

The nicotine concentrations for 3R4F were selected according to results from a previous study (Kogel et al., 2014), which showed that the selected concentrations were suitable for detecting differences in severity of effects throughout the respiratory tract without causing significant increase in morbidity due to high carbon monoxide (CO) concentration in the aerosol. The highest test atmosphere nicotine concentration that was selected for the

THS2.2 exposure groups, 50 μg nicotine/l aerosol, was based on the findings from a concentration range-finding study conducted prior to the study reported here (results not shown), which showed that this nicotine concentration caused mild toxicity but not an increase in morbidity. Exposing rats to MS from 3R4F at such high test atmosphere nicotine concentrations would not be possible because of the CO content in 3R4F smoke. THS2.2 aerosol contains much lower levels of CO and other constituents (see Schaller et al., 2016), allowing test atmospheres up to 50 μg nicotine/l. Consequently, the target nicotine concentration of the 3R4F_23 group was matched to that of the THS2.2_23 group, and the target nicotine concentration of the 3R4F_15 group was matched to that of the THS2.2_15 group.

The test atmospheres were characterized by measuring selected aerosol constituents throughout the study. Data were collected for clinical observations, aerosol uptake (biomonitoring), clinical pathology, gross pathology, organ weights, and histopathology according to the OECD 413 specifications. Supplementary Table 3 summarizes all OECD and molecular endpoints (OECD Plus groups) collected in this study. The exposure part of the study, as well as the determination of all OECD endpoints, was conducted in compliance with the OECD Principles on Good Laboratory Practice (GLP) (OECD, 1997), with the exception of bronchoalveolar lavage fluid (BALF) analytics using RodentMAP®, determination of biomarkers of exposure for acrolein, (4-Methylnitrosamino)-1-(3-Pyridyl)-1-butanone (NNK), benzene, acrylonitrile, and the exploratory transcriptomics/miRNA investigations.

2.2. THS2.2 tobacco sticks and cigarettes

THS2.2 is a heat-not-burn tobacco product, consisting of an electrically operated chargeable heating element (stick holder) and THS2.2 *tobacco stick* containing a tobacco plug. THS2.2 *tobacco stick* consist of a tobacco plug made out of specially processed reconstituted tobacco (cast leaf), a transfer section, and a mouthpiece, with an over-wrapping of cigarette paper. THS2.2 *tobacco sticks* are designed to be inserted into the stick holder that includes a battery, electronics for heat control, a heating element (blade), and the cigarette extractor. The heating element of the holder heats the tobacco plug in a temperature-controlled manner to a maximum of 350 °C. The comparative analytical characteristics of THS2.2 aerosol and 3R4F smoke are reported in part 2 of this series of publications (Schaller et al., submitted (this issue)-a). The tobacco blend designated 'FR1' was used in the THS2.2 *tobacco sticks* in this study. The *tobacco sticks* were provided by Philip Morris Products S.A., Neuchâtel, Switzerland.

Reference research cigarettes 3R4F were purchased from the University of Kentucky (http://www2.ca.uky.edu/refcig/). The 3R4F reference cigarette is constructed to represent the "full flavor" segment of the American market. Detailed 3R4F smoke analytics can be found in Roemer et al., (Roemer et al., 2012).

2.3. Animals

All procedures involving animals were performed in an AAALAC (American Association for the Accreditation of Laboratory Animal Care) accredited, AVA (Agri-Food & Veterinary Authority of Singapore) licensed facility with approval from an Institutional Animal Care and Use Committee, and performed in compliance with guidelines set by the National Advisory Committee for Laboratory Animal Research (NACLAR, 2004).

Outbred male and female Sprague Dawley rats (Crl:CD(SD)), bred under specific pathogen-free conditions, were obtained from Charles River, USA (breeding area Raleigh R04). Sprague Dawley rats were selected because of the extensive experience with this strain in previous inhalation studies conducted by Philip Morris International (PMI) and extensive published literature (Kogel et al., 2014; Moennikes et al., 2008; Phillips et al., 2015a; Terpstra et al., 2003; Vanscheeuwijck et al., 2002). The rats were approximately 8 weeks old at arrival and were acclimatized for 17 days for OECD groups and 24 days for OECD Plus groups prior to exposure (exposure of OECD Plus groups commenced 1 week after the OECD group). Serological testing was performed on 6 male and 6 female sentinel rats in week 10 of the study. Additional sentinel animals were sent for comprehensive microbiological, serological and histopathological evaluation at Envigo, UK: 6 live male and 6 live female rats before exposure, 2 live male and 2 live female rats on week 13, and 4 live male and 4 live female rats after week 19. Only *Staphylococcus* species, *Streptococcus* species, *Proteus* species, *Lactobacillus* species, and *Escherichia coli* that were considered normal flora in rats were detected in the cecum and/or nasopharynx.

The rats were housed in animal laboratory units with restricted access and under specific hygienic conditions. Frequent bacteriological testing performed on the laboratory air and surfaces, diet and drinking water during the course of the study showed microbial counts that were within internal specifications. The laboratory air was filtered fresh air, and positive pressure was maintained inside the laboratories. The housing temperature for the 2 animal housing rooms used was 21.0 ± 0.2 and 21.8 ± 0.4 °C (mean ± SD), and the relative humidity was 59.1± 1.0% and 51.6± 1.5% (mean ± S.D.), both conditions were within the specifications (22 ± 3 °C and 30–70%). The light/dark cycle was 12 h/12 h, with the light period beginning at 7 am.

All rats were individually identified by subcutaneously implanted transponders. The rats were housed in pairs throughout the exposure period with the exception of rare cases where the group size was odd (i.e., after a death or dissection), in which some rats were housed singly. The bedding material (Lignocel® BK 8–15, J. Rettenmaier & Sohne, GmbH + Co KG.) was composed of autoclaved softwood granulate. A gamma-irradiated pellet diet (T2914C irradiated rodent diet, Harlan) was provided on the cage top from cage lids, and tap water (filtered 0.45 and 0.2 μm pore size in series) from water bottles with steam-sterilized sipper tubes were supplied ad libitum for each cage except during exposure. Chemical analysis of food, water and bedding material confirmed that no contaminants were present that could adversely affect the outcomes of the study or hinder the interpretation of the data (such as aflatoxins, selected pesticides, heavy metals, and polychlorinated biphenyls; diet was also analyzed for nitrate, nitrite, nitrosamines, and organophosphates). A total of 209 male and 179 nulliparous and non-pregnant female rats were randomly allocated based on sex and body weight simultaneously to 10 OECD groups and 7 OECD Plus groups by an animal management software, Provantis (Instem, UK). The mean body weight of the rats at the beginning of the exposure period was similar in all exposure groups, and ranged from 284.8 to 286.2 g for male rats and 212.8–213.6 g for female rats, with a maximum relative standard deviation of 4.3% in male rats and 5.2% in female rats.

2.4. Aerosol generation and exposure

Both test and reference items were stored in the original packaging in a room with controlled room temperature of 2–10 °C, but uncontrolled humidity. Conditioning of reference and test articles was performed according to ISO standard 3402 (ISO3402, 1999) for 7–21 days to achieve a temperature of 22 ± 1 °C and relative humidity of 60 ± 3% before being used for aerosol generation.

MS from 3R4F was generated on 30-port rotary smoking machines (15 ports blocked) equipped with a Programmable Dual-port Syringe Pump (PDSP) with active side stream exhaust (type PMRL-

G, SM2000) (Kogel et al., 2014). Smoking machines were designed by Philip Morris Products S.A. and manufactured by Burghart Messtechnik, Weidel, Germany (http://www.burghart-mt.de/). MA from THS2.2 was generated using 30-port carousel smoking machines equipped with stick holders, a PDSP, and a temperature-controlled insulation kit (Tube Warming System) in the undiluted aerosol pathway, to reduce aerosol condensation prior to diluting the aerosol. The 3R4F cigarette MS and THS2.2 aerosol were generated according to the Health Canada Intensive Smoking Protocol (Health Canada, 1999), which is based on ISO standard 3308 (ISO3308, 2000), with the exceptions of the puff volume (55 ml), puff duration (2 s), puff frequency (one puff every 30 s), and closed ventilation holes. Several minor deviations from ISO standard 3308 were necessary for technical reasons (see Supplementary Table 4). The aerosols generated were diluted with filtered, conditioned air to obtain the target nicotine exposure concentrations.

The rats were individually nose-only exposed in flow-pass inhalation chambers of the type FPC-232 and in glass tubes matching their body size. The position of the rats in the chamber was changed on a daily basis according to a predetermined rotation scheme. To allow for acclimatization to the target aerosol concentrations, a time-adaptation phase was included in week 1 of the study during which animals were exposed 1.5 h during the first and second day, 3 h during the third and fourth day, and 4.5 h on days 5–7 at the target nicotine concentration. From day 8 onwards, rats were exposed for 6 h per day. Sham rats were exposed to filtered and conditioned fresh air, the exposure conditions being the same as those for the smoke-exposed rats. The relative humidity in the sham exposure chamber was 55± 1% (mean ± S.D.), and the temperature within the exposure chambers ranged from 21.7 to 22.4 °C (S.D. < 0.3 °C). Both conditions were in compliance with those specified by OECD TG 413 (OECD, 2009).

2.5. Analytical characterization of the test atmosphere

To characterize the test atmosphere and to check the reproducibility of aerosol generation and dilution, several analytical parameters were measured at the breathing zone of the rats in the inhalation chambers according to previously described analytical methods (Haussmann et al., 1998): Total particulate matter (TPM), CO, nicotine, formaldehyde, acetaldehyde, acrolein, and particle size distribution (PSD). For details of the frequency and methods of determination, see Supplementary Table 5.

2.6. Biological parameters

2.6.1. General conditions and health

Body weights, food consumption, ophthalmoscopy, and health status of the rats were monitored throughout the study (Supplementary Table 6). Individual body weight and group food consumption were determined at least once per week. Rats were checked at least once each day for mortality and morbidity. Detailed checks of the general condition and behavior of individual rats were performed at least 4 times during the 90-day exposure period, shortly after completion of the daily exposure. Ophthalmological examinations by indirect ophthalmoscopy were performed on all OECD group rats before the start of the 90-day exposure period, once during exposure, and once during the 42-day recovery period.

2.6.2. Biomonitoring

To monitor aerosol uptake by the rats, biomonitoring was performed through analysis of biomarkers of exposure for particulate and gas vapor phase constituents, such as steady-state blood carboxyhemoglobin (COHb) concentration and urinary metabolites of representative aerosol constituents. In addition, respiratory physiology measurements were performed. For detailed schedules, see Supplementary Table 7.

Determination of carboxyhemoglobin in blood

Once during the 90-day exposure period and once during the 42-day recovery period, blood was collected from the saphenous vein of isoflurane-anesthetized rats; levels of COHb were determined by spectrophotometric measurement of absorbance at several wavelengths of the mixed hemoglobins in hemolysate using the NPT 7 blood gas analyzer (Radiometer, Denmark).

Urine nicotine metabolites and biomarkers of exposure

Nicotine metabolites (*trans*-3′-hydroxycotinine (HOCOT), norcotinine (NCOT), cotinine (COT), nicotine-N'-oxide (NNO), nornicotine (NNIC)) were determined by high-performance liquid chromatography (HPLC) after derivatization with 1,3-diethyl-2-thiobarbituric acid as previously described (Rustemeier et al., 1993) in 24-h urine that was collected once before the 90-day exposure phase started (baseline), three times during the inhalation period, and once during the 42-day recovery period. The same samples were submitted to Analytisch-biologisches Forschungslabor GmbH (ABF, Germany) to quantify other metabolites of aerosols constituents: 3-hydroxypropylmercapturic acid (HPMA, metabolite of acrolein), 4-(methylnitrosamino)-1-(3-pyridyl)-1-butanol (NNAL, metabolite of NNK), S-phenylmercapturic acid (SPMA, metabolite of benzene), and 2-cyanoethylmercapturic acid (CEMA, metabolite of acrylonitrile). For these determinations, liquid chromatography-tandem mass spectrometry (LC-MS)/MS based methods were used as previously described (Mascher et al., 2001; Meger et al., 2000; Minet et al., 2011; Scherer et al., 2007). For a detailed schedule of the sample collection, see Supplementary Table 7.

Respiratory physiology

Respiratory frequency, tidal volume, peak inspiratory flow, and respiratory minute volume were determined once in the study for 10 male and 10 female animals per OECD group using head-out plethysmography (EMKA Technologies, France) to provide an estimate of the irritant potential of the test atmospheres. Briefly, animals were placed in modified plethysmograph exposure restraint tubes with a latex cuff fitted over the neck. After a period of acclimatization to the plethysmograph of approximately 30 min, the breathing patterns of the animals were recorded in 10 30-s measurements. The plethysmograph was attached to the pressure transducers that acquired the air flow and air pressure signals. The signals from the transducers were amplified by the bridge amplifiers, and data acquisition was performed using the IOX 2.9.4.32 software package (EMKA Technologies, France).

2.6.3. Hematology and clinical chemistry

Several parameters to assess systemic effects were investigated: Hematology and clinical chemistry were performed according to standard laboratory methods, as previously described (Phillips et al., 2015a). At necropsy, blood samples were taken from rats under pentobarbital anesthesia from the retro-orbital venous plexus, and analyzed using the Sysmex XT2000i system (Sysmex Canada Inc., Canada); plasma samples in citrated tubes were analyzed for prothrombin time (PT) and activated partial thromboplastin time (APTT) using the STA Compact coagulation analyzer (Stago, USA). For assessment of clinical chemistry in serum, blood samples were taken from rats at dissection under pentobarbital anesthesia by exsanguination via the abdominal aorta, and analyzed using the UniCel DxC 600i system (Beckman Coulter, USA). In some instances, sample analysis was not possible or data had to be suppressed because of insufficient volume, blood clotting, or other technical reasons. Please refer to the Results section for actual group sizes.

2.6.4. Lung lavage and analysis

Bronchoalveolar lavage fluid (BALF) was collected from the right lungs during dissection using five consecutive cycles of instillation at 15 cm H_2O pressure and fluid drawn out of the lung by gravity and pressure from the filled lung. For the first cycle, pre-warmed calcium- and magnesium-free phosphate-buffered saline (PBS) was used. For cycles 2–5, bovine serum albumin (BSA, 0.325% final) was added to the PBS. The lavage fluid of the first cycle was collected separately, centrifuged, and the supernatant was used for Luminex-based analysis of a panel of 60 selected proteins (RodentMAP®v3.0; Life Technologies, USA) performed by Myriad Rules-Based Medicine (Myriad RBM, USA). Cell pellets obtained from the first lavage cycle were re-suspended in ice cold PBS/BSA and pooled into the BALF from cycles 2–5. The number and viability of the free lung cells were determined, and they were further analyzed by flow cytometry (FACSCanto II, BD Biosciences, USA) to differentiate alveolar macrophages, neutrophils, lymphocytes, and eosinophils after staining with cell-type specific antibodies (Supplementary Table 8)(Friedrichs et al., 2006).

2.6.5. Necropsy, gross pathology and organ weights

Full necropsy was performed without prior fasting the day after the last exposure, according to previously described methods (Vanscheeuwijck et al., 2002). The weights of the spleen, thymus, lung with larynx and trachea, heart, kidneys, adrenal glands, testes, brain, and liver were determined. Organs were weighed separately for paired organs.

2.6.6. Histopathology

At the dissection time points, gross pathology was performed and the organs listed in OECD TG 413 (see Supplementary Table 9, pathology section) were harvested, followed by placement in appropriate fixative solutions at room temperature. The non-respiratory tract organs were fixed in a 4% formaldehyde solution except for the eyes, sternum, and testes, which were fixed in Davidson's, Schaffer and Bouin solutions, respectively. Lungs with larynx and trachea were removed together. After determination of weight, the right lung was separated for BALF collection. The left lung was fixed by instillation at 20 cm H_2O pressure via the left bronchus with ethanol glycerol acetic acid formaldehyde saline (EGAFS) and subsequent immersion. Histological sections of the respiratory tract organs were prepared at defined levels (Supplementary Table 9), and stained with hematoxylin and eosin (H&E). In addition, to allow for the identification of goblet cells, sections from nose at level 1, trachea at level 4 (bifurcation), and left lung at level 1 were stained with alcian blue/periodic acid-Schiff's reagent (AB-PAS) and evaluated. The laryngeal epithelial thickness was determined at the floor of the larynx and at the lower medial region of the vocal cords (level of arytenoid projections). Histopathological evaluation was performed by the histopathologist Dr. A. Buettner at the Laboratory of Pharmacology and Toxicology GmbH & Co. KG (Germany). Incidence of findings was recorded and the severity of the lesions was evaluated using a scoring system of 0–5 in a blinded manner adapted from the published literature (Coggins et al., 1980; Lewis, 1981; Young, 1981).

Bone marrow smears were prepared from sham, 3R4F_23, and THS2.2_50 groups and recovery groups for sham, 3R4F_23, and THS2.2_50. Bone marrow was collected from the left femur by flushing with HEPES-buffered saline solution (HBSS). Smears were prepared by cytospin of bone marrow suspension onto glass slides. Two bone marrow smears per animal were evaluated. Smears were stained with Pappenheimer solution. The myeloid: erythroid ratio was determined by evaluating cell differentiation of 200 nucleus-containing cells.

2.6.7. Statistical evaluation

Descriptive statistics (N, mean or median, standard deviation or geometric standard deviation) of the main aerosol parameters (TPM, CO, nicotine, formaldehyde, acetaldehyde, acrolein, and PSD) were computed for each exposure chamber. For PSD, calculation was performed using the SAR application. For the parameters of aerosol biomonitoring (blood carboxyhemoglobin, selected nicotine and aerosol metabolites in urine, and respiratory physiology), the number of valid measurements, mean, and standard deviation or standard error of the mean were computed for each exposure group and sex. For biological endpoints (body weight, food consumption, lung inflammation, hematology, clinical chemistry, organ weight, and pathology), descriptive statistics were computed for each exposure group and sex. If the parameters were evaluated on a continuous scale (e.g. body weights, organ weights, clinical chemistry, and hematology parameters), basic statistics (number of valid measurements, mean, standard deviation, standard error of the mean) were computed. For ordinal parameters, such as histopathology scorings, the number of valid measurements and frequency table (absolute and relative to the number of valid observations) were computed, as well as mean and standard deviation or standard error of the mean. For incidence parameters, the number of valid measurements and frequency table (absolute and relative to the number of valid observations) were computed.

Additionally and separately for each sex, pairwise differences between groups were estimated. Comparative statistics for respiratory physiology, clotting potential, FACS cell counts, and relative organ weights were computed using Student's two-sample *t*-test. Comparative statistics for body weight, hematology, and clinical chemistry were performed using the Provantis statistical reporting template (Instem, UK); depending on the normality of data, either a parametric test (ANOVA) or a non-parametric test was performed. For incidences, comparative statistics were computed using Fisher's exact test. For ordinal variables, the Cochran-Mantel-Haenszel test was used with the row mean scores statistic (with the alternative hypothesis that mean responses differ across compared groups, the scores being defined as integer scores). Finally, for data from multi-analyte profiles in BALF, as the number of values below the limit of detection/quantification was high for some analytes, a Mann-Whitney- Wilcoxon rank sum test was performed.

2.7. Transcriptomics endpoints

The transcriptomics analyses were performed on samples from OECD Plus groups described in section 2.1.

2.7.1. Tissue preparation

Prior to organ removal, the rats were whole-body perfused with cold saline to remove blood cells through the heart ventricles. Saline was introduced by insertion of a 20G needle into the left ventricle of the heart at 30 ml/min using a peristaltic pump. An exit cut was made at the right atrium of the heart to complete the flow. The perfusion was continued for approximately 8 min until the lungs and liver lobes were blanched. The lung lobes were embedded in optimal cutting temperature (OCT) compound and cut along the coronal plane using a cryostat (Leica CM3050b). The medial region of the left lung was cryosliced into serial sections of 40 μm each for total RNA including miRNA isolation. To isolate the left respiratory nasal epithelium (RNE), the head was excised and the lower jaw, fur, calvaria, and brain were removed from the skull. An incision sagittal to the nose was made, and the nose was pried into left and right halves before removing the RNE from the exposed grooves. The RNE was removed using forceps and snap frozen in liquid nitrogen for RNA/miRNA analysis.

Table 1
Characterization of test atmospheres – determinations performed in the exposure chambers.

Chamber	TPM (μg/l)	Particle size distribution		Nicotine (μg/l)	Carbon monoxide (ppm)	Acetaldehyde (μg/l)	Acrolein (μg/l)	Formaldehyde (μg/l)
		MMAD (μm)	GSD					
Sham	0.0 ± 0.0[a] (76)	NM	NM	<LOQ	<LOQ	NM	NM	NM
3R4F_8	86.2 ± 9.9 (76)	0.56–0.86 (8)	1.11–1.44	7.20 ± 0.81 (32)	108.6 ± 10.5	5.68 ± 1.09 (15)	0.56 ± 0.11 (15)	0.19 ± 0.04 (15)
3R4F_15	168.6 ± 8.9 (76)	0.59–0.84 (11)	1.18–1.44	13.33 ± 1.22 (29)	196.0 ± 8.9	10.29 ± 1.28 (15)	1.00 ± 0.12 (15)	0.36 ± 0.05 (15)
3R4F_23	273.5 ± 17.1 (76)	0.59–0.76 (12)	1.19–1.42	21.68 ± 1.64 (28)	333.4 ± 15.2	16.77 ± 0.78 (14)	1.61 ± 0.11 (14)	0.53 ± 0.05 (14)
THS2.2_15	89.4 ± 10.2 (76)	0.45–0.87 (11)	1.01–1.64	13.66 ± 1.37 (76)	4.5 ± 0.5	2.20 ± 0.14 (14)	0.09 ± 0.01 (14)	0.07 ± 0.01 (14)
THS2.2_23	124.7 ± 27 (76)	0.40–0.98 (10)	1.24–1.63	21.72 ± 3.00 (76)	6.4 ± 0.6	3.37 ± 0.45 (15)	0.13 ± 0.02 (15)	0.10 ± 0.02 (15)
THS2.2_50	319.8 ± 33.8 (76)	0.44–0.83 (13)	1.20–1.58	47.25 ± 4.83 (76)	12.9 ± 0.8	6.81 ± 0.72 (15)	0.25 ± 0.03 (15)	0.19 ± 0.03 (15)

Results represent medians or mean ± standard deviation. Abbreviations: TPM, total particulate matter; MMAD, mass median aerodynamic diameter; GSD, geometric standard deviation; NM, not measured. The sample size is in parentheses.
[a] TPM in Sham is defined as zero where the difference in filter weight before and after collection is negative.

2.7.2. Total RNA preparation and whole genome expression arrays

Lung sections were lysed in RLT buffer (Qiagen, Germany) and β-mercaptoethanol using ceramic beads for homogenization. Total RNA, including miRNA, was isolated using the miRNeasy Mini Kit (Qiagen, Germany). RNA extraction from RNE was done using QIAzol (Qiagen, Germany) lysis buffer and the miRNeasy Mini Kit. The RNA quality of the RNE samples from the sham female group was not sufficient to reach a significant sample size. Therefore, only data from the male RNE and male lung are reported (section 3.7). Transcriptomics data obtained from the female lung samples are shown in Supplementary Fig. 3.

2.7.3. Gene expression array data analysis

RNA was processed with the High Throughput 3′ In Vitro Transcription PLUS kit (Affymetrix, USA) for chip hybridization on GeneChip® Rat Genome 230 2.0 arrays (Affymetrix, USA). Raw data files were processed with the custom Chip Description File environment Rat2302_Rn_ENTREZG v19.0.0 (rat2302rnentrezgcdf) (Dai et al., 2005), and normalized using frozen-Robust Microarray Analysis (fRMA) (McCall et al., 2010). The normalization vector needed for fRMA was created using a set of 1023 microarray rat samples from 11 tissues and the R package *frmaTools version 1.18.0*. Quality controls, including log-intensities, normalized-unscaled standard error, relative log expression, median absolute value RLE, and pseudo-images, as well as raw image plots, were performed with the affyPLM package (Bioconductor, USA) (Bolstad et al., 2003). Following these quality control procedures, raw *p*-values were generated for contrasts between sham and exposed groups with the limma package (Smyth, 2004), and adjusted using the Benjamini–Hochberg false discovery rate (FDR) multiple test correction (Gentleman et al., 2004). The gene expression data used in this publication have been deposited in ArrayExpress (http://www.ebi.ac.uk/arrayexpress/), and are accessible through accession number E-MTAB-4492.

2.7.4. Systems biology network analysis

To quantitatively assess the perturbation of relevant biological response systems, previously defined causal network models were used (Boue et al., 2015; Gebel et al., 2013; Schlage et al., 2011; Westra et al., 2011, 2013) in conjunction with a network scoring algorithm that predicts the perturbation of these networks based on transcriptomics data (Martin et al., 2012, 2014). Briefly, this approach relies on two-layer causal network models, in which the lower layer represents the transcriptional changes, and the upper layer represents the actual causal network model. Both layers are linked, and transcriptional changes in the lower layer are used to deduce the activity of the components in the upper layer, which are then aggregated into the final network score. The method uses gene expression data without a fold change or *p*-value cutoff. The biological mechanisms covered by the networks included in this study are inflammation, cellular fate, tissue repair and angiogenesis, cellular stress, and cellular proliferation. Each biological process can be decomposed into biological sub-processes to further investigate the nature of the perturbation (Boue et al., 2015; Kogel et al., 2014).

3. Results

3.1. Test atmosphere composition

The concentrations of nicotine, TPM, CO, and aldehydes were determined in the test atmospheres; Table 1 summarizes the results. Analysis of the test atmospheres throughout the inhalation period indicated that the aerosol was reproducibly generated and delivered to the exposure chambers. Nicotine concentrations achieved for 3R4F_23 and THS2.2_23 were very similar. At the same nicotine concentration, the MA generated from THS2.2 contained approximately 2-fold less TPM, 50-fold less CO, 5-fold less formaldehyde and acetaldehyde, and 12-fold less acrolein compared with MS from 3R4F (Table 1). The PSD measurements indicated that particle sizes and distributions were similar between the exposure groups (Table 1), and were therefore similarly deposited in the respiratory tract. Based on the PSD data, our results indicate that particles were compatible with inhalation, and equally respirable between all aerosol-exposed groups.

3.2. In-life observations

After the exposure, the animals showed typical signs of stress related to tube restraint and/or smoke exposure, regardless of the type and concentration of test atmosphere they were exposed to (Dalbey et al., 1980; Gaworski et al., 2009; Vanscheeuwijck et al., 2002). This was manifested by post-exposure Harderian gland secretion, wet fur, decreased reflexes, and increased irritability. Observations made at the fundus of the eye during ophthalmoscopy examinations were similar in both sham and aerosol exposed groups, and no concentration- or test atmosphere-dependent effects were noted (data not shown). There were no numerical differences in mortality between THS2.2 and 3R4F groups. Deaths were considered either incidental or of technical origin (Supplementary Table 10).

In contrast to the above signs and symptoms that were observed across all exposure groups, higher incidences of wounds (on paws, tail base), sneezing, and/or closed eyes were noted in the 3R4F_23 groups (25 incidences) and THS2.2_50 groups (18 incidences). Wounds were probably due to animal movement in the exposure tube and abrasion through contact with the restraint plunger; closed eyelids were probably related to irritation from the aerosol

Table 2
In-life measurements during 90 day exposure to test atmosphere of the reference cigarette 3R4F, THS2.2, or air (sham).

Parameter	Sex	Sham	3R4F_8	3R4F_15	3R4F_23	THS2.2_15	THS2.2_23	THS2.2_50
Body weight on day 1 (g)	M	372.1 ± 4.79 (16)	374.9 ± 7.85 (10)	372.3 ± 7.01 (10)	368.1 ± 5.25 (16)	370.0 ± 4.32 (10)	380.2 ± 8.11 (10)	367.9 ± 4.19 (20)
	F	240.6 ± 3.95 (16)	243.4 ± 2.92 (10)	240.4 ± 4.35 (10)	244.3 ± 3.50 (16)	241.0 ± 4.24 (10)	247.8 ± 5.15 (10)	243.8 ± 3.52 (20)
Body weight on day 88 (g)	M	489.9 ± 9.63 (16)	434.4 ± 13.92 (10)**	441.0 ± 15.76 (10)**	402.8 ± 8.49 (15)**	443.4 ± 9.12 (10)**	449.1 ± 13.26 (10)**	421.4 ± 7.37 (20)**
	F	256.3 ± 6.02 (16)	270.2 ± 5.60 (10)	285.0 ± 6.48 (10)**	272.2 ± 3.40 (15)	275.3 ± 6.92 (10)*	301.0 ± 7.54 (10)**	300.2 ± 6.42 (20)**
Food consumption (g/day/100 g body weight)	M	6.1 ± 0.17 (10)	6.2 ± 0.07 (10)	6.2 ± 0.08 (10)	6.4 ± 0.09 (10)	6.5 ± 0.13 (10)	6.3 ± 0.13 (10)	7.0 ± 0.15 (10)**
	F	7.5 ± 0.26 (10)	7.9 ± 0.08 (10)	7.7 ± 0.14 (10)	7.2 ± 0.13 (10)	8.0 ± 0.07 (10)	8.2 ± 0.09 (10)*	8.3 ± 0.13 (10)*
Respiratory minute volume (ml/min)	M	212.3 ± 17.00 (10)	190.0 ± 10.10 (10)	161.8 ± 15.80 (10)*	123.7 ± 11.00 (10)***	220.0 ± 9.10 (10)	187.8 ± 13.80 (10)	186.9 ± 7.50 (10)
	F	147.0 ± 11.80 (10)	166.5 ± 13.80 (10)	121.0 ± 9.80 (10)	108.8 ± 5.90 (10)**	175.5 ± 23.80 (10)	149.6 ± 12.60 (10)	142.6 ± 9.50 (10)

Body weight measurements from day 1 and day 88 represent the starting and final measurements taken in the 90 day inhalation period. Food consumption was measured once per week over 10 weeks of the study, and reported as daily food consumed normalized to mean body weight (g/day per 100g body weight). Respiratory minute volume was measured once during the study. Results are presented as mean or least squares mean ± standard error. The sample size is in parentheses. Difference from sham group: Significance: $^{*}p < 0.05$; $^{**}p < 0.01$; $^{***}p < 0.001$. Abbreviations: M, male; F, female.

exposure.

The occurrence of tremors in rats was more frequent in the THS2.2_50 group, mainly during the first 15 days of exposure (7 incidences in female rats, 2 incidences in male rats), and after day 50 of the study (37 incidences in female rats, 14 incidences in male rats). This may be attributed to the nicotine effect that was observed in past study (Phillips et al., 2015a). The lower body weights in female rats, in combination with high nicotine concentration exposure, may account for the higher incidence of tremors. The animals with tremors recovered within 30 min upon removal from the exposure. This is typical of nicotine toxicity, and is related to the short half-life of nicotine in rats (Abobo et al., 2012; Silvette et al., 1962).

3.3. Biomonitoring

3.3.1. Respiratory physiology

Determination of respiratory physiology parameters was performed to assess the degree of irritation to the respiratory tract (Alarie, 1981). Exposure to 3R4F caused a concentration-dependent reduction in respiratory minute volume in both male and female rats that was significantly lower in the 3R4F_15 (male only) and 3R4F_23 (both male and female) groups, compared with the sham group (Tables 2 and 3). In contrast, the respiratory minute volumes of rats exposed to MA generated from THS2.2 were largely unaffected compared with sham groups (both sexes), and were significantly higher in comparison with 3R4F groups at the same nicotine concentrations of 15 μg/l (male only) and 23 μg/l (both sexes). The reduction in respiratory minute volume in 3R4F groups was mainly attributed to a reduction in respiratory frequency (both sexes) and tidal volume in male rats (Supplementary Tables 11,12). Respiratory frequency and tidal volume remained largely unaffected in THS2.2-exposed rats, and were higher than those in the 3R4F_15 (female) and 3R4F_23 (male and female rats) groups at the same nicotine concentrations. There was no significant change in peak inspiratory flow in male groups except in the 3R4F_8 group, where it was considered an incidental finding. The peak inspiratory flow in the female THS2.2_15 and THS2.2_23 groups was higher compared with the sham group.

3.3.2. Biomarkers of exposure

Measurement of COHb in blood was performed to assess the exposure and uptake of aerosols by the rats (Table 4). The proportions of COHb were up to 26.5% in male rats exposed to 3R4F, and only 4.5% in rats exposed to THS2.2. Similar results were obtained from the exposed female rats (Supplementary Table 13). There was also a good linear correlation between the proportions of COHb in the exposed animals and the CO concentrations in the test atmospheres, indicating efficient uptake of the aerosols by the animals (Supplementary Fig. 1). Measurements were repeated at the end of the recovery period, and showed that all COHb values were at baseline level (data not shown).

The second approach to assess aerosol exposure and uptake was the quantification of total nicotine metabolites in 24-h urine (during and after exposure) collected from rats at defined intervals during the study. As controls, nicotine metabolites quantified before the 90-day exposure phase and during the 42-day recovery phase were determined; the results obtained were all below the limit of quantification. The lower limits of quantification (LOQ) were 1.73 μmol/l for 3′HOCOT, 0.91 μmol/l for NCOT, 1.31 μmol/l for COT, 5.23 μmol/l for NNO, and 1.75 μmol/l for NNIC. In exposed animals, the total quantity of nicotine metabolites excreted was proportional to the nicotine test atmosphere concentrations (Table 1, Supplementary Table 13). Similar results were obtained for both sexes. At equal nicotine concentrations in the test

Table 3
Statistically significant differences in body weight, food consumption, and respiratory minute volume between animals exposed to aerosol from THS2.2 and cigarette smoke from 3R4F.

Parameter	Sex	THS2.2_15 vs. 3R4F_15	THS2.2_23 vs. 3R4F_23	THS2.2_50 vs. 3R4F_23
Body weight on day 88	M	=	↑*	=
	F	=	↑**	↑**
Food consumption	M	=	=	↑**
	F	=	↑***	↑***
Respiratory minute volume	M	↑**	↑**	↑***
	F	=	↑*	↑**

Difference between groups: Significance: *, $p < 0.05$; **$p < 0.01$; ***, $p < 0.001$. Symbols, ↑ indicates response higher in THS2.2 relative to 3R4F;=indicates no difference. Abbreviations: M, male; F, female.

atmosphere, the total quantity of nicotine metabolites excreted was higher in the THS2.2-exposed rats than in the 3R4F-exposed rats. This is suggestive of an overall higher uptake of aerosol constituents in the THS2.2-exposed rats. In the exposed animals, the total quantity of nicotine metabolites excreted was similar across the 3 time points (week 2, week 4, and week 12), indicating a stable exposure and uptake of aerosol by the rats throughout the study (Supplementary Fig. 1). The relative distribution of the 5 nicotine metabolites measured was in line with observations in past studies, where NNO and COT were the major metabolites excreted (Supplementary Fig. 1)(Kogel et al., 2014; Vanscheeuwijck et al., 2002).

The third approach to assess aerosol exposure and uptake was the quantification of CEMA (metabolite of acrylonitrile), HPMA (metabolite of acrolein), total NNAL (metabolite of NNK), and SPMA (metabolite of benzene) in 24-h urine of exposed rats (Table 4). In males, the levels of CEMA, HPMA, NNAL, and SPMA were approximately 48-fold, 2-fold, 5-fold, and 38-fold, respectively, lower in the THS2.2-exposed groups than in the 3R4F groups at equal nicotine exposure concentrations. Among these 4 biomarkers of exposure, the concentration of HPMA was notably higher compared with NNAL, CEMA, and SPMA in the sham and pre-exposed animals. This may be related to endogenous production of acrolein that contributes to the baseline levels of HPMA in urine (Stevens, 2008). The baseline levels of the 4 biomarkers were reflected in the urine samples collected before the 90-day exposure phase and during the 42-day recovery phase (Supplementary Fig. 1). As observed with nicotine metabolites, the excretion of CEMA, HPMA, NNAL, and SPMA was also fairly stable across the 13-week exposure period (measured in week 2, week 4, and week 12), indicating a reproducible aerosol generation and uniform uptake of aerosol constituents by the rats throughout the study (Supplementary Fig. 1). The concentration of HPMA excreted in the urine was proportional to the acrolein levels in the test atmosphere supplied (Supplementary Fig. 1).

3.4. General and systemic effects

3.4.1. Body weight and food consumption. The animals gained weight over time throughout the exposure period, and more rapidly during the recovery period (Fig. 1). Body weight determination was made one day after the weekend exposure break, during which animals had a short recovery, but also at the end of a week of exposure. This explains the zig-zag pattern of the body weights. In male rats, all aerosol-exposed animals showed lower body weight when compared with sham. After the 90-day exposure period to the test atmospheres, body weight was 10–18% lower in the 3R4F groups, and 8–14% lower in THS2.2 groups, compared with sham (Table 2). At equivalent nicotine concentrations (23 μg/l nicotine), the mean body weight in the male

Table 4
Bio-monitoring parameters in male animals.

Parameter	Sham	3R4F_8	3R4F_15	3R4F_23	THS2.2_15	THS2.2_23	THS2.2_50
COHb (%)	3.5 ± 0.42 (6)	11.3 ± 1.52 (6)	18.3 ± 1.04 (6)	26.5 ± 1.85 (6)	3.7 ± 0.42 (6)	4.0 ± 0.34 (5)	4.5 ± 0.81 (6)
Total nicotine metabolites (nmol)	12.9 ± 7.38 (8)	603.4 ± 99.83 (8)	1071.0 ± 268.16 (8)	1548.4 ± 355.49 (8)	1944.9 ± 343.03 (8)	2619.3 ± 306.20 (8)	5146.1 ± 648.85 (8)
CEMA (ng/ml)	4.1 ± 1.32 (8)	260.3 ± 121.01 (8)	375.9 ± 132.33 (8)	494.2 ± 108.39 (8)	7.7 ± 2.35 (8)	8.7 ± 2.00 (8)	10.0 ± 2.66 (8)
HPMA (ng/ml)	2610.6 ± 783.0 (8)	7389.9 ± 2522.6 (8)	10565.6 ± 3547.7 (8)	13213.8 ± 3393.7 (8)	4401.4 ± 1408.9 (8)	4035.8 ± 1005.5 (8)	4179.4 ± 1576.3 (8)
Total NNAL (pg/ml)	38.4 ± 9.65 (8)	147.0 ± 61.06 (8)	254.9 ± 56.64 (8)	412.0 ± 102.11 (8)	48.2 ± 28.71 (8)	46.6 ± 17.25 (8)	73.3 ± 37.46 (8)
SPMA (ng/ml)	3.1 ± 0.87 (8)	109.4 ± 55.07 (8)	171.9 ± 57.67 (8)	309.9 ± 109.5 (8)	4.5 ± 1.00 (8)	5.0 ± 1.05 (8)	5.4 ± 1.30 (8)

Carboxyhemoglobin (COHb) was measured in the blood of the exposed male rats immediately after the 6-h exposure period. Total nicotine metabolites, 3-hydroxypropylmercapturic acid (HPMA, biomarker for acrolein uptake), 4-(methylnitrosamino)-1-(3-pyridyl)-1-butanol (NNAL total, biomarker for NNK uptake), *S*-phenylmercapturic acid (SPMA, biomarker for benzene uptake), and 2-cyanoethylmercapturic acid (CEMA, marker for acrylonitrile uptake) in urine were measured at 3 time points across the 90-day study. Data from 1 representative time point (week 4) are shown. Urine biomarkers of exposure were measured from 24 h urine (collected during 6 h exposure and 18 h post-exposure). Results are presented as mean ± standard deviation. The sample size is in parentheses.

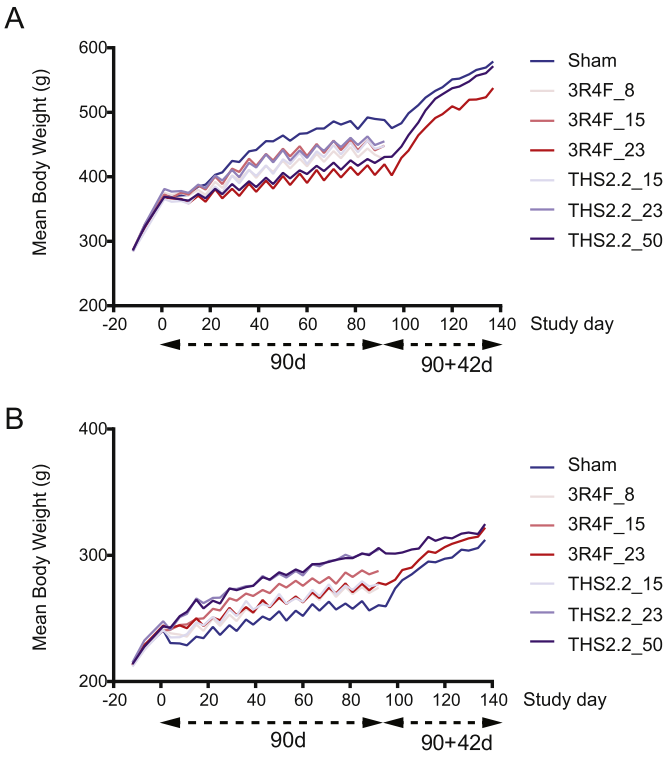

Fig. 1. Mean body weights of (A) male and (B) female rats exposed to fresh air (sham) and aerosols from THS2.2 and 3R4F. Animals were weighed twice per week. Day 1 represents the exposure start date. N = 6–20.

3R4F_23 group was lower than that in the THS2.2_23 group, while no difference was found between the 3R4F_15 group and the THS2.2_15 group (Table 3). In female rats, the body weight loss in the sham group during the first week of dose adaptation and slow weight gain in subsequent exposure weeks resulted in lower mean body weight in the sham group compared with the test and reference groups throughout the study (Fig. 1). As a result, body weight after the 90-day exposure period was 5–11% higher in the 3R4F groups and 7–17% higher in the THS2.2 groups, compared with the sham group (Table 2). The mean body weight in the 3R4F_23 female group was lower than that in both the THS2.2_23 and THS2.2_50 groups (Table 3). Similar findings have been reported for MS inhalation studies (Terpstra et al., 2003; Vanscheeuwijck et al., 2002). The reduction in body weight is likely due to the aerosol toxicity and irritation-dependent stress; both nicotine (Chowdhury, 1990; Chowdhury et al., 1989) and acrolein (Bouley et al., 1975; Feron et al., 1978) have been shown to cause this effect.

Food consumption did not differ between the 3R4F and sham groups. However, food consumption was higher in the male THS2.2_50 group compared with the sham and 3R4F_23 groups. In female rats, food consumption in the THS2.2_23 and THS2.2_50 groups was statistically higher than in the sham and 3R4F_23 groups (Tables 2 and 3).

3.4.2. Hematology. Blood neutrophil counts were significantly higher in the 3R4F_15 and 3R4F_23 male groups, as well as in the THS2.2_50 male 90-day exposed groups, compared with the sham group (Table 5). An aerosol concentration-dependent increase in neutrophil counts was observed for all 3R4F and THS2.2 90-day exposed female rats. No significant difference in neutrophil counts was observed between the 3R4F and THS2.2 exposed groups. After the 42-day recovery period, the neutrophil counts in

Table 5
Blood lymphocyte and neutrophil counts in male and female rats after 90-day inhalation period or 42-day recovery period following 90-day exposure to test atmosphere of the reference cigarette 3R4F, THS2.2, or air (sham).

Parameter	Sex	90d						90 + 42d		
		Sham	3R4F_8	3R4F_15	3R4F_23	THS2.2_15	THS2.2_23	THS2.2_50	Sham	3R4F_23	THS2.2_50
Neutrophil count	M	1.3 ± 0.31 (8)	1.8 ± 0.23 (6)	2.6 ± 0.50 (8)*	2.7 ± 0.44 (9)**	2.6 ± 0.88 (7)	2.2 ± 0.34 (6)	4.8 ± 2.13 (8)**	1.5 ± 0.19 (6)	1.7 ± 0.51 (3)	2.0 ± 0.32 (8)
	F	0.6 ± 0.10 (10)	1.2 ± 0.12 (8)**	1.7 ± 0.34 (8)**	2.0 ± 0.34 (7)**	1.8 ± 0.49 (6)**	1.9 ± 0.37 (8)**	3.5 ± 0.57 (7)**	0.7 ± 0.08 (5)	1.0 ± 0.20 (5)	1.6 ± 0.32 (8)#
Lymphocyte count	M	5.6 ± 0.79 (8)	4.4 ± 0.82 (6)	4.1 ± 0.49 (8)	3.8 ± 0.38 (9)*	3.7 ± 0.40 (7)*	5.0 ± 0.60 (6)	4.1 ± 0.72 (8)	7.8 ± 0.58 (6)	6.1 ± 0.59 (3)	6.1 ± 0.44 (8)#
	F	4.6 ± 0.62 (10)	4.1 ± 0.40 (8)	3.6 ± 0.46 (8)	4.2 ± 0.43 (7)	4.2 ± 0.52 (6)	3.7 ± 0.44 (8)	3.8 ± 0.34 (7)	3.8 ± 0.48 (5)	5.4 ± 0.86 (5)	4.9 ± 0.38 (8)

Blood neutrophil and lymphocyte counts measured after 90-day exposure (90d) and 42-day recovery period following a 90-day exposure (90 + 42d). Counts are reported as $x10^9$/l. Results are presented as mean ± standard error. The sample size is in parentheses. Difference from sham group at 90d: Significance: *, $p < 0.05$; **$p < 0.01$. Difference from sham group at 90 + 42d: Significance: #$p < 0.05$. Abbreviations: M, male; F, female.

Table 6
Clinical chemistry parameters from male and female rats after 90-day inhalation period or 42-day recovery period following 90-day exposure to test atmosphere of the reference cigarette 3R4F, THS2.2, or air (sham).

Parameter	Sex	90d							90 + 42d		
		Sham	3R4F_8	3R4F_15	3R4F_23	THS2.2_15	THS2.2_23	THS2.2_50	Sham	3R4F_23	THS2.2_50
Alkaline phosphatase (IU/l)	M	162.0 ± 16.00 (10)	191.5 ± 16.00 (10)	193.9 ± 17.60 (10)	255.0 ± 20.70 (10)**	186.4 ± 15.90 (10)	235.0 ± 19.00 (9)**	254.0 ± 24.70 (10)**	149.6 ± 14.70 (6)	133.2 ± 15.60 (5)	169.8 ± 13.60 (10)
	F	111.0 ± 9.60 (10)	158.2 ± 19.40 (10)*	149.1 ± 11.50 (9)*	182.0 ± 19.20 (9)**	146.7 ± 15.50 (10)	179.3 ± 22.80 (10)**	265.0 ± 32.70 (10)**	128.0 ± 15.00 (6)	129.0 ± 15.00 (5)	83.9 ± 7.40 (10)#
Alanine aminotransferase (IU/l)	M	57.0 ± 6.50 (10)	52.3 ± 5.00 (10)	63.7 ± 4.00 (10)	68.0 ± 5.80 (10)	64.2 ± 4.60 (10)	98.0 ± 18.00 (8)**	75.0 ± 6.70 (10)*	61.3 ± 11.50 (6)	47.9 ± 5.00 (5)	57.3 ± 7.50 (10)
	F	51.0 ± 4.40 (10)	54.9 ± 6.90 (10)	55.9 ± 4.30 (9)	54.0 ± 2.60 (9)	67.6 ± 6.10 (10)*	74.6 ± 7.20 (10)**	73.0 ± 3.20 (10)**	68.5 ± 14.30 (6)	47.0 ± 2.00 (5)	52.4 ± 8.90 (9)
Aspartate aminotransferase (IU/l)	M	121.0 ± 8.90 (10)	134.2 ± 7.70 (10)	164.6 ± 10.70 (10)*	152.0 ± 16.80 (10)	160.5 ± 13.60 (10)*	209.0 ± 30.00 (8)**	158.0 ± 16.00 (10)*	108.4 ± 17.30 (6)	89.5 ± 2.80 (5)	108.5 ± 8.80 (10)
	F	146.6 ± 13.40 (10)	165.5 ± 36.70 (10)	130.2 ± 12.50 (9)	122.8 ± 11.10 (9)	147.7 ± 13.70 (10)	124.0 ± 7.80 (10)	146.0 ± 7.50 (10)	166.0 ± 24.50 (6)	91.0 ± 8.00 (5)##	114.6 ± 17.50 (9)#
Total protein (g/l)	M	58.8 ± 0.80 (10)	57.4 ± 1.00 (10)	58.2 ± 1.00 (10)	58.4 ± 0.40 (10)	56.2 ± 0.80 (10)	61.0 ± 3.00 (9)	58.3 ± 1.40 (10)	59.7 ± 1.30 (6)	62.9 ± 1.80 (5)	59.4 ± 0.90 (10)
	F	64.0 ± 1.30 (10)	56.0 ± 1.60 (10)**	57.4 ± 0.90 (9)**	57.0 ± 0.90 (9)**	56.8 ± 0.90 (10)**	54.7 ± 0.80 (10)**	58.0 ± 0.60 (10)**	71.0 ± 1.20 (6)	66.0 ± 3.50 (5)#	62.8 ± 1.10 (10)##
Albumin (g/l)	M	34.8 ± 0.40 (10)	33.7 ± 0.70 (10)	34.1 ± 0.70 (10)	34.7 ± 0.20 (10)	32.6 ± 0.40 (10)**	35.7 ± 1.30 (9)	34.4 ± 0.80 (10)	34.9 ± 0.60 (6)	35.0 ± 0.90 (5)	33.6 ± 0.60 (10)
	F	38.9 ± 0.80 (10)	34.2 ± 0.90 (10)**	34.0 ± 0.70 (9)**	33.6 ± 0.40 (9)**	33.6 ± 1.00 (10)**	33.1 ± 0.60 (10)**	34.3 ± 0.50 (10)**	42.7 ± 0.80 (6)	38.1 ± 2.30 (5)##	36.6 ± 0.90 (10)##
Globulin (g/l)	M	23.9 ± 0.50 (10)	23.7 ± 0.60 (10)	24.2 ± 0.50 (10)	24.0 ± 0.40 (10)	23.5 ± 0.60 (10)	24.2 ± 1.60 (10)	23.8 ± 0.90 (10)	25.0 ± 0.70 (6)	27.9 ± 1.20 (5)#	25.7 ± 0.50 (10)
	F	25.0 ± 0.60 (10)	21.8 ± 0.90 (10)*	23.5 ± 0.40 (9)	23.8 ± 1.10 (9)	23.2 ± 0.70 (10)	21.6 ± 0.70 (10)**	24.1 ± 0.80 (10)	28.7 ± 0.50 (6)	28.0 ± 1.80 (5)	26.1 ± 1.20 (10)
Cholesterol (mmol/l)	M	1.3 ± 0.08 (10)	1.1 ± 0.08 (10)	1.0 ± 0.05 (10)**	0.9 ± 0.04 (10)**	1.1 ± 0.05 (10)**	1.0 ± 0.07 (9)**	1.0 ± 0.08 (10)**	1.2 ± 0.07 (6)	1.3 ± 0.10 (5)	1.3 ± 0.11 (10)
	F	1.4 ± 0.09 (10)	0.9 ± 0.06 (10)**	0.8 ± 0.07 (9)**	0.8 ± 0.08 (9)**	1.0 ± 0.08 (10)**	0.9 ± 0.07 (10)**	1.0 ± 0.06 (10)**	1.7 ± 0.09 (6)	1.6 ± 0.26 (5)	1.4 ± 0.07 (10)#
Triglyceride (mmol/l)	M	1.2 ± 0.16 (10)	1.0 ± 0.09 (10)	0.7 ± 0.11 (10)**	0.8 ± 0.09 (10)	0.7 ± 0.08 (10)**	1.2 ± 0.12 (8)	0.8 ± 0.15 (10)*	1.3 ± 0.24 (6)	1.4 ± 0.33 (5)	1.5 ± 0.24 (10)
	F	0.9 ± 0.11 (10)	0.8 ± 0.10 (10)	0.4 ± 0.08 (9)**	0.3 ± 0.05 (9)**	0.9 ± 0.15 (10)	0.7 ± 0.14 (10)	0.4 ± 0.06 (10)**	1.8 ± 0.32 (6)	1.2 ± 0.27 (5)	1.5 ± 0.17 (10)
Glucose (mmol/l)	M	12.5 ± 0.70 (10)	10.9 ± 0.50 (10)*	11.5 ± 1.40 (10)	10.0 ± 0.60 (10)**	11.4 ± 0.50 (10)	16.6 ± 4.10 (8)	9.6 ± 0.60 (10)**	13.4 ± 0.70 (6)	14.5 ± 2.70 (5)	14.5 ± 3.00 (10)
	F	10.5 ± 0.40 (10)	11.6 ± 1.10 (10)	10.9 ± 1.30 (9)	8.6 ± 0.30 (9)**	11.5 ± 1.50 (10)	9.4 ± 0.40 (10)	8.4 ± 0.40 (10)**	10.2 ± 0.40 (6)	11.6 ± 1.80 (5)	11.0 ± 0.30 (10)

Clinical chemistry parameters measured after 90-day exposure (90d) and 42-day recovery period following a 90-day exposure (90 + 42d). Results represent mean ± standard error. The sample size is in parentheses. Difference from sham group at 90d: Significance: *, $p < 0.05$; **$p < 0.01$. Difference from sham group at 90 + 42d: Significance: #, $p < 0.05$; ##$p < 0.01$. Abbreviations: M, male; F, female.

Table 7
Statistical significance difference in activities of liver enzymes and triglycerides present in serum.

Parameter	Sex	90d			90 + 42d
		THS2.2_15 vs. 3R4F_15	THS2.2_23 vs. 3R4F_23	THS2.2_50 vs. 3R4F_23	THS2.2_50 vs. 3R4F_23
Alkaline phosphatase (IU/L)	M	=	=	=	=
	F	=	=	↑*	↓*
Alanine aminotransferase (IU/L)	M	=	=	=	=
	F	=	↑*	↑**	=
Aspartate aminotransferase (IU/L)	M	=	↑*	=	=
	F	=	=	=	=
Triglyceride (mmol/L)	M	=	↑*	=	=
	F	↑**	↑**	=	=

Difference between groups: Significance: *, $p < 0.05$; **$p < 0.01$. Symbols, ↓ indicates response lower in THS2.2 relative to 3R4F; ↑ indicates response higher in THS2.2 relative to 3R4F; =indicates no difference. Abbreviations: M, male; F, female.

Table 8
Differential cell counts in BALF from male and female rats after 90-day inhalation period or 42-day recovery period following 90-day exposure to test atmosphere of the reference cigarette 3R4F, THS2.2, or air (sham).

Parameter	Sex	90d						90 + 42d		
		Sham	3R4F_8	3R4F_15	3R4F_23	THS2.2_15	THS2.2_23	THS2.2_50	Sham	3R4F_23	THS2.2_50
Total cell count	M	39.4 ± 6.08 (10)	49.4 ± 8.06 (10)	76.0 ± 13.40 (10)*	103.4 ± 17.32 (10)**	36.7 ± 7.29 (10)	34.9 ± 7.14 (10)	39.0 ± 8.67 (10)	41.5 ± 10.95 (6)	84.8 ± 24.26 (5)	45.6 ± 9.59 (10)
	F	22.9 ± 3.36 (10)	55.0 ± 11.21 (10)*	58.7 ± 8.85 (10)**	116.4 ± 13.40 (9)***	26.7 ± 5.56 (9)	42.5 ± 7.13 (10)*	27.8 ± 3.23 (10)	37.4 ± 11.73 (6)	73.4 ± 22.56 (6)	41.9 ± 9.57 (10)
Macrophage count	M	37.3 ± 6.20 (10)	42.7 ± 7.34 (10)	52.0 ± 9.57 (10)	67.0 ± 13.78 (10)	35.6 ± 7.20 (10)	33.5 ± 7.11 (10)	35.7 ± 8.15 (10)	40.1 ± 10.53 (6)	70.7 ± 20.84 (5)	44.6 ± 9.39 (10)
	F	22.0 ± 3.36 (10)	45.5 ± 9.82 (10)*	39.8 ± 7.52 (10)	67.2 ± 10.02 (9)**	25.3 ± 5.59 (9)	40.0 ± 6.64 (10)*	26.5 ± 3.16 (10)	36.9 ± 11.60 (6)	59.4 ± 17.82 (6)	40.9 ± 9.32 (10)
Lymphocyte count	M	1.3 ± 0.43 (10)	1.0 ± 0.19 (10)	1.7 ± 0.25 (10)	2.4 ± 0.34 (10)	0.5 ± 0.08 (10)	0.7 ± 0.11 (10)	1.2 ± 0.46 (10)	0.9 ± 0.38 (6)	3.0 ± 0.80 (5)#	0.6 ± 0.14 (10)
	F	0.6 ± 0.16 (10)	1.7 ± 0.45 (10)*	1.6 ± 0.39 (10)*	2.4 ± 0.46 (9)**	0.8 ± 0.52 (9)	1.1 ± 0.53 (10)	0.6 ± 0.13 (10)	0.5 ± 0.12 (6)	3.5 ± 1.11 (6)#	0.7 ± 0.24 (10)
Neutrophil count	M	0.8 ± 0.25 (10)	5.7 ± 1.18 (10)***	22.1 ± 4.74 (10)***	33.7 ± 6.68 (10)***	0.5 ± 0.10 (10)	0.7 ± 0.24 (10)	2.1 ± 0.98 (10)	0.5 ± 0.17 (6)	11.0 ± 3.13 (5)##	0.3 ± 0.09 (10)
	F	0.3 ± 0.11 (10)	7.6 ± 1.47 (10)***	17.1 ± 1.95 (10)***	46.5 ± 4.46 (9)***	0.6 ± 0.21 (9)	1.3 ± 0.65 (10)	0.7 ± 0.19 (10)	0.1 ± 0.03 (6)	10.4 ± 3.72 (6)#	0.3 ± 0.10 (10)
Eosinophil count	M	0.0 ± 0.01 (10)	0.0 ± 0.01 (10)	0.2 ± 0.12 (10)	0.3 ± 0.07 (10)**	0.0 ± 0.01 (10)	0.0 ± 0.01 (10)	0.0 ± 0.00 (10)	0.0 ± 0.01 (6)	0.2 ± 0.06 (5)#	0.0 ± 0.00 (10)
	F	0.0 ± 0.00 (10)	0.1 ± 0.02 (10)**	0.1 ± 0.02 (10)***	0.3 ± 0.07 (9)***	0.0 ± 0.01 (9)	0.0 ± 0.02 (10)	0.0 ± 0.01 (10)	0.0 ± 0.00 (6)	0.1 ± 0.04 (6)#	0.0 ± 0.01 (10)

Cell numbers are quantified by fluorescence-activated cell sorting (FACS) after 90-day exposure (90d) and 42-day recovery period following a 90-day exposure (90 + 42d). Cell numbers are reported as 10^5/right lung. Results represent mean ± standard error. The sample size is in parentheses. Difference from sham group at 90d: Significance: *, $p < 0.05$; **$p < 0.01$; ***, $p < 0.001$. Difference from sham group at 90 + 42d: Significance: #, $p < 0.05$; ##$p < 0.01$. Abbreviations: M, male; F, female.

male rats declined to levels similar to those in the sham group. In female rats, the neutrophil counts were significantly lower after the 42-day recovery period, compared with the 90-day exposure groups, even though the level in the THS2.2_50 group was still slightly higher than in the sham recovery group.

Lymphocyte counts were statistically significantly lower in the 3R4F_23 male group when compared with the sham group on day 90 (Table 5). No change in lymphocyte counts was observed for the female animals. Lymphocyte counts were slightly lower in the male THS2.2 groups, compared with the sham group. A statistically significant difference was observed for the THS2.2_15 group, even though no concentration-dependent effect was observed. No significant difference in lymphocyte counts was observed between the 3R4F and THS2.2 exposed groups. After the 42-day recovery period, the lymphocyte counts in the sham, 3R4F_23, and THS2.2_50 male groups were increased, compared with the same groups at 90-day. A statistically significant difference was observed for the THS2.2_50 group compared with the sham group after the 42-day recovery period.

A small but significantly higher monocyte count in the THS2.2_23 and THS2.2_50 groups was observed relative to the sham group in female rats (Supplementary Table 14). The monocyte count, however, was not different between the 3R4F- and THS2.2-exposed groups.

The red blood cell (RBC) parameters (erythrocyte count, reticulocyte count, blood hemoglobin (Hb) concentration, mean corpuscular volume (MCV), mean cell hemoglobin content (MCHC), mean corpuscular hemoglobin (MCH), and hematocrit (HCT)) did not show any consistent exposure-related effects (Supplementary Table 14), and results for all groups were within the range of normal values provided by the breeders (Thrall, 2012).

3.4.3. Clinical chemistry. Serum was collected during necropsy after 90 days of exposure and after 42 days post-exposure from the abdominal aorta of rats for the analysis of various clinical chemistry parameters. The most obvious aerosol effects were observed in the activities of liver-derived enzymes. The activity of alkaline phosphatase (ALP) was increased and statistically significant compared with the sham after 90 days of exposure in the male 3R4F_23 group and in all female 3R4F groups, while aspartate aminotransferase (AST) activity was higher in the male 3R4F_15 group (Table 6). Compared with sham, the ALP and alanine aminotransferase (ALT) activities were higher in the male and female THS2.2 groups, while AST activity was higher in the male THS2.2-exposed groups. The liver-derived enzyme activities were in general similar between the THS2.2 and 3R4F groups at the same nicotine concentrations (Table 7). The enzyme activities in the 3R4F and THS2.2_50 groups reverted back to levels similar to those in the sham group after the 42-day recovery period.

Some aerosol-dependent effects were also observed in the markers of nutritional/metabolic status, including proteins, lipids, and glucose (Table 6). The concentrations of albumin and total protein were unchanged in the male 3R4F groups. Albumin was reduced relative to the sham group in the male THS2.2_15 group, but not in the other concentration groups, and hence is considered an incidental observation. The 3R4F- and THS2.2-exposed female groups had lower albumin and total serum protein concentrations compared with the sham group after a 90-day exposure. The concentrations of albumin and total protein in the female sham group were also lower compared with the same group after the 42-day recovery period. The levels of both analytes in exposed groups were partially reversed toward sham group levels in the post-exposure recovery animals.

Serum cholesterol concentration was lowered in a concentration-dependent manner in all the 3R4F- and THS2.2-

Table 9
Statistical significance difference in BALF cell counts between animals exposed to aerosol from THS2.2 and cigarette smoke from 3R4F.

Parameter	Sex	90d			90 + 42d
		THS2.2_15 vs. 3R4F_15	THS2.2_23 vs. 3R4F_23	THS2.2_50 vs. 3R4F_23	THS2.2_50 vs. 3R4F_23
Total cell count	M	$\downarrow^{*}$	$\downarrow^{**}$	$\downarrow^{**}$	=
	F	$\downarrow^{**}$	$\downarrow^{***}$	$\downarrow^{***}$	=
Macrophage count	M	=	$\downarrow^{*}$	=	=
	F	=	$\downarrow^{*}$	$\downarrow^{**}$	=
Lymphocyte count	M	$\downarrow^{**}$	$\downarrow^{***}$	=	$\downarrow^{*}$
	F	=	=	$\downarrow^{**}$	$\downarrow^{*}$
Neutrophil count	M	$\downarrow^{***}$	$\downarrow^{***}$	$\downarrow^{***}$	$\downarrow^{***}$
	F	$\downarrow^{***}$	$\downarrow^{***}$	$\downarrow^{***}$	$\downarrow^{**}$
Eosinophil count	M	=	$\downarrow^{***}$	$\downarrow^{***}$	$\downarrow^{***}$
	F	$\downarrow^{***}$	$\downarrow^{**}$	$\downarrow^{***}$	$\downarrow^{**}$

Difference between groups: Significance: *, $p < 0.05$; **$p < 0.01$; ***$p < 0.001$. Symbols, ↓ indicates response lower in THS2.2 relative to 3R4F; =indicates no difference. Abbreviations: M, male; F, female.

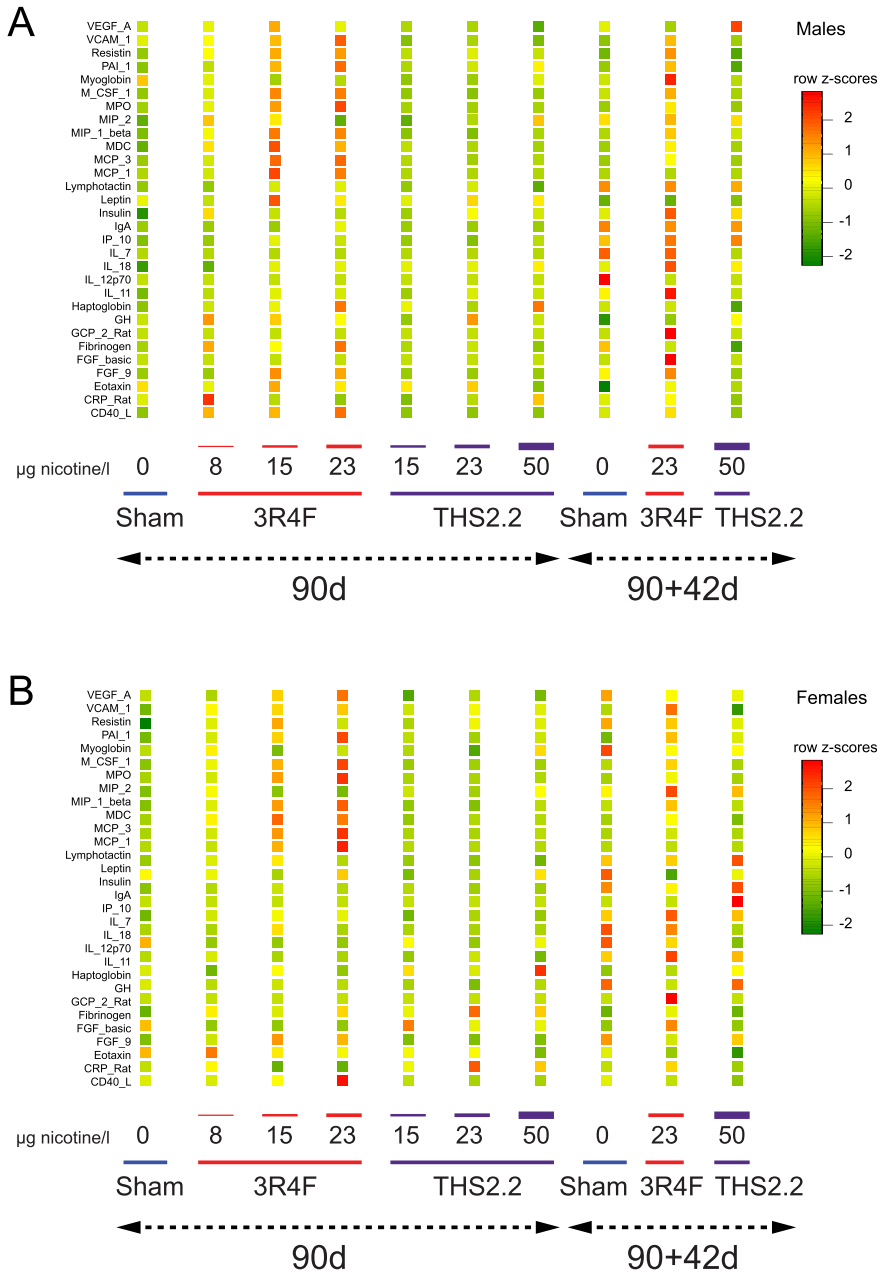

Fig. 2. Analytes present in bronchoalveolar lavage fluid after 90 days of exposure and 42 days of recovery (R). Data shown are row z-scores for each analyte (y-axis) and for each exposure group (x-axis) in (A) male and (B) female rats. Note: Analytes with 50% or more values below limit of quantification (LOQ) were excluded from the heatmaps. N = 5–10.

Table 10
Organ weights relative to body weight in male and female rats after 90-day inhalation period or 42-day recovery period following 90-day exposure to test atmosphere of the reference cigarette 3R4F, THS2.2, or air (sham).

Parameter	Sex	90d						90 + 42d		
		Sham	3R4F_8	3R4F_15	3R4F_23	THS2.2_15	THS2.2_23	THS2.2_50	Sham	3R4F_23	THS2.2_50
Lung, larynx, trachea	M	35.8 ± 1.37 (10)	41.7 ± 1.33 (9)**	47.9 ± 1.81 (8)***	50.6 ± 1.42 (9)***	44.0 ± 3.45 (9)	39.0 ± 0.74 (9)	40.3 ± 0.97 (8)*	30.6 ± 1.42 (6)	35.9 ± 1.74 (4)#	32.3 ± 0.86 (10)
	F	51.4 ± 4.06 (7)	57.4 ± 2.32 (10)	57.4 ± 1.31 (10)	62.7 ± 2.17 (9)*	54.2 ± 2.68 (9)	49.1 ± 1.17 (9)	48.7 ± 2.43 (9)	42.5 ± 1.08 (6)	49.5 ± 0.95 (6)###	46.1 ± 1.18 (10)#
Left adrenal	M	0.6 ± 0.03 (8)	0.8 ± 0.00 (9)**	0.8 ± 0.07 (9)**	0.9 ± 0.03 (10)***	0.9 ± 0.11 (9)*	0.8 ± 0.06 (9)**	0.9 ± 0.03 (9)***	0.5 ± 0.03 (6)	0.5 ± 0.05 (4)	0.4 ± 0.02 (10)
	F	1.3 ± 0.11 (8)	1.6 ± 0.10 (9)	1.6 ± 0.00 (9)*	1.7 ± 0.07 (9)*	1.6 ± 0.10 (9)	1.6 ± 0.06 (10)	1.9 ± 0.15 (8)**	1.0 ± 0.09 (6)	1.2 ± 0.05 (6)	1.1 ± 0.04 (10)
Right adrenal	M	0.6 ± 0.04 (9)	0.8 ± 0.00 (9)**	0.8 ± 0.05 (9)**	0.9 ± 0.04 (10)***	0.8 ± 0.10 (9)*	0.8 ± 0.04 (9)**	0.9 ± 0.03 (9)***	0.5 ± 0.03 (6)	0.5 ± 0.12 (4)	0.4 ± 0.02 (10)#
	F	1.3 ± 0.08 (9)	1.6 ± 0.12 (9)	1.4 ± 0.00 (10)	1.6 ± 0.11 (9)*	1.5 ± 0.07 (8)	1.5 ± 0.05 (10)*	1.7 ± 0.09 (9)**	1.0 ± 0.04 (6)	1.1 ± 0.05 (6)	1.0 ± 0.05 (10)
Thymus	M	4.0 ± 0.40 (9)	3.8 ± 0.69 (10)	2.4 ± 0.42 (8)*	2.5 ± 0.30 (9)**	3.2 ± 0.39 (7)	2.8 ± 0.37 (9)*	2.6 ± 0.57 (7)*	3.5 ± 0.48 (6)	3.5 ± 0.60 (4)	3.9 ± 0.40 (10)
	F	4.8 ± 0.81 (7)	5.4 ± 0.93 (9)	4.9 ± 0.86 (10)	4.3 ± 0.42 (8)	4.5 ± 0.64 (8)	4.4 ± 0.57 (9)	3.8 ± 0.55 (8)	4.8 ± 0.41 (6)	7.5 ± 0.48 (6)##	5.6 ± 0.53 (10)
Spleen	M	15.4 ± 1.58 (10)	15.8 ± 0.66 (10)	14.7 ± 0.59 (9)	13.2 ± 0.44 (10)	17.6 ± 1.95 (9)	15.7 ± 0.41 (9)	15.8 ± 1.55 (10)	16.0 ± 0.74 (6)	15.7 ± 1.19 (4)	15.9 ± 0.95 (10)
	F	19.4 ± 1.10 (9)	18.0 ± 1.32 (10)	16.7 ± 0.63 (10)*	16.1 ± 0.45 (9)*	18.2 ± 1.05 (9)	15.5 ± 0.60 (10)**	16.6 ± 0.74 (10)*	16.6 ± 0.76 (6)	20.0 ± 0.74 (6)##	20.9 ± 1.35 (10)#
Liver	M	329.3 ± 5.09 (10)	340.5 ± 6.49 (10)	331.3 ± 7.62 (9)	373.0 ± 7.85 (10)***	363.8 ± 36.36 (9)	374.1 ± 13.96 (10)*	381.7 ± 13.18 (10)**	328.7 ± 6.62 (6)	354.2 ± 14.76 (4)	331.9 ± 8.90 (10)
	F	339.6 ± 6.58 (9)	366.1 ± 11.72 (10)	382.4 ± 11.35 (10)**	386.7 ± 15.10 (9)*	385.2 ± 15.15 (10)*	419.1 ± 13.67 (10)***	442.6 ± 10.21 (10)***	353.5 ± 13.87 (6)	354.6 ± 10.87 (6)	346.7 ± 5.21 (10)
Uterus	F	30.3 ± 2.95 (9)	22.7 ± 1.93 (10)*	20.9 ± 2.73 (10)*	18.2 ± 2.26 (9)**	23.3 ± 2.51 (9)	16.0 ± 1.58 (10)***	12.7 ± 0.66 (10)***	30.7 ± 4.79 (6)	20.3 ± 3.56 (6)	18.8 ± 2.02 (10)#

Organ weights were taken after 90-day exposure (90d) and 42-day recovery period following a 90-day exposure (90 + 42d). Organ weights are normalized to body weight and reported as $x10^{-4}$. Results represent mean ± standard error. The sample size is in parentheses. Difference from sham group at 90d: Significance: *, $p < 0.05$; **$p < 0.01$; ***$p < 0.001$. Difference from sham group at 90 + 42d: Significance: # $p < 0.05$; ##$p < 0.01$; ###$p < 0.001$. Abbreviations: M, male; F, female.

exposed male and female groups. Triglyceride levels showed the same general trend in the 3R4F- and THS2.2-exposed male and female groups compared with the sham groups (Table 6). There was no difference in cholesterol (both sexes) and triglycerides (male only) concentration between the 3R4F and THS2.2 groups; in female rats, the concentrations of triglycerides in the 3R4F groups were lower than those in the THS2.2 groups at the same nicotine exposure concentrations. The concentrations returned to basal levels similar to those in the sham group in the post-exposure recovery animals (Table 6).

Serum glucose concentrations were slightly lower in the male 3R4F_8 and 3R4F_23 groups relative to the sham group on day 90 (Table 6). No difference was observed compared with the male recovery groups. In female rats, blood glucose was lower in the 3R4F_23 group, and the levels returned to baseline in the recovery groups. Blood glucose was lower in both the male and female THS2.2_50 groups, compared with the sham group. The glucose concentrations returned to sham levels (female only) after the post-exposure recovery period. The remaining serum analytes showed either minor changes or no exposure effects (data not shown).

3.4.4. Clotting potential. The results from PT and APTT were used to determine the efficiency of extrinsic and intrinsic pathways of coagulation, respectively. In male rats, the measured PTs were either within or marginally above the reference range for this strain of rat (Lee et al., 2012). The PT data from female rats and APTT from both sexes were within the reference range for this strain (Lee et al., 2012). No significant difference was detected between the 3R4F and THS2.2 groups for both PT and APTT (data not shown).

3.4.5. Lung lavage and analysis. The degree of inflammation in the lungs caused by test atmosphere from 3R4F and THS2.2 was evaluated by the quantification of free lung cells and the profiling of cytokines present in BALF. Exposure to 3R4F in both male and female groups caused a concentration-dependent increase in total free lung cell count compared with sham, whereas only the female THS2.2_23 group showed statistically significant higher count (Tables 8 and 9). Among the free lung cells, the neutrophil and eosinophil cell counts were increased in a concentration-dependent manner in all 3R4F groups for both male and female rats compared with the sham groups, while no significant increase was noted in the THS2.2-exposed groups. The macrophage and lymphocyte counts showed a trend of increase in the male 3R4F-exposed groups, while no increase was noted in the THS2.2 groups (Tables 8 and 9). In females, macrophage and lymphocyte counts were increased in the 3R4F groups compared with the sham group, while no increase was noted in the THS2.2 groups, with the exception of a marginal increase in macrophage counts in the THS2.2_23 female group. In summary, the accumulation of inflammatory cells in the BALF of 3R4F-exposed rats was consistent with findings from previous studies (Fujimoto et al., 2015; Kogel et al., 2014; Piade et al., 2014). Low numbers of immune cells in rats exposed to THS2.2 aerosol are reflective of a low degree of pulmonary inflammation in the lung, and are consistent with lower concentrations of irritants in the aerosol of the THS2.2 test atmosphere, compared with 3R4F (Schaller et al., submitted (this issue)-a).

Multiple analyte profiling (RodentMAP™) was performed on BALF to quantify 60 analytes; 30 out of 60 analytes had at least 50% of values below the lower limit of quantification for all the OECD groups. Data from the quantifiable analytes are summarized in Fig. 2. Analytes with significant exposure effects can be summarized as follows: Exposure to 3R4F caused a concentration-

Table 11
Statistical significance difference in relative organ weights between animals exposed to aerosol from THS2.2 and cigarette smoke from 3R4F.

Parameter	Sex	90d			90 + 42d
		THS2.2_15 vs. 3R4F_15	THS2.2_23 vs. 3R4F_23	THS2.2_50 vs. 3R4F_23	THS2.2_50 vs. 3R4F_23
Lung, larynx, trachea	M	=	↓***	↓***	=
	F	=	↓***	↓***	↓*
Left adrenal	M	=	=	=	=
	F	=	=	=	=
Right adrenal	M	=	↓*	=	=
	F	=	=	=	=
Thymus	M	=	=	=	=
	F	=	=	=	↓*
Spleen	M	=	↑***	=	=
	F	=	=	=	=
Liver	M	=	=	=	=
	F	=	=	↑**	=
Uterus	F	=	=	↓*	=

Difference between groups: Significance: $^{*}p < 0.05$; $^{**}p < 0.01$; $^{***}p < 0.001$. Symbols, ↓ indicates response lower in THS2.2 relative to 3R4F; ↑ indicates response higher in THS2.2 relative to 3R4F; =indicates no difference. Abbreviations: M, male; F, female.

dependent increase in some inflammatory cytokines and factors associated with inflammation (e.g. M-CSF, MCP1, MDC, FGF9, and VEGFA) relative to sham, but the levels were not significantly higher in any of the THS2.2-exposed groups. The concentrations of other analytes (e.g. MIP-1β, MCP3, MPO and PAI-1), although increased in the THS2.2-exposed groups, were significantly lower when compared with the 3R4F_15 and 3R4F_23 groups of both sexes. At the end of the 42-day recovery period, the effects of 3R4F exposure on most of the previously upregulated analytes were reduced but still higher than those in the sham group (Fig. 2). The RodentMAP™ results are consistent with lowered numbers of inflammatory cells in the BALF collected from THS2.2-exposed rats.

3.5. Respiratory tract organs

Higher weights of lungs relative to body weight compared with sham were observed in the 3R4F-exposed animals, and to a lesser extent in THS2.2 and post-exposure groups (Tables 10 and 11). Higher relative weights of lungs (with trachea and larynx) are typical of smoke-exposed lungs (Gaworski et al., 1997, 1999; Vanscheeuwijck et al., 2002). Lower organ weights in the THS2.2 groups compared with 3R4F were consistent with reduced infiltration of inflammatory cells in the lung, and corroborated with the histopathological findings. Histopathological findings in 3R4F-exposed groups were consistent with published data (Coggins et al., 1980, 1989; Gaworski et al., 1997; Piade et al., 2014; Vanscheeuwijck et al., 2002). Histopathological evaluation of the lungs and other respiratory tract organs showed significantly lower severity scores in the THS2.2-exposed animals compared with 3R4F-exposed animals. The parameters listed in Table 12 are summarized here.

The nasal lesions observed predominantly in 3R4F-exposed rats included reserve cell hyperplasia of the respiratory epithelium, squamous epithelial metaplasia of the respiratory epithelium and olfactory epithelium, cornification of the metaplastic respiratory epithelium, presence of neutrophilic granulocytes, loss of goblet cells at the septum, atrophy of olfactory epithelium, loss of nerve bundles at the lamina propria of olfactory epithelium, and mixed inflammatory cells at the lamina propria of the olfactory epithelium. Severity scores observed in THS2.2-exposed animals were significantly lower than those in 3R4F-exposed groups (Table 12, Table 13). The incidences of the changes described above at nose level 2 to 4 were significantly lower in the THS2.2 groups, compared with the 3R4F groups. Being obligatory nose breathers, an exception was at the more sensitive nose level 1 of the rats (Renne et al., 2009), where the incidences of reserve cell hyperplasia, squamous cell metaplasia, and the loss of goblet cells do not differ between the 3R4F- and THS2.2-exposed groups. After the 42-day recovery period, the severity scores of many of the findings in the 3R4F-exposed groups were reduced. For the findings at nose level 1, the mean severity scores were still lower for the THS2.2_50 group, compared with the 3R4F_23 group after the 42-day recovery period.

Changes observed in the larynx in response to 3R4F exposure (moderate to high severity score) were significantly lower in THS2.2-exposed animals (low severity score); these changes included squamous epithelial metaplasia, cornification, and hyperplasia of the epithelium (Tables 12,13). While the incidences of the observed laryngeal changes were significantly lower in the THS2.2 groups compared with the 3R4F groups, only the incidence of hyperplasia at the lower medial region of the larynx was the same in the test and reference item groups. At 42 days post exposure, the severity and incidences of squamous epithelial metaplasia and the amount of cornification were reduced in all locations, exposure groups and sexes. Epithelial hyperplasia and squamous epithelial metaplasia at the laryngeal epithelia, the epithelial thickness measured at the floor of the larynx and at the lower medial region of the vocal cords, were larger in the 3R4F groups compared with the THS2.2 groups (Supplementary Tables 15,16). At 42 days post exposure, a reduction was observed in the epithelial thickness in the 3R4F- and THS2.2-exposed groups, but the epithelial thickness measured in the 3R4F_23 group was still greater than that in the THS2.2_50 group.

Histopathological findings, including reserve cell hyperplasia and goblet cell hyperplasia at the tracheal epithelium, were observed at the tracheal ring and bifurcation in response to 3R4F exposure (low severity score) but absent from THS2.2-exposed animals (Table 13). Both findings were reversed in the 3R4F 42-day post-exposure groups.

The severity scores for changes observed in the left lung in response to 3R4F exposure were moderate to high. The severity scores were significantly lower in THS2.2-exposed animals, where the changes were either of low severity score or absent (Table 13). The changes included the presence of macrophages with and without yellow pigmentation in the alveolar lumen, the presence of neutrophilic granulocytes in the alveolar lumen, and goblet cell hyperplasia at the main bronchus. Incidences of these findings were also significantly lower in the THS2.2-exposed animals. The severity scores of the findings were reduced in the post-exposure groups.

Table 12
Histopathological findings in the respiratory tract of male and female rats after 90-day inhalation period or 42-day recovery period following 90-day exposure to test atmosphere of the reference cigarette 3R4F, THS2.2, or air (sham).

Localization	Tissue type	Observation	Sex	90d							90 + 42d		
				Sham	3R4F_8	3R4F_15	3R4F_23	THS2.2_15	THS2.2_23	THS2.2_50	Sham	3R4F_23	THS2.2_50
Nose level 1	Respiratory epithelium	Reserve cell	M	0.5 ± 0.17 (5/10)	3.6 ± 0.16 (10/10)***	4.1 ± 0.10 (10/10)***	4.6 ± 0.16 (10/10)***	2.2 ± 0.36 (10/10)***	2.9 ± 0.10 (10/10)***	3.7 ± 0.15 (10/10)***	0.5 ± 0.22 (3/6)	2.6 ± 0.40 (5/5)##	1.3 ± 0.26 (8/10)
		hyperplasia	F	0.1 ± 0.10 (1/10)	3.9 ± 0.18 (10/10)***	4.1 ± 0.10 (10/10)***	4.8 ± 0.15 (9/9)***	2.0 ± 0.21 (10/10)***	2.6 ± 0.16 (10/10)***	3.6 ± 0.16 (10/10)***	0.0 ± 0.00 (0/6)	2.5 ± 0.22 (6/6)##	1.2 ± 0.28 (7/9)##
		Squamous epithelial	M	0.0 ± 0.00 (0/10)	2.5 ± 0.17 (10/10)***	3.4 ± 0.16 (10/10)***	4.0 ± 0.00 (10/10)***	0.7 ± 0.40 (4/10)*	1.5 ± 0.17 (10/10)***	2.9 ± 0.23 (10/10)***	0.2 ± 0.17 (1/6)	4.0 ± 0.00 (5/5)##	0.8 ± 0.36 (4/10)
		metaplasia	F	0.0 ± 0.00 (0/10)	3.0 ± 0.00 (10/10)***	3.9 ± 0.10 (10/10)***	4.0 ± 0.00 (9/9)***	1.0 ± 0.21 (8/10)***	1.5 ± 0.17 (10/10)***	3.2 ± 0.25 (10/10)***	0.0 ± 0.00 (0/6)	4.0 ± 0.00 (6/6)###	1.3 ± 0.41 (6/9)#
		Amount of	M	0.0 ± 0.00 (0/10)	0.0 ± 0.00 (0/10)	1.0 ± 0.39 (5/10)*	2.8 ± 0.29 (10/10)***	0.4 ± 0.40 (1/10)	0.0 ± 0.00 (0/10)	0.4 ± 0.31 (2/10)	0.0 ± 0.00 (0/6)	2.2 ± 0.37 (5/5)##	0.0 ± 0.00 (0/10)
		cornification	F	0.0 ± 0.00 (0/10)	0.0 ± 0.00 (0/10)	1.2 ± 0.44 (6/10)**	3.9 ± 0.11 (9/9)***	0.0 ± 0.00 (0/10)	0.0 ± 0.00 (0/10)	1.0 ± 0.42 (4/10)*	0.0 ± 0.00 (0/6)	2.5 ± 0.22 (6/6)##	0.0 ± 0.00 (0/9)
		Loss of goblet cells	M	0.4 ± 0.22 (3/10)	3.1 ± 0.18 (10/10)***	4.5 ± 0.17 (10/10)***	4.6 ± 0.16 (10/10)***	1.9 ± 0.46 (9/10)**	2.0 ± 0.26 (10/10)***	3.4 ± 0.16 (10/10)***	0.8 ± 0.31 (4/6)	2.2 ± 0.66 (4/5)	1.4 ± 0.31 (8/10)
		(septum)	F	0.3 ± 0.17 (3/9)	3.8 ± 0.20 (10/10)***	4.6 ± 0.16 (10/10)***	4.7 ± 0.17 (9/9)***	1.3 ± 0.26 (9/10)**	2.1 ± 0.23 (10/10)***	3.9 ± 0.10 (10/10)***	0.2 ± 0.17 (1/6)	3.7 ± 0.21 (6/6)##	1.4 ± 0.44 (7/9)#
		Neutrophilic	M	0.1 ± 0.10 (1/10)	0.3 ± 0.15 (3/10)	0.5 ± 0.22 (4/10)	0.8 ± 0.29 (5/10)*	0.0 ± 0.00 (0/10)	0.0 ± 0.00 (0/10)	0.1 ± 0.10 (1/10)	0.0 ± 0.00 (0/6)	0.2 ± 0.22 (1/5)	0.1 ± 0.1 (1/10)
		granulocytes	F	0.0 ± 0.00 (0/10)	0.2 ± 0.13 (2/10)	1.0 ± 0.33 (5/10)*	1.2 ± 0.28 (7/9)***	0.0 ± 0.00 (0/10)	0.0 ± 0.00 (0/10)	0.4 ± 0.16 (4/10)*	0.0 ± 0.00 (0/6)	0.8 ± 0.31 (4/6)#	0.0 ± 0.00 (0/9)
Nose level 2	Respiratory epithelium	Reserve cell	M	0.0 ± 0.00 (0/10)	0.6 ± 0.18 (5/9)**	2.9 ± 0.23 (10/10)***	3.8 ± 0.13 (10/10)***	0.2 ± 0.13 (2/10)	0.1 ± 0.10 (1/10)	0.2 ± 0.13 (2/10)	0.0 ± 0.00 (0/6)	0.8 ± 0.20 (4/5)##	0.1 ± 0.13 (1/8)
		hyperplasia	F	0.3 ± 0.15 (3/10)	0.7 ± 0.21 (6/10)	3.2 ± 0.13 (10/10)***	4.4 ± 0.18 (9/9)***	0.1 ± 0.10 (1/10)	0.2 ± 0.15 (2/9)	0.7 ± 0.26 (5/10)	0.0 ± 0.00 (0/6)	1.0 ± 0.26 (5/6)##	0.1 ± 0.10 (1/10)
		Squamous epithelial	M	0.0 ± 0.00 (0/10)	0.0 ± 0.00 (0/9)	1.2 ± 0.33 (7/10)**	2.2 ± 0.20 (10/10)***	0.0 ± 0.00 (0/10)	0.0 ± 0.00 (0/10)	0.0 ± 0.00 (0/10)	0.0 ± 0.00 (0/6)	0.0 ± 0.00 (0/5)	0.0 ± 0.00 (0/8)
		metaplasia	F	0.0 ± 0.00 (0/10)	0.0 ± 0.00 (0/10)	1.1 ± 0.31 (7/10)**	2.8 ± 0.15 (9/9)***	0.0 ± 0.00 (0/10)	0.0 ± 0.00 (0/9)	0.0 ± 0.00 (0/10)	0.0 ± 0.00 (0/6)	0.0 ± 0.00 (0/6)	0.0 ± 0.00 (0/10)
	Olfactorepithelium	Atrophy	M	0.0 ± 0.00 (0/10)	0.0 ± 0.00 (0/9)	2.0 ± 0.69 (5/9)**	4.5 ± 0.17 (10/10)***	0.0 ± 0.00 (0/10)	0.0 ± 0.00 (0/9)	0.1 ± 0.10 (1/10)	0.2 ± 0.17 (1/6)	3.0 ± 0.77 (4/5)#	0.5 ± 0.50 (1/8)
			F	0.0 ± 0.00 (0/10)	0.4 ± 0.31 (2/10)	3.6 ± 0.22 (10/10)***	4.9 ± 0.11 (9/9)***	0.0 ± 0.00 (0/10)	0.0 ± 0.00 (0/10)	0.7 ± 0.26 (5/10)*	0.0 ± 0.00 (0/6)	3.2 ± 0.17 (6/6)##	0.2 ± 0.20 (1/10)
		Squamous epithelial	M	0.0 ± 0.00 (0/10)	0.0 ± 0.00 (0/9)	1.0 ± 0.41 (4/9)*	2.1 ± 0.38 (8/10)***	0.0 ± 0.00 (0/10)	0.0 ± 0.00 (0/9)	0.0 ± 0.00 (0/10)	0.0 ± 0.00 (0/6)	1.2 ± 0.37 (4/5)#	0.1 ± 0.13 (1/8)
		metaplasia	F	0.0 ± 0.00 (0/10)	0.0 ± 0.00 (0/10)	2.6 ± 0.22 (10/10)***	2.8 ± 0.40 (8/9)***	0.0 ± 0.00 (0/10)	0.0 ± 0.00 (0/10)	0.0 ± 0.00 (0/10)	0.0 ± 0.00 (0/6)	0.7 ± 0.33 (3/6)	0.0 ± 0.00 (0/10)
	Lamina propria	Loss of nerve bundles	M	0.0 ± 0.00 (0/10)	0.0 ± 0.00 (0/9)	1.6 ± 0.58 (5/9)**	4.3 ± 0.52 (9/10)***	0.0 ± 0.00 (0/10)	0.0 ± 0.00 (0/9)	0.0 ± 0.00 (0/10)	0.0 ± 0.00 (0/6)	4.0 ± 1.00 (4/5)##	0.6 ± 0.63 (1/8)
			F	0.0 ± 0.00 (0/10)	0.3 ± 0.30 (1/10)	4.0 ± 0.52 (9/10)***	5.0 ± 0.00 (9/9)***	0.0 ± 0.00 (0/10)	0.0 ± 0.00 (0/10)	0.0 ± 0.00 (0/10)	0.0 ± 0.00 (0/6)	4.8 ± 0.17 (6/6)##	0.3 ± 0.30 (1/10)
		Mixed inflammatory	M	0.0 ± 0.00 (0/10)	0.0 ± 0.00 (0/9)	0.2 ± 0.22 (1/9)	1.3 ± 0.21 (9/10)***	0.0 ± 0.00 (0/10)	0.0 ± 0.00 (0/9)	0.0 ± 0.00 (0/10)	0.0 ± 0.00 (0/6)	0.8 ± 0.20 (4/5)##	0.1 ± 0.13 (1/8)
		cell infiltrates	F	0.0 ± 0.00 (0/10)	0.0 ± 0.00 (0/10)	0.4 ± 0.22 (3/10)	1.8 ± 0.22 (9/9)***	0.0 ± 0.00 (0/10)	0.0 ± 0.00 (0/10)	0.0 ± 0.00 (0/10)	0.0 ± 0.00 (0/6)	1.2 ± 0.17 (6/6)##	0.0 ± 0.00 (0/10)
Nose level 3	Olfactory epithelium	Atrophy	M	0.0 ± 0.00 (0/10)	0.0 ± 0.00 (0/10)	0.7 ± 0.47 (2/9)	4.0 ± 0.00 (10/10)***	0.0 ± 0.00 (0/8)	0.0 ± 0.00 (0/10)	0.0 ± 0.00 (0/10)	0.0 ± 0.00 (0/6)	3.2 ± 0.80 (4/5)##	0.0 ± 0.00 (0/10)
			F	0.0 ± 0.00 (0/10)	0.0 ± 0.00 (0/10)	3.4 ± 0.43 (9/10)***	4.0 ± 0.00 (9/9)***	0.0 ± 0.00 (0/10)	0.0 ± 0.00 (0/10)	0.0 ± 0.00 (0/10)	0.0 ± 0.00 (0/6)	3.2 ± 0.65 (5/6)##	0.0 ± 0.00 (0/10)
		Squamous epithelial	M	0.0 ± 0.00 (0/10)	0.0 ± 0.00 (0/10)	0.4 ± 0.29 (2/9)	3.1 ± 0.10 (10/10)***	0.0 ± 0.00 (0/8)	0.0 ± 0.00 (0/10)	0.0 ± 0.00 (0/10)	0.0 ± 0.00 (0/6)	1.0 ± 0.32 (4/5)#	0.0 ± 0.00 (0/10)
		metaplasia	F	0.0 ± 0.00 (0/10)	0.0 ± 0.00 (0/10)	2.5 ± 0.34 (9/10)***	3.0 ± 0.00 (9/9)***	0.0 ± 0.00 (0/10)	0.0 ± 0.00 (0/10)	0.0 ± 0.00 (0/10)	0.0 ± 0.00 (0/6)	0.8 ± 0.17 (5/6)##	0.0 ± 0.00 (0/10)
	Lamina propria	Loss of nerve bundles	M	0.0 ± 0.00 (0/10)	0.0 ± 0.00 (0/10)	0.4 ± 0.29 (2/9)	3.7 ± 0.21 (10/10)***	0.0 ± 0.00 (0/8)	0.0 ± 0.00 (0/10)	0.0 ± 0.00 (0/10)	0.0 ± 0.00 (0/6)	3.2 ± 0.80 (4/5)##	0.0 ± 0.00 (0/10)
			F	0.0 ± 0.00 (0/10)	0.0 ± 0.00 (0/10)	3.4 ± 0.43 (9/10)***	4.0 ± 0.00 (9/9)***	0.0 ± 0.00 (0/10)	0.0 ± 0.00 (0/10)	0.0 ± 0.00 (0/10)	0.0 ± 0.00 (0/6)	3.2 ± 0.65 (5/6)##	0.0 ± 0.00 (0/10)
Nose level 4	Olfactory epithelium	Atrophy	M	0.0 ± 0.00 (0/10)	0.0 ± 0.00 (0/10)	0.2 ± 0.22 (1/9)	3.3 ± 0.40 (9/10)***	0.0 ± 0.00 (0/10)	0.0 ± 0.00 (0/10)	0.0 ± 0.00 (0/10)	0.0 ± 0.00 (0/6)	0.2 ± 0.20 (1/5)	0.0 ± 0.00 (0/10)
			F	0.0 ± 0.00 (0/10)	0.0 ± 0.00 (0/10)	2.4 ± 0.34 (9/9)***	3.0 ± 0.29 (9/9)***	0.0 ± 0.00 (0/10)	0.0 ± 0.00 (0/9)	0.0 ± 0.00 (0/10)	0.0 ± 0.00 (0/6)	0.8 ± 0.31 (4/6)#	0.0 ± 0.00 (0/10)
		Squamous epithelial	M	0.0 ± 0.00 (0/10)	0.0 ± 0.00 (0/10)	0.1 ± 0.11 (1/9)	2.9 ± 0.35 (9/10)***	0.0 ± 0.00 (0/10)	0.0 ± 0.00 (0/10)	0.0 ± 0.00 (0/10)	0.0 ± 0.00 (0/6)	0.0 ± 0.00 (0/5)	0.0 ± 0.00 (0/10)
		metaplasia	F	0.0 ± 0.00 (0/10)	0.0 ± 0.00 (0/10)	1.8 ± 0.43 (7/9)***	2.0 ± 0.37 (8/9)***	0.0 ± 0.00 (0/10)	0.0 ± 0.00 (0/9)	0.0 ± 0.00 (0/10)	0.0 ± 0.00 (0/6)	0.0 ± 0.00 (0/6)	0.0 ± 0.00 (0/10)
	Lamina propria	Loss of nerve bundles	M	0.0 ± 0.00 (0/10)	0.0 ± 0.00 (0/10)	0.2 ± 0.22 (1/9)	3.0 ± 0.37 (9/10)***	0.0 ± 0.00 (0/10)	0.0 ± 0.00 (0/10)	0.0 ± 0.00 (0/10)	0.0 ± 0.00 (0/6)	0.0 ± 0.00 (0/5)	0.0 ± 0.00 (0/10)
			F	0.0 ± 0.00 (0/10)	0.0 ± 0.00 (0/10)	1.8 ± 0.49 (6/9)**	2.7 ± 0.37 (8/9)***	0.0 ± 0.00 (0/10)	0.0 ± 0.00 (0/9)	0.0 ± 0.00 (0/10)	0.0 ± 0.00 (0/6)	0.0 ± 0.00 (0/6)	0.0 ± 0.00 (0/10)
Larynx	Ventral depression	Squamous epithelial	M	0.0 ± 0.00 (0/10)	2.1 ± 0.28 (10/10)***	4.2 ± 0.33 (10/10)***	4.3 ± 0.41 (8/8)***	0.0 ± 0.00 (0/10)	0.3 ± 0.16 (2/8)	0.4 ± 0.24 (3/9)	0.0 ± 0.00 (0/6)	0.4 ± 0.24 (2/5)	0.0 ± 0.00 (0/10)
		metaplasia	F	0.0 ± 0.00 (0/10)	4.1 ± 0.46 (10/10)***	4.8 ± 0.13 (10/10)***	3.9 ± 0.61 (8/9)***	0.5 ± 0.50 (1/10)	0.0 ± 0.00 (0/9)	0.8 ± 0.42 (4/10)*	0.0 ± 0.00 (0/6)	0.0 ± 0.00 (0/6)	0.0 ± 0.00 (0/10)
		Amount of	M	0.0 ± 0.00 (0/10)	0.0 ± 0.00 (0/10)	2.8 ± 0.73 (7/10)**	3.1 ± 0.83 (6/8)**	0.0 ± 0.00 (0/10)	0.0 ± 0.00 (0/8)	0.0 ± 0.00 (0/9)	0.0 ± 0.00 (0/6)	0.0 ± 0.00 (0/5)	0.0 ± 0.00 (0/10)
		cornification	F	0.0 ± 0.00 (0/10)	3.3 ± 0.72 (8/10)***	4.0 ± 0.67 (8/10)***	3.3 ± 0.83 (6/9)**	0.5 ± 0.50 (1/10)	0.0 ± 0.00 (0/9)	0.0 ± 0.00 (0/10)	0.0 ± 0.00 (0/6)	0.0 ± 0.00 (0/6)	0.0 ± 0.00 (0/10)
	Lower medial region	Hyperplasia	M	0.3 ± 0.21 (2/10)	3.6 ± 0.18 (9/9)***	4.1 ± 0.11 (9/9)***	4.1 ± 0.13 (8/8)***	1.6 ± 0.18 (9/9)**	2.3 ± 0.26 (10/10)***	2.8 ± 0.15 (9/9)***	0.5 ± 0.50 (1/6)	2.6 ± 0.51 (5/5)#	1.0 ± 0.17 (8/9)#
			F	0.1 ± 0.11 (1/9)	4.1 ± 0.10 (10/10)***	4.3 ± 0.15 (10/10)***	4.5 ± 0.19 (8/8)***	1.8 ± 0.43 (8/9)**	2.3 ± 0.26 (10/10)***	3.2 ± 0.25 (10/10)***	0.0 ± 0.00 (0/6)	3.2 ± 0.20 (5/5)##	0.5 ± 0.22 (4/10)
		Amount of	M	0.0 ± 0.00 (0/10)	1.7 ± 0.55 (5/9)**	3.7 ± 0.24 (9/9)***	3.4 ± 0.53 (7/8)***	0.0 ± 0.00 (0/9)	0.4 ± 0.31 (2/10)	0.0 ± 0.00 (0/9)	0.0 ± 0.00 (0/6)	0.2 ± 0.20 (1/5)	0.0 ± 0.00 (0/9)
		cornification	F	0.0 ± 0.00 (0/9)	3.0 ± 0.47 (9/10)***	4.3 ± 0.21 (10/10)***	4.6 ± 0.38 (8/8)***	0.1 ± 0.11 (1/9)	0.0 ± 0.00 (0/10)	0.1 ± 0.10 (1/10)	0.0 ± 0.00 (0/6)	2.0 ± 0.71 (4/5)#	0.0 ± 0.00 (0/10)
	Upper medial region	Squamous epithelial	M	0.0 ± 0.00 (0/9)	1.9 ± 0.45 (7/9)**	3.9 ± 0.39 (9/9)***	3.9 ± 0.30 (8/8)***	0.2 ± 0.22 (1/9)	0.6 ± 0.40 (3/10)	1.2 ± 0.49 (5/9)*	0.0 ± 0.00 (0/6)	0.2 ± 0.20 (1/5)	0.3 ± 0.25 (1/8)
		metaplasia	F	0.0 ± 0.00 (0/9)	3.5 ± 0.45 (9/10)***	4.6 ± 0.16 (10/10)***	4.9 ± 0.13 (8/8)***	0.9 ± 0.51 (3/9)	0.9 ± 0.41 (5/10)*	1.4 ± 0.60 (5/10)*	0.0 ± 0.00 (0/6)	0.4 ± 0.40 (1/5)	0.0 ± 0.00 (0/10)
		Amount of	M	0.0 ± 0.00 (0/9)	0.0 ± 0.00 (0/9)	0.4 ± 0.29 (2/9)	1.1 ± 0.74 (2/8)	0.0 ± 0.00 (0/9)	0.0 ± 0.00 (0/10)	0.0 ± 0.00 (0/9)	0.0 ± 0.00 (0/6)	0.0 ± 0.00 (0/5)	0.0 ± 0.00 (0/8)
		cornification	F	0.0 ± 0.00 (0/9)	0.5 ± 0.50 (1/10)	1.0 ± 0.56 (3/10)	3.9 ± 0.64 (7/8)***	0.0 ± 0.00 (0/9)	0.0 ± 0.00 (0/10)	0.5 ± 0.50 (1/10)	0.0 ± 0.00 (0/6)	0.0 ± 0.00 (0/5)	0.0 ± 0.00 (0/10)
	Vocal folds, pseudostratified epithelium	Squamous epithelial	M	0.0 ± 0.00 (0/10)	0.0 ± 0.00 (0/9)	0.0 ± 0.00 (0/8)	0.4 ± 0.24 (3/9)	0.0 ± 0.00 (0/10)	0.0 ± 0.00 (0/10)	0.0 ± 0.00 (0/8)	0.0 ± 0.00 (0/6)	0.0 ± 0.00 (0/5)	0.0 ± 0.00 (0/10)
		metaplasia	F	0.0 ± 0.00 (0/10)	0.0 ± 0.00 (0/9)	0.0 ± 0.00 (0/9)	0.6 ± 0.50 (2/8)	0.0 ± 0.00 (0/9)	0.0 ± 0.00 (0/10)	0.0 ± 0.00 (0/9)	0.0 ± 0.00 (0/5)	0.0 ± 0.00 (0/5)	0.0 ± 0.00 (0/9)
	Vocal folds, squamous epithelium	Hyperplasia	M	0.1 ± 0.10 (1/10)	2.4 ± 0.34 (10/10)***	3.8 ± 0.22 (9/9)***	4.0 ± 0.00 (10/10)***	0.7 ± 0.26 (5/10)*	1.1 ± 0.23 (8/10)**	1.4 ± 0.38 (7/9)**	0.8 ± 0.48 (2/4)	1.8 ± 0.49 (4/5)	0.9 ± 0.45 (4/9)
			F	0.0 ± 0.00 (0/10)	3.2 ± 0.28 (9/9)***	3.9 ± 0.10 (10/10)***	3.5 ± 0.53 (7/8)***	1.5 ± 0.50 (7/10)**	1.1 ± 0.38 (7/10)**	2.1 ± 0.38 (9/10)***	0.0 ± 0.00 (0/6)	2.2 ± 0.58 (4/5)#	0.4 ± 0.22 (3/10)
		Amount of	M	0.0 ± 0.00 (0/10)	1.2 ± 0.39 (6/10)**	2.4 ± 0.53 (8/9)***	3.9 ± 0.31 (10/10)***	0.0 ± 0.00 (0/10)	0.1 ± 0.10 (1/10)	0.4 ± 0.29 (2/9)	0.0 ± 0.00 (0/4)	0.0 ± 0.00 (0/5)	0.3 ± 0.33 (1/9)
		cornification	F	0.0 ± 0.00 (0/10)	1.6 ± 0.50 (6/9)**	4.1 ± 0.23 (10/10)***	3.9 ± 0.61 (7/8)***	0.8 ± 0.51 (3/10)	0.3 ± 0.30 (1/10)	0.5 ± 0.27 (3/10)	0.0 ± 0.00 (0/6)	1.6 ± 0.40 (4/5)##	0.1 ± 0.10 (1/10)
	Bifurcation	Squamous epithelial	M	0.0 ± 0.00 (0/10)	0.0 ± 0.00 (0/9)	0.1 ± 0.10 (1/10)	0.4 ± 0.16 (4/10)*	0.1 ± 0.10 (1/10)	0.0 ± 0.00 (0/9)	0.1 ± 0.10 (1/10)	0.0 ± 0.00 (0/6)	0.0 ± 0.00 (0/4)	0.0 ± 0.00 (0/9)
		metaplasia	F	0.0 ± 0.00 (0/9)	0.0 ± 0.00 (0/10)	0.0 ± 0.00 (0/8)	0.8 ± 0.48 (3/6)*	0.0 ± 0.00 (0/10)	0.0 ± 0.00 (0/10)	0.1 ± 0.10 (1/10)	0.0 ± 0.00 (0/6)	0.0 ± 0.00 (0/6)	0.0 ± 0.00 (0/10)
		Goblet cell hyperplasia	M	0.0 ± 0.00 (0/10)	0.2 ± 0.15 (2/9)	0.7 ± 0.26 (5/10)*	1.1 ± 0.23 (8/10)***	0.0 ± 0.00 (0/10)	0.1 ± 0.10 (1/10)	0.0 ± 0.00 (0/10)	0.0 ± 0.00 (0/6)	0.0 ± 0.00 (0/5)	0.0 ± 0.00 (0/10)
			F	0.1 ± 0.11 (1/9)	0.3 ± 0.21 (2/10)	0.1 ± 0.11 (1/9)	0.6 ± 0.38 (3/8)	0.2 ± 0.20 (1/10)	0.0 ± 0.00 (0/10)	0.0 ± 0.00 (0/10)	0.0 ± 0.00 (0/6)	0.2 ± 0.17 (1/6)	0.0 ± 0.00 (0/10)
Left lung	Alveolar lumen	Macrophages without	M	1.4 ± 0.22 (10/10)	2.0 ± 0.21 (10/10)*	3.1 ± 0.18 (10/10)***	3.4 ± 0.16 (10/10)***	0.8 ± 0.20 (7/10)	0.9 ± 0.31 (6/10)	1.4 ± 0.27 (9/10)	0.5 ± 0.22 (3/6)	1.0 ± 0.00 (5/5)	0.8 ± 0.25 (6/10)
		pigmentation	F	0.7 ± 0.15 (7/10)	2.7 ± 0.15 (10/10)***	2.8 ± 0.20 (10/10)***	3.4 ± 0.18 (9/9)***	0.9 ± 0.18 (8/10)	0.7 ± 0.21 (6/10)	1.5 ± 0.17 (10/10)**	0.8 ± 0.31 (4/6)	1.3 ± 0.21 (6/6)	0.5 ± 0.17 (5/10)
		Macrophages with	M	0.0 ± 0.00 (0/10)	0.9 ± 0.31 (5/10)*	2.7 ± 0.30 (10/10)***	3.4 ± 0.22 (10/10)***	0.1 ± 0.10 (1/10)	0.3 ± 0.21 (2/10)	0.7 ± 0.40 (3/10)	0.2 ± 0.17 (1/6)	1.4 ± 0.24 (5/5)##	0.2 ± 0.13 (2/10)
		pigmentation (yellow)	F	0.0 ± 0.00 (0/10)	1.5 ± 0.31 (8/10)***	2.2 ± 0.29 (9/10)***	3.6 ± 0.18 (9/9)***	0.1 ± 0.10 (1/10)	0.0 ± 0.00 (0/10)	0.0 ± 0.00 (0/10)	0.0 ± 0.00 (0/6)	2.3 ± 0.21 (6/6)##	0.3 ± 0.15 (3/10)
		Neutrophilic	M	0.6 ± 0.40 (3/10)	0.3 ± 0.15 (3/10)	1.0 ± 0.26 (7/10)	1.2 ± 0.20 (9/10)*	0.0 ± 0.00 (0/10)	0.4 ± 0.16 (4/10)	0.5 ± 0.27 (3/10)	0.0 ± 0.00 (0/6)	0.0 ± 0.00 (0/5)	0.0 ± 0.00 (0/10)
		granulocytes	F	0.2 ± 0.13 (2/10)	0.6 ± 0.22 (5/10)	1.2 ± 0.25 (8/10)**	1.6 ± 0.18 (9/9)***	0.2 ± 0.13 (2/10)	0.3 ± 0.30 (1/10)	0.1 ± 0.10 (1/10)	0.0 ± 0.00 (0/6)	0.0 ± 0.00 (0/6)	0.0 ± 0.00 (0/10)
	Main bronchus	Goblet cell hyperplasia	M	0.5 ± 0.27 (3/8)	1.7 ± 0.40 (10/10)*	3.2 ± 0.36 (9/9)***	4.8 ± 0.15 (9/9)***	0.4 ± 0.44 (1/9)	0.8 ± 0.57 (2/9)	0.5 ± 0.19 (4/8)	0.0 ± 0.00 (0/5)	1.0 ± 0.45 (3/5)	0.3 ± 0.25 (1/8)
			F	0.4 ± 0.22 (3/10)	2.1 ± 0.64 (7/10)*	3.2 ± 0.46 (9/9)***	4.0 ± 0.24 (9/9)***	0.8 ± 0.33 (5/10)	0.2 ± 0.13 (2/10)	0.8 ± 0.39 (5/10)	0.0 ± 0.00 (0/5)	0.8 ± 0.31 (4/6)#	0.0 ± 0.00 (0/10)

Histopathological evaluation was performed after 90-day exposure (90d) and 42-day recovery following a 90-day exposure period (90 + 42d). Results represent mean score ±standard error; incidence and sample size are in parentheses. Difference from sham group at 90d: Significance: *$p < 0.05$; **$p < 0.01$; ***$p < 0.001$. Difference from sham group at 90 + 42d: Significance: #$p < 0.05$; ##$p < 0.01$; ###$p < 0.001$. Abbreviations: M, male; F, female.

3.6. Non-respiratory tract organs

Most findings in non-respiratory tract organs were incidental, did not reach statistical significance in comparison to control groups, and were considered normal background levels for Sprague Dawley rats. Even though the mean myeloid: erythroid cell ratios in the bone marrow of the male 3R4F_23 and THS2.2_50 groups were showing trend of increased compared with the sham group, the mean ratio was not statistically significant and did not differ between the 3R4F and THS2.2 groups; the ratios were within the expected physiological range (data not shown). Lower relative thymus weights were observed in the 3R4F- and THS2.2-exposed groups relative to sham (Table 10). The organ weight effect was correlated with mild to moderate thymus atrophy in the 3R4F- and THS2.2-exposed groups (Table 14). In general, the magnitude of the effect did not differ between the 3R4F- and THS2.2-exposed groups. Higher relative adrenal gland weights, indicative of a stress response (Coggins et al., 1989; Everds et al., 2013; Gaworski et al., 2009), were observed in both the 3R4F- and THS2.2-exposed animals compared with the sham group; this finding was reversed at the end of the post-exposure recovery period (Table 10). The relative weights of adrenal glands were similar between the 3R4F- and THS2.2-exposed groups, with the exception of the incidental lower right adrenal gland weights in THS2.2_23 males, compared with the 3R4F_23 group (Table 11). No consistent exposure-related histopathological changes were observed in the adrenal glands (data not shown). Also consistent with the stress response in exposed rats, a reduction in relative spleen weights was seen in both the 3R4F- and THS2.2-exposed female groups relative to sham, which was reversed in the post-exposure recovery groups. The relative weights of the spleen did not differ between the THS2.2 and 3R4F groups at the same nicotine exposure concentrations. Other than reduced yellow pigmentation in the red pulp in the female 3R4F_8, 3R4F_15, THS2.2_23, and THS2.2_50 groups, no other statistically significant histopathological findings were found (Table 14). The relative weights of the livers were higher in the male 3R4F_23 and THS2.2_23 and THS2.2_50 groups when compared with the sham group. The liver weights were higher in the female 3R4F_15 and 3R4F_23 groups and in all THS2.2 groups compared with the sham (Table 10). In female rats, the relative liver weights were higher in the THS2.2_50 group but not in the THS2.2_23 compared with the 3R4F_23 group (Table 11). An increase in the severity score and incidence of cytoplasmic vacuolization was observed in the hepatocytes of the THS2.2_23 and THS2.2_50 female groups compared with the sham (Table 14). However, when compared with the 3R4F groups, no concentration-dependent difference was found. Both severity score and incidence of cytoplasmic vacuolization in the liver reverted back to baseline levels after the 42 days' recovery period.

An aerosol-induced reduction in relative uterus weights was seen in both the 3R4F- and THS2.2-exposed female groups, and was reversed in the post-exposure recovery groups (Table 10). The relative uterus weights did not differ between the THS2.2 and 3R4F groups at the same nicotine concentrations (Table 11). A lower level of eosinophilic granulocytes in the stroma of the uterus was found in the 3R4F_15, 3R4F_23, THS2.2_23, and THS2.2_50 groups, with no differences observed between the test and reference groups. No other structural changes to uterine cells were found (Table 14).

3.7. Transcriptomics

Gene expression changes in RNE and lung tissue of 3R4F- and THS 2.2-exposed male rats after 90 days of exposure or after a 42-day recovery period were compared with their respective sham exposed group. The amplitude (expressed as negative log-fold change) and statistical significance of gene expression changes are shown in volcano plots (Fig. 3).

After 90 days of exposure, the number of differentially expressed genes in the RNE and in the lung tissue increased with increasing 3R4F smoke concentration in male rats, and to a lesser extent in the THS 2.2-exposed rats. No differentially expressed genes were detected above the applied threshold of false discovery rate (FDR) corrected p-value < 0.05 in the RNE and lung tissues of the THS2.2-exposed animals. After the 42-day recovery period, the observed effects in male rats were generally lower than in the 90-day exposure groups, with only a few differentially expressed genes in the RNE and lung tissues of the 3R4F groups. However, it should be noted that despite not reaching statistical significance, some genes showed high fold changes in expression in 3R4F_15 and 3R4F_23 post-exposure groups that were not seen in the THS2.2_50 post-exposure groups (see volcano plots in Fig. 3).

A heatmap was generated to obtain an overview of the overlap of differentially expressed genes between the groups (Supplementary Fig. 2). The visualization of the changes in transcriptional profiles provided by a heatmap offers the advantage that each gene which was significantly differentially expressed in one group could be compared with its fold change in the other groups. The heatmap shows that differential gene expression (fold change) in the RNE of male rats increased steeply with the highest 3R4F concentration, whereas the differential gene expression in lung tissue increased more gradually with increasing 3R4F concentration. In both tissues, the amplitude of change of the differentially expressed genes was clearly lower in the THS2.2-exposed groups, compared with the 3R4F-exposed groups. Even though THS2.2 exposure induced expression of some genes compared with the sham group, the fold change in expression did not reach statistical significance.

To examine which biological processes were affected by 3R4F and THS2.2 exposure in the RNE and in the lung tissue of male rats, the previously described network models reflecting the biological processes that are known to be perturbed by MS were used (Boue et al., 2015; Gebel et al., 2013; Schlage et al., 2011; Westra et al., 2011, 2013). The perturbation of those network models can be qualitatively assessed and mathematically quantified (Martin et al., 2014). As shown in Fig. 4, the affected biological processes in the RNE follow a steep exposure concentration-dependent increase in 3R4F-exposed groups after 90 days of exposure. The star plots in Fig. 4 show the biological processes scaled for their relative contribution to the overall affected network. The main affected biological processes in the 3R4F_23 group included the inflammatory processes, the cell fate processes, the tissue repair and angiogenesis processes, and cell stress processes. Only minimal network perturbation was detectable in the THS2.2-exposed groups. After the 42-day recovery period, most of the affected biological processes were still detectable in the 3R4F groups, even though obvious attenuation of the affected biological processes was observed, including the inflammatory and cell fate processes.

In the lung tissue, a strong effect on biological processes was observed following exposure to 3R4F. The inflammatory processes showed the greatest modifications in the 3R4F_23 group following a 90-day exposure. Other major perturbed processes in the 3R4F_23 group included the cell fate processes, tissue repair and angiogenesis, and cell stress processes (Fig. 4). In contrast, much weaker network perturbations were evident following THS2.2 exposure, which mainly showed perturbation of the inflammatory processes. The affected biological processes in the 90-day exposed 3R4F groups were also detectable after the 42-day recovery period. The extent to which the inflammation processes were affected was similar in the 3R4F post-exposure groups, compared with the 90-day exposed group. The extent of the effect on other perturbed networks was either small or none in the 3R4F post-exposure groups, compared with the 90-day exposed group. In contrast,

attenuation of the networks' perturbation was observed in the THS2.2 recovery groups. In summary, the transcriptomics analysis further supports an overall reduced biological impact of THS2.2 exposure on the nasal epithelium and lung tissue compared with 3R4F.

4. Discussion

A 90-day inhalation study was conducted to compare the sub-chronic inhalation toxicity in Sprague Dawley rats exposed to the aerosol from the MRTP THS2.2 and the 3R4F reference cigarette. Ninety-day inhalation studies conducted according to OECD Test Guideline 413 are a commonly used approach to assess general toxicity following inhalation exposure to MS from cigarettes or to other aerosols (Moennikes et al., 2008; Piade et al., 2014; Terpstra et al., 2003; Vanscheeuwijck et al., 2002). In this study, the testing approach was extended to include an evaluation of molecular endpoints to complement the classical methods of toxicological assessment, as well as provide insights into the mechanistic drivers for the changes observed (Kogel et al., 2014; Phillips et al., 2015b, 2016).

The overall study mean nicotine concentrations, along with reproducible PSD of the aerosols, indicate that the aerosol was generated and delivered in a consistent manner to the inhalation chambers with levels very close to the target concentrations. The measured PSD for the test atmospheres (mass median aerodynamic diameter (MMAD) ranging from 0.4 to 0.9 μm, see Table 1) was below the specification given in OECD TG 413 (MMAD ranging from 1 to 3 μm; geometric standard deviation (GSD) ranging from 1.5 to 3.0). The deposition fraction of the inhaled aerosol in the lung is shown to increase as the particle size decreases from 1–5 μm–0.5 μm MMAD (Kuehl et al., 2012). Hence, both aerosol from THS2.2 and MS from 3R4F have a similar PSD and should readily be deposited in the lungs and well taken up by the rats.

The maximum exposure concentrations selected for the 3R4F and THS2.2 groups were 23 μg/l and 50 μg/l nicotine, respectively. These concentrations were selected to detect the maximum possible toxicities induced by the test and reference items. Based on the formula described by Alexander et al. (Alexander et al., 2008), the test atmosphere concentration of nicotine (50 μg/l) at 0.187 l/min respiratory minute volume (value taken from current study) for a 250 g male rat generated a delivered dose (DD) of nicotine aerosol equivalent to (0.05 mg/l x 0.187 l/min x 360 min)/0.25 kg = 13.5 mg nicotine/kg body weight. An assumption based on 100% retention of nicotine in the respiratory tract was made, based on published data for humans (Baker and Dixon, 2006; Feng et al., 2007; Gowadia and Dunn-Rankin, 2010). According to this assumption and 1.39 mg nicotine per cigarette, and an average human adult body weight of 60 kg, the human equivalence daily dose is 13.5 mg/kg × 60 kg = 810 mg nicotine (or 583 cigarettes per day). Alternatively, the human equivalent daily dose based on body surface area (FDA, 2005) is 13.5 mg/kg/6.2 × 60 kg = 131 mg nicotine (or 94 cigarettes per day). Thus the applied exposure levels were high and suitable for a toxicity study.

Exposure was monitored by frequent measurements of nicotine concentrations at the breathing zone of the rats in the exposure chambers, as well as other smoke constituents. Biomonitoring of aerosol uptake was done by quantifying the metabolites of various aerosol components in the urine of exposed rats. The recovery of total nicotine metabolites was in direct correlation to the nicotine test atmosphere concentrations of the same inhaled aerosol. However, when compared with the 3R4F-exposed groups at the same target nicotine concentrations, the uptake of aerosol constituents was higher in the THS2.2-exposed rats, as evidenced in the higher levels of total nicotine metabolites excreted in 24-h urine. The lower degree of irritation to the respiratory tract organs and resultant higher respiratory minute volume in THS2.2-exposed animals relative to 3R4F-exposed rats likely explains the higher inhaled dose in the THS2.2-exposed groups. Measurement of representative urinary metabolites of other aerosol components indicated significantly lower levels of harmful constituents such as acrolein, NNK, benzene, and acrylonitrile in the aerosol from THS2.2 compared with cigarettes, consistent with the reduced HPHC present in the aerosol of THS2.2 (Schaller et al., submitted (this issue)-a).

Exposure-related reduction in body weight was significantly less pronounced in THS2.2- than in 3R4F-exposed rats; this was likely due to effects of harmful smoke constituents such as acrolein in the 3R4F aerosol, affecting body weight gain (Feron et al., 1978). Weight loss observed in the THS2.2 groups relative to sham may be attributed to the effects of nicotine. Reduced body weights were also observed in a nicotine-only inhalation study (Phillips et al., 2015a), as well as in other studies where nicotine was administered (Chowdhury, 1990; Ijomone et al., 2014; Seoane-Collazo et al., 2014). The higher mean body weight and food consumption indicated better general well-being and lower systemic toxicity in the THS2.2-exposed animals, compared with the 3R4F-exposed animals. However, when compared with the sham group animals, the aerosol-exposed males showed a reduction in body weight, while aerosol-exposed females showed higher body weights compared with their sham counterparts. The higher body weights in the THS2.2-exposed female animals (relative to sham) were also observed in a THS2.2 menthol study (Oviedo et al., submitted (this issue)). While higher food consumption correlated with higher body weights in the female THS2.2 groups, as also observed in the THS2.2 menthol study (Oviedo et al., submitted (this issue)), an increase in food consumption was not observed in a recent inhalation study involving nicotine pyruvate (Phillips et al., 2015a). Furthermore, there have been a number of conflicting published results pointing to the role of nicotine in appetite suppression (Chen et al., 2007; Grunberg et al., 1984; Mineur et al., 2011; Seoane-Collazo et al., 2014). Therefore more studies are needed to identify whether these results are due to nicotine only or to other constituents of the aerosol.

In comparison with MS from 3R4F, THS2.2 aerosol showed a significantly lower irritant effect on the respiratory tract. This was evident from the relatively unaffected respiratory frequencies in the THS2.2-exposed rats relative to sham. The histopathological assessment of the respiratory tract organs, as well as lung inflammation parameters (inflammatory cells and analytes in BALF), also indicated a much lower biological activity of the THS2.2 MA than the MS from 3R4F at equivalent nicotine concentrations. Aerosol-related histopathological findings in the respiratory tract included hyperplasia and squamous metaplasia in the epithelium of the nasal cavity and larynx, accumulation of neutrophilic granulocytes in the nasal cavity, and reserve cell and goblet cell hyperplasia at the tracheal epithelium. At equivalent nicotine concentrations in the test atmosphere, the incidence and severity of these lesions were significantly lower in the THS2.2-exposed rats. Lung inflammation, as reflected by the accumulation of pigmented alveolar macrophages and neutrophilic granulocytes, as well as the presence of pro-inflammatory and chemotactic cytokines in the bronchoalveolar lavage fluid, was significantly lower in THS2.2- than in 3R4F-exposed groups.

The toxicity due to sub-chronic inhalation of the test atmospheres was evaluated according to the recommendations stated in the OECD Test Guideline 413 (OECD, 2009). Exposure-related changes were not observed in the evaluated RBC parameters and most of the non-respiratory tract organs and clinical chemistry parameters. Inhalation exposure-induced responses, such as

Table 13
Statistical significance difference in histopathological findings in the respiratory tract organs between animals exposed to aerosol from THS2.2 and cigarette smoke from 3R4F.

Localization	Tissue type	Observation	Sex	90d			90 + 42d
				THS2.2_15 vs. 3R4F_15	THS2.2_23 vs. 3R4F_23	THS2.2_50 vs. 3R4F_23	THS2.2_50 vs. 3R4F_23
Nose level 1	Respiratory epithelium	Reserve cell hyperplasia	M	↓**	↓***	↓**	↓*
			F	↓***	↓***	↓***	↓**
		Squamous epithelial metaplasia	M	↓***	↓***	↓***	↓**
			F	↓***	↓***	↓**	↓***
		Amount of cornification	M	=	↓***	↓***	↓***
			F	↓**	↓***	↓***	↓***
		Loss of goblet cells (septum)	M	↓***	↓***	↓***	=
			F	↓***	↓***	↓**	↓**
		Neutrophilic granulocytes	M	↓*	↓*	↓*	=
			F	↓*	↓***	↓*	↓**
Nose level 2	Respiratory epithelium	Reserve cell hyperplasia	M	↓***	↓***	↓***	↓*
			F	↓***	↓***	↓***	↓**
		Squamous epithelial metaplasia	M	↓**	↓***	↓***	=
			F	↓**	↓***	↓***	=
	Olfactory epithelium	Atrophy	M	↓**	↓***	↓***	↓*
			F	↓***	↓***	↓***	↓***
		Squamous epithelial metaplasia	M	↓*	↓***	↓***	↓*
			F	↓***	↓***	↓***	↓*
	Lamina propria	Loss of nerve bundles	M	↓**	↓***	↓***	↓*
			F	↓***	↓***	↓***	↓***
		Mixed inflammatory cell infiltrates	M	=	↓***	↓***	↓*
			F	=	↓***	↓***	↓***
Nose level 3	Olfactory epithelium	Atrophy	M	=	↓***	↓***	↓**
			F	↓***	↓***	↓***	↓***
		Squamous epithelial metaplasia	M	=	↓***	↓***	↓**
			F	↓***	↓***	↓***	↓***
	Lamina propria	Loss of nerve bundles	M	=	↓***	↓***	↓**
			F	↓***	↓***	↓***	↓***
Nose level 4	Olfactory epithelium	Atrophy	M	=	↓***	↓***	=
			F	↓***	↓***	↓***	↓**
		Squamous epithelial metaplasia	M	=	↓***	↓***	=
			F	↓***	↓***	↓***	=
	Lamina propria	Loss of nerve bundles	M	=	↓***	↓***	=
			F	↓**	↓***	↓***	=
Larynx	Ventral depression	Squamous epithelial metaplasia	M	↓***	↓***	↓***	↓*
			F	↓***	↓***	↓**	=
		Amount of cornification	M	↓**	↓**	↓**	=
			F	↓**	↓**	↓**	=
	Lower medial region	Hyperplasia	M	↓***	↓***	↓***	↓**
			F	↓***	↓***	↓**	↓**
		Amount of cornification	M	↓***	↓**	↓***	=
			F	↓***	↓***	↓***	↓**
	Upper medial region	Squamous epithelial metaplasia	M	↓***	↓***	↓**	=
			F	↓***	↓***	↓***	=
		Amount of cornification	M	=	=	=	=
			F	=	↓***	↓**	=
	Vocal folds, pseudostratified epithelium	Squamous epithelial metaplasia	M	=	=	=	=
			F	=	=	=	=
	Vocal folds, squamous epithelium	Hyperplasia	M	↓***	↓***	↓***	=
			F	↓**	↓*	↓*	↓*
		Amount of cornification	M	↓***	↓***	↓***	=
			F	↓**	↓***	↓**	↓**
	Bifurcation	Squamous epithelial metaplasia	M	=	↓*	=	=
			F	=	↓*	=	=
		Goblet cell hyperplasia	M	↓*	↓**	↓***	=
			F	=	↓*	↓*	=
Left lung	Alveolar lumen	Macrophages without pigmentation	M	↓***	↓***	↓***	=
			F	↓***	↓***	↓***	↓*
		Macrophages with pigmentation (yellow)	M	↓***	↓***	↓***	↓**
			F	↓***	↓***	↓***	↓***
		Neutrophilic granulocytes	M	↓**	↓*	↓*	=
			F	↓**	↓**	↓***	=
	Main bronchus	Goblet cell hyperplasia	M	↓**	↓***	↓***	=
			F	↓**	↓***	↓***	↓**

Difference between groups: Significance: $^{*}p < 0.05$; $^{**}p < 0.01$; $^{***}p < 0.001$. Symbols, ↓ indicates response lower in THS2.2 relative to 3R4F; =indicates no difference. Abbreviations: M, male; F, female.

changes in differential leukocyte counts in blood, lower serum cholesterol, and glucose levels, higher activities of liver-related enzymes in serum, higher organ weights for liver and adrenal glands, cytoplasmic vacuolization in the liver (female), and reduced thymus (male), spleen (female) and uterus weights were observed in both 3R4F- and THS2.2-exposed rats. The extent of change for

Table 14
Histopathological findings in non-respiratory organs of male and female rats after 90-day inhalation period or 42-day recovery period following 90-day exposure to test atmosphere of the reference cigarette 3R4F, THS2.2, or air (sham).

Localization	Observation	Sex	90d						90 + 42d		
			Sham	3R4F_8	3R4F_15	3R4F_23	THS2.2_15	THS2.2_23	THS2.2_50	Sham	3R4F_23	THS2.2_50
Liver	Cytoplasmic vacuolization	M	1.4 ± 0.34 (7/10)	0.8 ± 0.33 (4/10)	0.6 ± 0.22 (5/10)	1.8 ± 0.32 (8/9)	0.9 ± 0.31 (6/10)	1.0 ± 0.33 (6/10)	0.8 ± 0.36 (4/10)	0.2 ± 0.17 (1/6)	0.4 ± 0.40 (1/5)	0.8 ± 0.29 (5/10)
		F	0.7 ± 0.40 (3/10)	0.4 ± 0.22 (3/10)	0.4 ± 0.22 (3/10)	1.2 ± 0.32 (7/9)	1.3 ± 0.33 (7/10)	1.8 ± 0.39 (9/10)*	1.5 ± 0.17 (10/10)*	0.2 ± 0.17 (1/6)	0.5 ± 0.34 (2/6)	0.1 ± 0.10 (1/10)
Spleen, red pulp	Yellow pigmentation	M	2.4 ± 0.22 (10/10)	2.2 ± 0.25 (10/10)	2.5 ± 0.17 (10/10)	2.7 ± 0.15 (10/10)	2.6 ± 0.16 (10/10)	2.6 ± 0.16 (10/10)	2.6 ± 0.31 (9/10)	2.2 ± 0.17 (6/6)	2.8 ± 0.20 (5/5)#	2.4 ± 0.22 (10/10)
	Yellow pigmentation	F	3.2 ± 0.20 (10/10)	2.2 ± 0.25 (10/10)**	2.2 ± 0.20 (10/10)**	2.8 ± 0.15 (9/9)	2.6 ± 0.22 (10/10)	2.4 ± 0.16 (10/10)*	2.6 ± 0.16 (10/10)*	3.3 ± 0.21 (6/6)	3.0 ± 0.26 (6/6)	2.8 ± 0.20 (10/10)
Thymus	Atrophy	M	0.1 ± 0.10 (1/10)	0.3 ± 0.21 (2/10)	0.9 ± 0.28 (6/10)*	1.1 ± 0.39 (5/9)*	0.4 ± 0.22 (3/10)	0.7 ± 0.26 (5/10)*	1.8 ± 0.40 (7/9)**	1.2 ± 0.54 (3/6)	1.2 ± 0.58 (3/5)	0.8 ± 0.25 (6/10)
	Atrophy	F	0.2 ± 0.20 (1/10)	0.1 ± 0.10 (1/10)	0.3 ± 0.21 (2/10)	0.6 ± 0.24 (4/9)	0.5 ± 0.27 (3/10)	0.5 ± 0.31 (3/10)	1.2 ± 0.29 (8/10)**	0.2 ± 0.17 (1/6)	0.0 ± 0.00 (0/6)	0.6 ± 0.16 (6/10)
Uterus, stroma	Eosinophilic granulocytes	F	1.2 ± 0.36 (6/10)	0.4 ± 0.22 (3/10)	0.1 ± 0.10 (1/10)*	0.1 ± 0.11 (1/9)*	0.7 ± 0.30 (4/10)	0.2 ± 0.20 (1/10)*	0.0 ± 0.00 (0/10)**	0.3 ± 0.33 (1/6)	0.3 ± 0.33 (1/6)	0.4 ± 0.27 (2/10)

Histopathological evaluation was performed after 90-day exposure (90d) and 42-day recovery following a 90-day exposure period (90 + 42d). Results represent mean score ±standard error; incidence and sample size are in parentheses. Difference from sham group at 90d: Significance: $^{*}p < 0.05$; $^{**}p < 0.01$; $^{***}p < 0.001$. Difference from sham group at 90 + 42d: Significance: #$p < 0.05$; ##$p < 0.01$; ###, $p < 0.001$. Abbreviations: M, male; F, female.

most of these mentioned responses did not differ between the 3R4F- and THS2.2-exposed groups at the same nicotine concentration. Similar effects were observed in published data involving nicotine-containing aerosols (Moennikes et al., 2008; Oviedo et al., submitted (this issue); Piade et al., 2014; Terpstra et al., 2003; Vanscheeuwijck et al., 2002; Werley et al., 2008), and in a nicotine-only exposure study (Phillips et al., 2015a). Higher blood neutrophil counts and lower blood lymphocyte counts, in combination with the increase in the weights of adrenal glands and decreased weights for thymus and spleen, and are likely due to stress (Everds et al., 2013) and/or the effects of nicotine (Phillips et al., 2015a). The fold change in lymphocyte counts, as well as adrenal, thymus and spleen weights in the 3R4F- and THS2.2-exposed groups are very similar to those seen with nicotine-only or nicotine pyruvate exposures at matched nicotine concentrations, as reported in a 28-day inhalation study by Phillips et al. (Phillips et al., 2015a), suggesting a dominant effect of nicotine on these parameters. The fold change in neutrophil counts is approximately 2–3 times higher in this study than in the 28-day nicotine-only inhalation study (Phillips et al., 2015a), suggesting that additional factors, such as the length of the study, the age of the animals, or residual HPHCs, can influence neutrophil counts. The decrease in serum cholesterol and glucose levels was also observed in our nicotine pyruvate 28-day inhalation study (Phillips et al., 2015a) and in other inhalation and nicotine administration studies (Latha et al., 1988; Seoane-Collazo et al., 2014; Vu et al., 2014), thereby supporting the hypothesis that chronic nicotine administration affects glucose and lipid metabolism. The increased levels of activity of alkaline phosphatase and alanine aminotransferase in serum and liver weights seen in this study were very similarly observed in the 28-day inhalation study involving nicotine pyruvate (Phillips et al., 2015a), suggesting a dominant role for nicotine amongst the many components of cigarette MS and THS2.2 aerosol in regulating these processes. The underlying changes in lipid peroxidation in the liver, as observed in response to cigarette MS exposure (Watanabe et al., 1995) and nicotine administration (Kalpana and Menon, 2004a, 2004b), may contribute to changes in enzymatic activities in the liver. An increase in glycogen content in the liver, as reflected by periodic acid-Schiff (PAS)-positive granules (with and without diastase treatment) in the livers of nicotine-exposed rats is also in alignment with proposed metabolic activity changes in the livers of nicotine-exposed rats (Phillips et al., 2015a). A higher incidence of cytoplasmic vacuolization in the livers of female THS2.2-exposed rats is possibly related to glycogen content in the liver, and points to a role for nicotine in its regulation. Lastly, lowered uterus weights (measured in the 3R4F MS- and THS2.2 aerosol-exposed rats) have also been reported in nicotine-only administration studies (Iranloye and Bolarinwa, 2009; Patil et al., 1999). The published literature indicates that nicotine may exert an effect on rodent ovarian function (Blackburn et al., 1994), which may explain the influence of exposure on uterus weights.

Of the 3R4F- and THS2.2-induced changes observed in this study, the lower levels of serum albumin, total protein, and triglycerides were not observed in the nicotine-only 28-day inhalation study (Phillips et al., 2015a). Reduced protein synthesis by the liver in response to cigarette MS is a possible mechanism to reduce serum albumin and total protein concentrations (Sershen et al., 1981). To address whether chronic exposure to nicotine or other aerosol components may be the cause for lower levels of serum albumin would require further testing of total protein and triglycerides. The influence of aerosol from cigarettes or nicotine on decreasing serum triglyceride levels is likely multi-factorial, possibly due to a reduction in nutritional status (food consumption) and/or changes in lipid metabolism in response to cigarette

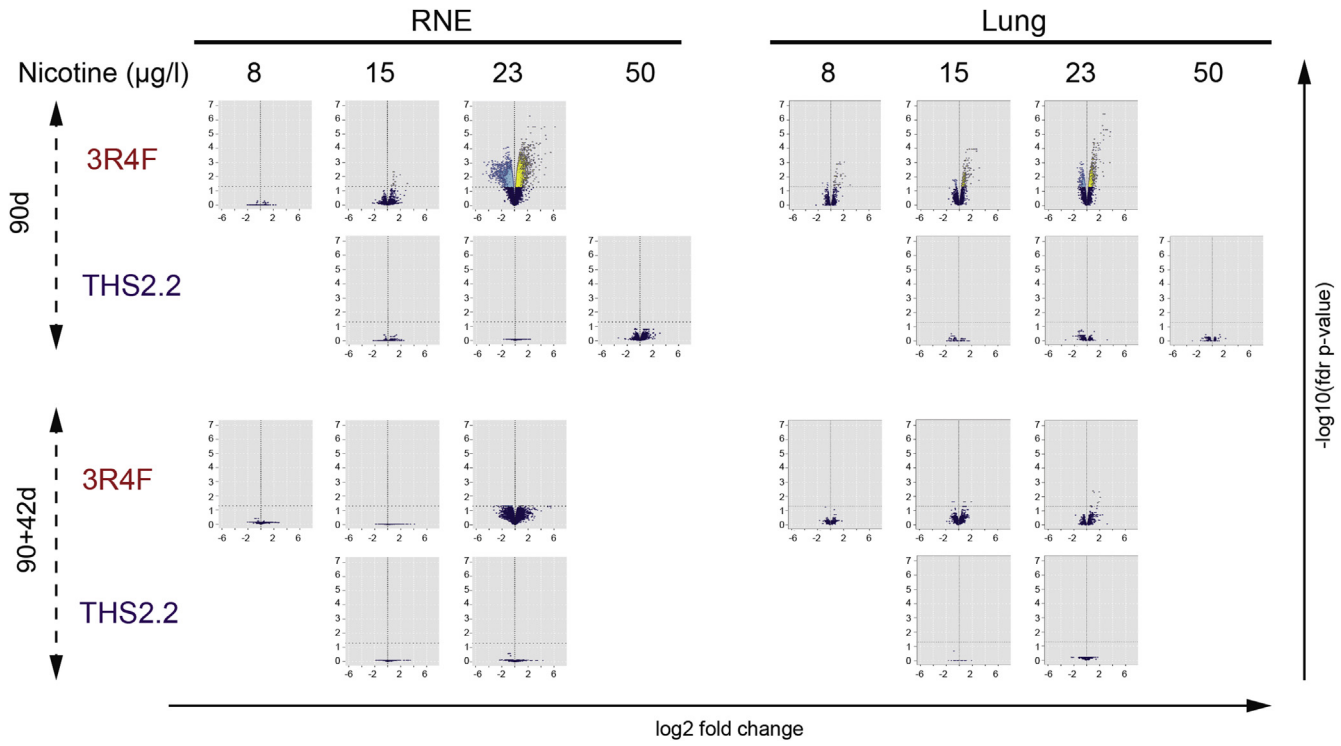

Fig. 3. Effects of 3R4F and THS2.2 exposure on the respiratory nasal epithelium (RNE) and lung transcriptome in male rats. For each gene, the gene expression change, calculated as [log2(fold change)], is plotted on the x-axis and the statistical significance, proportional to the [−log10(adjusted p-value FDR)], was plotted on the y-axis. Yellow and light blue dots indicate genes that were statistically significantly up- or down-regulated, respectively, compared with sham exposed groups. The horizontal line represents statistical significance [$-\log_{10}(0.05)$].The left side RNE and right lung lobes were analyzed following a 90-day exposure and 42-day post-exposure period. FDR, false discovery rate.

MS exposure (Maida and Howlett, 1990; Seoane-Collazo et al., 2014; Winders and Grunberg, 1990). The effect of the reduction in serum albumin and total protein concentrations measured is likely to be minimal, as these changes fall within the normal physiological

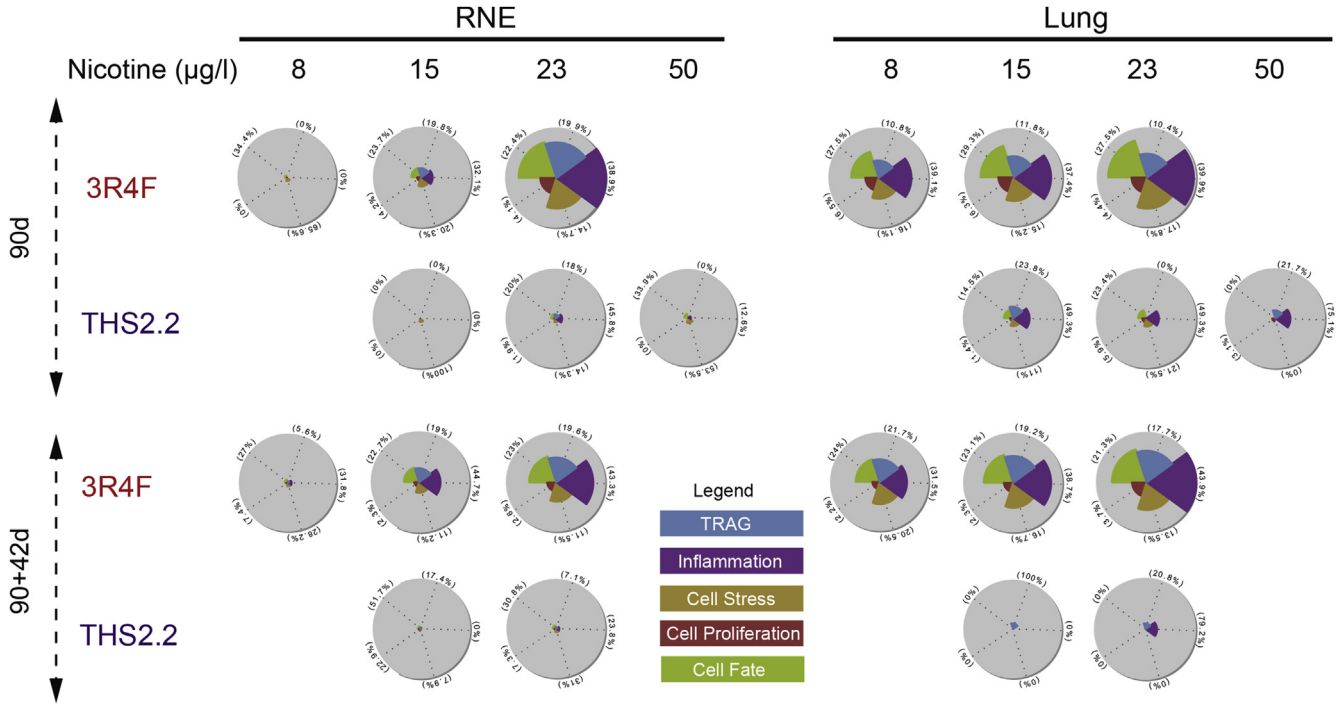

Fig. 4. Star plots showing relative network-level biological impact in the respiratory nasal epithelium (RNE) and lung tissues for all exposure groups. The relative network-level biological impact for each exposure group was compared with the sham groups after a 90-day exposure and following a 42-day recovery period in RNE and lungs of male animals. The surface area of each segment is proportional to the contribution of each network perturbation (shown as percentage in the labels) within each exposure group. The sum of surface area for each exposure group is shown relative to the perturbation in the sham group.

ranges in rats (Seibel et al., 2010). The interpretation of changes in concentrations of triglycerides and the comparison with the normal physiological ranges in rats (Seibel et al., 2010) are complicated by the fact that the animals were not diet-restricted prior to blood collection and analysis. In summary, the toxicological changes observed in the respiratory tract organs of the THS2.2 MA-exposed rats were much less pronounced than in 3R4F MS-exposed rats. No additional changes was trigged by THS2.2 compared with cigarettes and most observed changes are likely a reflection of the response to nicotine exposure.

The systems toxicology-based assessment using transcriptomics analysis further supports an overall reduced biological impact of THS2.2 exposure on the RNE and the lung tissue when compared with 3R4F exposure. The number of differentially expressed genes was markedly lower in THS2.2-exposed animals, compared with 3R4F-exposed animals. The overall lower biological effect is consistent with the histopathological evaluation and BALF analysis of the THS2.2-exposed animals. Additionally, the use of gene expression analysis in sub-acute toxicity testing can potentially provide information on the toxicity mechanisms. The network-based approach that was performed relies on the fold change of the differentially expressed genes, and is a threshold-free method. As a network-based approach integrates many genes in a single network, it has higher statistical power than a gene-level analysis. Consistent with published data, the network model-based analysis used in this study suggested that inflammatory processes were the major affected biological processes in the RNE and lungs of the 3R4F-exposed groups (Boue et al., 2013; Kogel et al., 2014; Phillips et al., 2015b). Histologically, the presence of increased neutrophilic granulocytes on the respiratory epithelium of nose level 1, the findings of increased macrophages and neutrophilic granulocytes in the alveolar lumen of the lungs, and increased levels of neutrophils, eosinophils, and inflammatory mediators in BALF, all correlated well with the increased perturbation of the inflammatory processes network in 3R4F-exposed animals. In contrast, the inflammatory processes were much less affected in THS2.2-exposed groups relative to the 3R4F-exposed groups; this finding is consistent with the low level of accumulation of immune cells in the respiratory tissues (nose and lungs) and inflammatory cytokines in the BALF. Additionally, other molecular networks were minimally affected in the RNE and lung tissues of THS2.2-exposed animals, compared with 3R4F-exposed animals. After a 42-day recovery, the inflammatory processes network was still detectable in the lungs of 3R4F-exposed animals, correlating with the persistence of immune cells and inflammatory cytokines in the BALF. Similarly, other molecular networks remained perturbed in the 3R4F recovery groups, suggesting repair and long lasting post-inhalation effect of MS on critical biological processes. In contrast, amplitudes of minimally affected molecular networks in the THS2.2- exposed animals were negligible in RNE and lungs of recovery animals.

In conclusion, the data indicated that the MA from THS2.2 did not cause additional toxicity compared with MS from the 3R4F cigarette, while the toxicity to respiratory tract organs in THS2.2-exposed animals was much lower than in rats exposed to 3R4F. Following exposure to THS2.2, most of the responses were considerably reduced in comparison to 3R4F. Where findings were similar between the 2 products, the responses were similar to effects caused by nicotine-alone exposure at comparable test atmosphere concentrations.

Conflict of interest

The work reported in this publication involved a candidate Modified Risk Tobacco Product developed by Philip Morris International (PMI) and was solely funded by PMI. All authors are (or were) employees of PMI R&D or worked for PMI R&D under contractual agreements.

Acknowledgements

The work was solely funded by PMI. The authors would like to thank the study team. We acknowledge the technical assistance and support of the bioresearch and aerosol team at PMIRL Singapore. We are also grateful for the technical assistance in lung slicing, RNA isolation, and gene chip preparation provided by Abdelkader Benyagoub, Karin Baumer, and Remi Dulize, respectively. The authors want further to than Jan Verbeeck for the optimization and technical support on the smoking machines and test atmosphere generation.

Appendix A. Supplementary data

Supplementary data related to this article can be found at http://dx.doi.org/10.1016/j.yrtph.2016.10.015.

Transparency document

Transparency document related to this article can be found online at http://dx.doi.org/10.1016/j.yrtph.2016.10.015.

References

Abobo, C.V., et al., 2012. Effect of menthol on nicotine pharmacokinetics in rats after cigarette smoke inhalation. Nicotine Tob. Res. 14, 801–808.
Alarie, Y., 1981. Bioassay for evaluating the potency of airborne sensory irritants and predicting acceptable levels of exposure in man. Food Cosmet. Toxicol. 19, 623–626.
Alexander, D.J., et al., 2008. Association of Inhalation Toxicologists (AIT) working party recommendation for standard delivered dose calculation and expression in non-clinical aerosol inhalation toxicology studies with pharmaceuticals. Inhal. Toxicol. 20, 1179–1189.
Baker, R.R., Dixon, M., 2006. The retention of tobacco smoke constituents in the human respiratory tract. Inhal. Toxicol. 18, 255–294.
Blackburn, C.W., et al., 1994. Nicotine, but not cotinine, has a direct toxic effect on ovarian function in the immature gonadotropin-stimulated rat. Reprod. Toxicol. 8, 325–331.
Bolstad, B.M., et al., 2003. A comparison of normalization methods for high density oligonucleotide array data based on variance and bias. Bioinformatics 19, 185–193.
Boue, S., et al., 2013. Cigarette smoke induces molecular responses in respiratory tissues of ApoE(-/-) mice that are progressively deactivated upon cessation. Toxicology 314, 112–124.
Boue, S., et al., 2015. Causal Biological Network Database: a Comprehensive Platform of Causal Biological Network Models Focused on the Pulmonary and Vascular Systems. Database, Oxford, p. bav030.
Bouley, G., et al., 1975. Effects in the rat of a weak dose of acrolein inhaled continuously. Eur. J. Toxicol. Environ. Hyg. 8, 291–297.
Chen, H., et al., 2007. Regulation of hypothalamic NPY by diet and smoking. Peptides 28, 384–389.
Chowdhury, P., 1990. Endocrine and metabolic regulation of body mass by nicotine: role of growth hormone. Ann. Clin. Lab. Sci. 20, 415–419.
Chowdhury, P., et al., 1989. Weight loss and altered circulating GI peptide levels of rats exposed chronically to nicotine. Pharmacol. Biochem. Behav. 33, 591–594.
Coggins, C.R., et al., 1989. Ninety-day inhalation study in rats, comparing smoke from cigarettes that heat tobacco with those that burn tobacco. Fundam. Appl. Toxicol. 13, 460–483.
Coggins, C.R., et al., 1980. Cigarette smoke induced pathology of the rat respiratory tract: a comparison of the effects of the particulate and vapour phases. Toxicology 16, 83–101.
Dai, M., et al., 2005. Evolving gene/transcript definitions significantly alter the interpretation of GeneChip data. Nucleic Acids Res. 33, e175.
Dalbey, W.E., et al., 1980. Chronic inhalation of cigarette smoke by F344 rats. J. Natl. Cancer Inst. 64, 383–390.
Everds, N.E., et al., 2013. Interpreting stress responses during routine toxicity studies: a review of the biology, impact, and assessment. Toxicol. Pathol. 41, 560–614.
Family Smoking Prevention and Tobacco Control Act, Public Law No. 111–131, 22 June 2009.
FDA, 2005. Guidance for Industry: Estimating the Maximum Safe Starting Dose in Initial Clinical Trials for Theraperutics in Adult Healthy Volunteers.

Feng, S., et al., 2007. Respiratory retention of nicotine and urinary excretion of nicotine and its five major metabolites in adult male smokers. Toxicol. Lett. 173, 101–106.
Feron, V.J., et al., 1978. Repeated exposure to acrolein vapour: subacute studies in hamsters, rats and rabbits. Toxicology 9, 47–57.
Friedrichs, B., et al., 2006. Lung inflammation in rats following subchronic exposure to cigarette mainstream smoke. Exp. Lung Res. 32, 151–179.
Fujimoto, H., et al., 2015. Biological responses in rats exposed to mainstream smoke from a heated cigarette compared to a conventional reference cigarette. Inhal. Toxicol. 27, 224–236.
Gaworski, C.L., et al., 1997. 13-week inhalation toxicity study of menthol cigarette smoke. Food Chem. Toxicol. 35, 683–692.
Gaworski, C.L., et al., 1999. Toxicologic evaluation of flavor ingredients added to cigarette tobacco: skin painting bioassay of cigarette smoke condensate in SENCAR mice. Toxicology 139, 1–17.
Gaworski, C.L., et al., 2009. Effect of filtration by activated charcoal on the toxicological activity of cigarette mainstream smoke from experimental cigarettes. Inhal. Toxicol. 21, 688–704.
Gebel, S., et al., 2013. Construction of a computable network model for DNA damage, autophagy, cell death, and senescence. Bioinform Biol. Insights 7, 97–117.
Gowadia, N., Dunn-Rankin, D., 2010. A transport model for nicotine in the tracheobronchial and pulmonary region of the lung. Inhal. Toxicol. 22, 42–48.
Gentleman, R.C., et al., 2004. Bioconductor: open software development for computational biology and bioinformatics. Genome Bio. 10, R80.
Grunberg, N.E., et al., 1984. Effects of nicotine on body weight and food consumption in rats. Psychopharmacol. Berl. 83, 93–98.
Haussmann, H.J., et al., 1998. Comparison of fresh and room-aged cigarette sidestream smoke in a subchronic inhalation study on rats. Toxicol. Sci. 41, 100–116.
Haziza, C., 2016. Evaluation of the Tobacco Heating System 2.2. Part 8: 5–Day randomized reduced exposure clinical trial in Poland. submitted (in this issue). Regul. Toxicol. Pharmacol.
Health Canada, 1999. Health Canada T-115: Determination of "Tar", Nicotine and Carbon Monoxide in Mainstream Tobacco Smoke.
Ijomone, O.M., et al., 2014. Effects of chronic nicotine administration on body weight, food intake and nitric oxide concentration in female and male rats. Pathophysiology 21, 185–190.
Iranloye, B.O., Bolarinwa, A.F., 2009. Effect of nicotine administration on weight and histology of some vital visceral organs in female albino rats. Niger. J. Physiol. Sci. 24, 7–12.
ISO3308, 2000. Cigarettes - Routine Analytical Cigarette-smoking Machine - Definitions and Standard Conditions. International Organization for Standardization.
ISO3402, 1999. Tobacco and Tobacco Products - Atmospheres for Conditioning and Testing. International Organization for Standardization.
Kalpana, C., Menon, V.P., 2004a. Modulatory effects of curcumin on lipid peroxidation and antioxidant status during nicotine-induced toxicity. Pol. J. Pharmacol. 56, 581–586.
Kalpana, C., Menon, V.P., 2004b. Protective effect of curcumin on circulatory lipid peroxidation and antioxidant status during nicotine-induced toxicity. Toxicol. Mech. Methods 14, 339–343.
Kogel, U., et al., 2014. A 28-day rat inhalation study with an integrated molecular toxicology endpoint demonstrates reduced exposure effects for a prototypic modified risk tobacco product compared with conventional cigarettes. Food Chem. Toxicol. 68, 204–217.
Kogel, U., et al., 2016. Evaluation of the Tobacco Heating System 2.2. Part 7: systems toxicological assessment of a mentholated version revealed reduced cellular and molecular exposure effects compared with mentholated and non-mentholated cigarette smoke. submitted (in this issue). Regul. Toxicol. Pharmacol.
Kuehl, P.J., et al., 2012. Regional particle size dependent deposition of inhaled aerosols in rats and mice. Inhal. Toxicol. 24, 27–35.
Latha, M.S., et al., 1988. Effect of exposure of rats to cigarette smoke on the metabolism of lipids. Atherosclerosis 70, 225–231.
Lee, J.M., et al., 2012. Historical control data from 13-week repeated toxicity studies in Crj:CD (SD) rats. Lab. Anim. Res. 28, 115–121.
Lewis, D.J., 1981. Factors affecting the distribution of tobacco smoke-induced lesions in the rodent larynx. Toxicol. Lett. 9, 189–194.
Maida, V., Howlett, G.J., 1990. Effects of cigarette smoking and dietary lipids on rat lipoprotein metabolism. Atherosclerosis 80, 209–216.
Martin, F., et al., 2014. Quantification of biological network perturbations for mechanistic insight and diagnostics using two-layer causal models. BMC Bioinforma. 15, 238.
Martin, F., et al., 2016. Evaluation of the Tobacco Heating System 2.2. Part 9: Application of systems pharmacology to identify exposure response markers in peripheral blood of smokers switching to THS2.2. submitted (in this issue). Regul. Toxicol. Pharmacol.
Martin, F., et al., 2012. Assessment of network perturbation amplitudes by applying high-throughput data to causal biological networks. BMC Syst. Biol. 6, 54.
Mascher, D.G., et al., 2001. High-performance liquid chromatographic-tandem mass spectrometric determination of 3-hydroxypropylmercapturic acid in human urine. J. Chromatogr. B Biomed. Sci. Appl. 750, 163–169.
McCall, M.N., et al., 2010. Frozen robust multiarray analysis (fRMA). Biostatistics 11, 242–253.
Meger, M., et al., 2000. Biomonitoring of environmental tobacco smoke (ETC)-related exposure to 4-(methylnitrosamino)-1-(3-pyridyl)-1-butanone (NNK). Biomarkers 5, 33–45.
Minet, E., et al., 2011. Urinary excretion of the acrylonitrile metabolite 2-cyanoethylmercapturic acid is correlated with a variety of biomarkers of tobacco smoke exposure and consumption. Biomarkers 16, 89–96.
Mineur, Y.S., et al., 2011. Nicotine decreases food intake through activation of POMC neurons. Science 332, 1330–1332.
Moennikes, O., et al., 2008. Reduced toxicological activity of cigarette smoke by the addition of ammonia magnesium phosphate to the paper of an electrically heated cigarette: subchronic inhalation toxicology. Inhal. Toxicol. 20, 647–663.
NACLAR, 2004. Guidelines on the Care and Use of Animals for Scientific Purposes. National Advisory Committee for Laboratory Animal Research.
OECD, 1997. OECD Test Guideline 1: OECD Series on Principles of Good Laboratory Practice and Compliance Monitoring.
OECD, 2009. OECD Test Guideline 413: Subchronic Inhalation Toxicity: 90-Day Study, Revised Toxicity Guideline.
Oviedo, A., et al., 2016. Evaluation of the Tobacco Heating System 2.2. Part 6: 90-day OECD 413 rat inhalation study with systems toxicology endpoints demonstrates reduced exposure effects of a mentholated version compared with mentholated and non-mentholated cigarette smoke. submitted (in this issue). Regul. Toxicol. Pharmacol.
Patil, S., et al., 1999. Effect of graded doses of nicotine on ovarian and uterine activities in albino rats. Indian J. Exp. Biol. 37, 184–186.
Phillips, B., et al., 2015a. Toxicity of aerosols of nicotine and pyruvic acid (separate and combined) in Sprague-Dawley rats in a 28-day OECD 412 inhalation study and assessment of systems toxicology. Inhal. Toxicol.
Phillips, B., et al., 2016. An 8-Month systems toxicology inhalation/cessation study in Apoe-/- mice to investigate cardiovascular and respiratory exposure effects of a candidate modified risk tobacco product, THS 2.2, compared with conventional cigarettes. Toxicol. Sci. 149, 411–432.
Phillips, B., et al., 2015b. A 7-month cigarette smoke inhalation study in C57BL/6 mice demonstrates reduced lung inflammation and emphysema following smoking cessation or aerosol exposure from a prototypic modified risk tobacco product. Food Chem. Toxicol. 80, 328–345.
Piade, J.J., et al., 2014. Toxicological assessment of kretek cigarettes Part 3: kretek and American-blended cigarettes, inhalation toxicity. Regul. Toxicol. Pharmacol. 70 (Suppl. 1), S26–S40.
Renne, R., et al., 2009. Proliferative and nonproliferative lesions of the rat and mouse respiratory tract. Toxicol. Pathol. 37, 5S–73S.
Roemer, E., et al., 2012. Mainstream smoke chemistry and in vitro and in vivo toxicity of the reference cigarettes 3R4F and 2R4F. Beiträge zur Tabakforschung/Contributions Tob. Res. 25, 316–335.
Rustemeier, K., et al., 1993. High-performance liquid chromatographic determination of nicotine and its urinary metabolites via their 1,3-diethyl-2-thiobarbituric acid derivatives. J. Chromatogr. 613, 95–103.
Schaller, J.-P., et al., 2016a. Evaluation of the Tobacco Heating System 2.2. Part 2: Chemical composition, genotoxicity, cytotoxicity, and physical properties of the aerosol. submitted (in this issue). Regul. Toxicol. Pharmacol.
Schaller, J.-P., et al., 2016b. Evaluation of the Tobacco Heating System 2.2. Part 3: influence of the tobacco blend on the formation of harmful and potentially harmful constituents in the aerosol. submitted (in this issue). Regul. Toxicol. Pharmacol.
Scherer, G., et al., 2007. Relationship between machine-derived smoke yields and biomarkers in cigarette smokers in Germany. Regul. Toxicol. Pharmacol. 47, 171–183.
Schlage, W.K., et al., 2011. A computable cellular stress network model for non-diseased pulmonary and cardiovascular tissue. BMC Syst. Biol. 5, 168.
Seibel, J., et al., 2010. Comparison of haematology, coagulation and clinical chemistry parameters in blood samples from the sublingual vein and vena cava in Sprague-Dawley rats. Lab. Anim. 44, 344–351.
Seoane-Collazo, P., et al., 2014. Nicotine improves obesity and hepatic steatosis and ER stress in diet-induced obese male rats. Endocrinology 155, 1679–1689.
Sershen, H., et al., 1981. Effect of cigarette smoke on protein synthesis in brain and liver. Neuropharmacology 20, 451–456.
Sewer, A., et al., 2016. Evaluation of the Tobacco Heating System 2.2. Part 5: MicroRNA expression from a 90-day rat inhalation study indicates reduced effects of the aerosol on lung tissue compared with cigarette smoke exposure. submitted (in this issue). Regul. Toxicol. Pharmacol.
Silvette, H., et al., 1962. The actions of nicotine on central nervous system functions. Pharmacol. Rev. 14, 137–173.
Smith, M., et al., 2016. Evaluation of the tobacco heating system 2.2. Part 1: description of the system and the scientific assessment program. submitted (in this issue). Regul. Toxicol. Pharmacol.
Smyth, G.K., 2004. Linear models and empirical bayes methods for assessing differential expression in microarray experiments. Stat. Appl. Genet. Mol. Biol. 3. Article3.
Stevens, J.M.C., 2008. Sources, metabolism, and biomolecular interactions relevant to human health and disease. Mol. Nutr. Food Res. 52, 7–25.
Terpstra, P.M., et al., 2003. Toxicological evaluation of an electrically heated cigarette. Part 4: subchronic inhalation toxicology. J. Appl. Toxicol. 23, 349–362.
Thrall, M.A., 2012. Veterinary Hematology and Clinical Chemistry. Wiley-Blackwell, Ames, Iowa.
Vanscheeuwijck, P.M., et al., 2002. Evaluation of the potential effects of ingredients added to cigarettes. Part 4: subchronic inhalation toxicity. Food Chem. Toxicol. 40, 113–131.
Vu, C.U., et al., 2014. Nicotinic acetylcholine receptors in glucose homeostasis: the

acute hyperglycemic and chronic insulin-sensitive effects of nicotine suggest dual opposing roles of the receptors in male mice. Endocrinology 155, 3793–3805.
Watanabe, K., et al., 1995. Effect of cigarette smoke on lipid peroxidation and liver function tests in rats. Acta Med. Okayama 49, 271–274.
Werley, M.S., et al., 2008. Smoke chemistry, in vitro and in vivo toxicology evaluations of the electrically heated cigarette smoking system series K. Regul. Toxicol. Pharmacol. 52, 122–139.
Westra, J.W., et al., 2011. Construction of a computable cell proliferation network focused on non-diseased lung cells. BMC Syst. Biol. 5, 105.
Westra, J.W., et al., 2013. A modular cell-type focused inflammatory process network model for non-diseased pulmonary tissue. Bioinform Biol. Insights 7, 167–192.
Winders, S.E., Grunberg, N.E., 1990. Effects of nicotine on body weight, food consumption and body composition in male rats. Life Sci. 46, 1523–1530.
Wong, E.T., et al., 2016. Evaluation of the Tobacco Heating System 2.2. Part 4: 90-day OECD 413 rat inhalation study with systems toxicology endpoints demonstrates reduced exposure effects compared with cigarette smoke. submitted (in this issue). Regul. Toxicol. Pharmacol.
Young, J.T., 1981. Histopathologic examination of the rat nasal cavity. Fundam. Appl. Toxicol. 1, 309–312.

Regulatory Toxicology and Pharmacology 81 (2016) S82–S92

Contents lists available at ScienceDirect

Regulatory Toxicology and Pharmacology

journal homepage: www.elsevier.com/locate/yrtph

Evaluation of the Tobacco Heating System 2.2 (THS2.2). Part 5: microRNA expression from a 90-day rat inhalation study indicates that exposure to THS2.2 aerosol causes reduced effects on lung tissue compared with cigarette smoke

Alain Sewer [a, *], Ulrike Kogel [a], Marja Talikka [a], Ee Tsin Wong [b], Florian Martin [a], Yang Xiang [a], Emmanuel Guedj [a], Nikolai V. Ivanov [a], Julia Hoeng [a], Manuel C. Peitsch [a]

[a] Philip Morris International R&D, Part of Philip Morris International Group of Companies, Philip Morris Products S.A., Quai Jeanrenaud 5, 2000, Neuchâtel, Switzerland

[b] Philip Morris International Research Laboratories Pte Ltd, Part of Philip Morris International Group of Companies, 50 Science Park Road, The Kendall #02-07, Science Park II, 117406, Singapore

ARTICLE INFO

Article history:
Received 4 July 2016
Received in revised form
7 November 2016
Accepted 16 November 2016
Available online 17 November 2016

Keywords:
Heat-not-burn
Modified risk tobacco product
Inhalation toxicology study
microRNA expression
Inflammation-related microRNAs

ABSTRACT

Modified-risk tobacco products (MRTP) are designed to reduce the individual risk of tobacco-related disease as well as population harm compared to smoking cigarettes. Experimental proof of their benefit needs to be provided at multiple levels in research fields. Here, we examined microRNA (miRNA) levels in the lungs of rats exposed to a candidate modified-risk tobacco product, the Tobacco Heating System 2.2 (THS2.2) in a 90-day OECD TG-413 inhalation study. Our aim was to assess the miRNA response to THS2.2 aerosol compared with the response to combustible cigarettes (CC) smoke from the reference cigarette 3R4F. CC smoke exposure, but not THS2.2 aerosol exposure, caused global miRNA downregulation, which may be explained by the interference of CC smoke constituents with the miRNA processing machinery. Upregulation of specific miRNA species, such as miR-146a/b and miR-182, indicated that they are causal elements in the inflammatory response in CC-exposed lungs, but they were reduced after THS2.2 aerosol exposure. Transforming transcriptomic data into protein activity based on corresponding downstream gene expression, we identified potential mechanisms for miR-146a/b and miR-182 that were activated by CC smoke but not by THS2.2 aerosol and possibly involved in the regulation of those miRNAs. The inclusion of miRNA profiling in systems toxicology approaches increases the mechanistic understanding of the complex exposure responses.

© 2016 The Authors. Published by Elsevier Inc. This is an open access article under the CC BY license (http://creativecommons.org/licenses/by/4.0/).

1. Introduction

The U.S. Family Smoking Prevention and Tobacco Control Act (FSPTCA) defines a MRTP as "any tobacco product that is sold or distributed for use to reduce harm or the risk of tobacco related disease associated with commercially marketed tobacco products" (Family Smoking Prevention and Tobacco Control Act). This publication is part of a series of nine publications describing the nonclinical and part of the clinical assessment of a candidate MRTP, THS2.2, and a mentholated version (THS2.2M). The series of publications provides part of the overall scientific program to assess the potential for THS2.2 to be a reduced-risk product. The first publication in this series describes THS2.2 and the assessment program for MRTPs (Smith et al., 2016). This is followed by six publications, including this one, that describe the nonclinical assessment of THS2.2 regular and THS2.2M (Kogel et al., 2016; Oviedo et al., 2016; Schaller et al., submitted (this issue)-a; Schaller et al., submitted (this issue)-b; Sewer et al., 2016; Wong et al., 2016). The eighth publication in the series describes a clinical study to assess whether the reduced formation of Harmful and Potentially Harmful Constituents (HPHC) for THS2.2 regular also leads to reduced-exposure to HPHCs when the product is used in a clinical setting (Haziza, 2016). A final publication utilizes data gathered from the reduced exposure clinical study on THS2.2 regular to determine if a systems pharmacology approach can identify exposure response markers in

* Corresponding author.
E-mail address: alain.sewer@pmi.com (A. Sewer).

http://dx.doi.org/10.1016/j.yrtph.2016.11.018
0273-2300/© 2016 The Authors. Published by Elsevier Inc. This is an open access article under the CC BY license (http://creativecommons.org/licenses/by/4.0/).

Abbreviations

CC	Combustible Cigarette
CS	Cigarette Smoke
FDR	False Discovery Rate
GC	Guanine-Cytosine
HPHC	Harmful and Potentially Harmful Constituents
IL-1	Interleukin 1
lncRNA	Long Non-Coding RNA
mRNA	Messenger RNA
miRNA	MicroRNA
MRTP	Modified Risk Tobacco Product
NPA	Network Perturbation Amplitude
NUSE	Normalized Unscaled Standard Error
OECD	Organisation for Economic Co-operation and Development
QC	Quality Control
Q-Q	Quantile-Quantile
RT-PCR	Reverse Transcription Polymerase Chain Reaction
TG	Test Guidelines
THS2.2	Tobacco Heating System 2.2
TNF	Tumor Necrosis Factor

peripheral blood of smokers switching to THS2.2 (Martin et al., 2016).

In this article, the expression of microRNA (miRNA) molecules in the lungs of rats exposed to the novel Tobacco Heating System (THS) 2.2 product in a 90-day OECD TG-413 inhalation study are investigated. One goal is to integrate the findings obtained from the analyses of miRNA exposure responses into the systems toxicology framework applied to the same study and reported earlier in this publication series (Wong et al., 2016).

miRNAs are noncoding regulatory RNA molecules that bind target messenger RNAs (mRNAs) and destabilize them or suppress their translation into proteins (Krol et al., 2010). There is increasing evidence that miRNA levels are affected by several known toxicants as well as oxidative and other forms of cellular stress. This suggests an important role for miRNAs in toxicology, which could provide a link between environmental influences and gene expression (Hong and Cho, 2015). Different types of cellular stress have been shown to affect genes encoding miRNAs as a mechanism of adaptation or tolerance to stress factors (Lema and Cunningham, 2010). In fact, multiple stressors including reactive oxygen species, phorbol esters, the RAS oncogene, double-stranded RNA, and interferons can affect the levels of the RNase III enzyme Dicer, which is critical for the generation of miRNAs (Wiesen and Tomasi, 2009).

miRNAs have also been linked to diseases etiologically related to smoking, such as lung cancer (Liu et al., 2009) and chronic obstructive pulmonary disease (De Smet et al., 2015). An alteration of the miRNA profile induced by CC smoke was found in target tissues even before disease manifestation, as recently reviewed (Vrijens et al., 2015). Izzotti et al. (2009a) showed that exposure to environmental CC smoke for 4 weeks resulted in downregulation of several miRNAs in rat lungs. Similar studies in mice showed that, in addition to sex and age, environmental CC smoke exposure for 5 weeks induced changes in the pulmonary miRNA profile. Mostly downregulated, the affected miRNAs were involved in adaptive mechanisms and the activation of pathways known to be associated with lung diseases (Izzotti et al., 2009b). Moreover, miRNA profiling of human bronchial brushings identified several miRNAs that were downregulated in smokers compared with those in nonsmokers and further *in vitro* tests showed that miR-218 in particular was suppressed by CC smoke condensate in cultured primary bronchial epithelial cells (Schembri et al., 2009). In organotypic bronchial epithelial cultures exposed to fresh cigarette smoke (CS) at the air–liquid interface, we previously observed reduced miR-146a/b levels related to inflammatory gene expression changes, and reduced levels of miR-449a/b/c and miR-107 related to changes in the expression of genes regulating the cell cycle (Mathis et al., 2013). In addition, different CC smoke-related miRNA response profiles were observed in lung tumors and tumor-free lung parenchyma samples from A/J mice exposed to CC smoke for 18 months when compared with spontaneous lung tumors and parenchyma from sham-exposed mice (Luettich et al., 2014).

The overall study was designed and conducted in accordance with the OECD TG-413 guidelines and the results are summarized in an accompanying manuscript (Wong et al., 2016). Briefly, rats exposed to mainstream CC smoke from 3R4F reference cigarettes for 90 days showed inflammation as indicated by the accumulation of immune cells in the lung tissue as well as proinflammatory and chemotactic cytokines in bronchoalveolar lavage fluid. Histopathological findings in the respiratory tract included epithelial cell hyperplasia, squamous metaplasia, atrophy in the airways, and the accumulation of pigmented alveolar macrophages in the lungs of 3R4F-exposed rats. All of these effects were markedly reduced in rats exposed to the aerosol from THS2.2. Here, we report on the pulmonary miRNA expression after 90-day inhalation of THS2.2 in comparison with 3R4F, as well as after a 42-day postexposure recovery period. The miRNA findings in the lung tissue of rats exposed to CC smoke or THS2.2 aerosol were complemented by transcriptomic profiling to obtain an insight into the mechanism behind the observed effects.

2. Materials and methods

2.1. Experimental design

Here, we report on the “OECD plus” part of a 90-day rat inhalation study in accordance with OECD test guidelines (TG) 413 (Wong et al., 2016). Experimental groups consisted of six male and six female rats. ‘Exposed’ experimental groups were scheduled for 13 weeks or 90 days (90d) of exposure for 5 days per week and 6 hours per day to *sham* (filtered air), *3R4F low* (8 μg/l nicotine), *3R4F medium* (15 μg/l nicotine), *3R4F high* (23 μg/l nicotine), *THS2.2 low* (15 μg/l nicotine), *THS2.2 medium* (23 μg/l nicotine), or *THS2.2 high* (50 μg/l nicotine) treatments, in accordance with OECD TG. ‘Recovery’ experimental groups consisted of rats concomitantly exposed with the 90-day animals, which were kept for additional 42 days of post-exposure recovery (90 + 42d). The *THS2.2 high* treatment was not included in the recovery groups because of the exposure chamber capacity. Here, we specifically report on the miRNA analysis of the lung after the inhalation and recovery period. After sample prioritization, all male rat exposed and recovery groups could be used for miRNA profiling, whereas the female rat *3R4F low* and *3R4F medium* groups (90d and 90 + 42d) were not available.

2.2. Animals

All procedures involving animals were performed in an American Association for the Accreditation of Laboratory Animal Care-accredited, Agri-Food & Veterinary Authority of Singapore-licensed facility with approval from an Institutional Animal Care and Use Committee, and performed in compliance with guidelines set by the National Advisory Committee for Laboratory Animal Research (NACLAR, 2004).

Outbred male and female Sprague–Dawley rats [Crl: CD (SD)], bred under specific pathogen-free conditions, were obtained from Charles River (Wilmington, MA, USA). The rats were approximately 8 weeks old at arrival and were acclimatized for at least 14 days prior to exposure.

2.3. Reference cigarettes and THS2.2 tobacco sticks

Reference 3R4F cigarettes were purchased from the University of Kentucky (Lexington, KY, USA; http://www.ca.uky.edu/refcig). THS2.2 *tobacco sticks* were provided by Philip Morris Products S.A. (Neuchâtel, Switzerland). THS2.2 sticks consist of a tobacco plug made of specially processed tobacco powder, a transfer section, and a mouthpiece, wrapped with cigarette paper. These sticks are designed to be inserted into a stick holder that includes a battery, electronics for controlling the temperature, a heating element (blade), and a cigarette extractor. The heating element heats the tobacco plug in a controlled manner to a maximum temperature of 350 °C. The comparative analytical specifications of the THS2.2 aerosol and 3R4F smoke are reported in part 2 of this series of publications (Schaller et al., 2016-a). The tobacco blend designated 'FR1' was used in the THS2.2 sticks in this study.

2.4. Smoke generation and animal exposure

Aerosol from 3R4F was generated on 30-port rotary smoking machines (Burghart Messtechnik, Wedel, Germany) (15 ports blocked) equipped with a Programmable Dual-port Syringe Pump (PDSP) with an active side stream exhaust (type PMRL-G, SM2000). Aerosol from THS2.2 was generated using 30-port carousel smoking machines (Burghart Messtechnik) equipped with stick holders and a PDSP. Animal exposure is described in detail in Part 4 of this series (Wong et al., 2016). Characterization of test atmospheres showed that target nicotine concentrations were met. Exposure intake was confirmed by quantification of total nicotine metabolites in 24-hour urine (Wong et al., 2016).

2.5. RNA isolation and miRNA profiling

Dissection took place 16 hours after the last exposure. Prior to organ removal, whole-body perfusion with cold saline was performed. The left lung lobe was cryosectioned into 40-μm slices, and the slices were collected alternately for transcriptomics and other analyses (not shown here). Lung samples were lysed in RLT buffer (Qiagen, Hilden, Germany) + β-mercaptoethanol using ceramic beads for homogenization. RNA including miRNA was isolated using the miRNeasy Mini Kit (Qiagen). miRNA was labeled with the FlashTag™ Biotin HSR Labeling Kit (Affymetrix, Santa Clara, CA, USA). miRNA analysis was performed on an Affymetrix GeneChip® miRNA 3.0 Array using 200 ng of RNA as a starting material.

2.6. miRNA data analysis

The raw data were preprocessed through a standard pipeline. Briefly, raw data CEL files were read using the *read.celfiles* function of the oligo packages in the Bioconductor suite of microarray analysis tools available in the R statistical software environment (Carvalho and Irizarry, 2010; Gentleman et al., 2004; R Core Team, 2014). The quality control (QC) was based on the *arrayQualityMetrics* package and examined four distinct metrics: Euclidean distances between arrays in raw and normalized data heat maps, normalized unscaled standard error (NUSE) plots, and intensity distribution box plots (Kauffmann et al., 2009). Arrays that were identified as outliers in at least two of the metrics were discarded, and the QC metrics were recalculated on the remaining arrays until all were accepted. This approach led to seven arrays being discarded in two iterations, so that the number of animal per experimental group decreased from 6 to an average of 5.25 ± 0.79. Normalized probe-level data were obtained by applying robust multiarray normalization and summarized at the probe set level using the median polish method (Irizarry et al., 2003). These miRNA expression data were submitted to ArrayExpress with the accession number E-MTAB-5296.

Only the miRNA probe sets that had significantly higher intensity values than their guanine-cytosine (GC) and sequence length-matched background probes (p-value cut-off = 0.01) were considered to be "present" or "detected," based on the manufacturer's instructions (see the Detection section in the Affymetrix® miRNA QCTool user guide; (Affymetrix, 2011). If a miRNA probe set was detected in more than half of the samples of at least one sample group, it was retained for the downstream analysis; if not, it was discarded together with all of the probe sets measured on the array that belonged to other species than rat. Overall, this preprocessing yielded 321 detected miRNA probe sets in the final expression miRNA matrix. When comparing experimental sample groups (Fig. 1B), the distributions of the numbers of detected miRNAs in individual samples can be used as an indicator of global downregulation. In doing so, we reasonably assume that the downregulation affecting the miRNA probe sets with intensities close to the detection threshold similarly affects all of the detected miRNA probe sets.

The design of our experiment entails 16 pairwise "treatment vs. control" comparisons so as to derive miRNA regulation upon exposure or recovery (e.g. low 3R4F male 90d vs. sham male 90d). For each comparison, a submatrix of the miRNA expression matrix was derived by keeping only the samples belonging to the treatment or control group, as well as the miRNA probe sets that were detected in more than 50% of the samples of at least one of two experimental groups. Linear models for differential expression were applied to the resulting submatrices using the moderated *t*-statistics implemented in the *limma* package (Ritchie et al., 2015). The obtained raw p-values were then adjusted for multiple testing by the Benjamini–Hochberg False Discovery Rate (FDR) method (Benjamini and Hochberg, 1995).

Besides the standard volcano plots (Allison et al., 2006), we used quantile-quantile (Q-Q) plots to represent the global significance of the differential miRNA expression. For each comparison, all of the detected miRNAs were ranked according to decreasing raw p-values. The −log10 values of the corresponding quantiles were plotted on the x-axis, while the y-axis contained the −log10 values of their raw p-values. Deviations of the resulting Q-Q curve above the diagonal line, which represents the random situation, indicate that a global signal was detected in the comparison. To assess the significance of these deviations, we estimated the 95% confidence intervals of each point of the diagonal by calculating the Q-Q curves of 1000 alternative expression matrices obtained by randomly permuting the columns of the original miRNA expression matrix. Merging these 95% confidence intervals yielded the gray surfaces drawn around the diagonal lines on the Q-Q plots. We also added three relevant boundary lines forming a "Z" shape: the lower one delimits the raw p-values smaller than 0.05, the upper one delimits the Bonferroni-corrected p-values smaller than 0.05 (Bonferroni, 1935), and the oblique one joining the other two delimits the Benjamini–Hochberg adjusted p-values (i.e. FDRs) smaller than 0.05 (Benjamini and Hochberg, 1995).

2.7. Quantitative RT-PCR

To confirm the findings from the miRNA experiment, real-time PCR profiling of miRNAs using the miScript PCR System (SYBR®

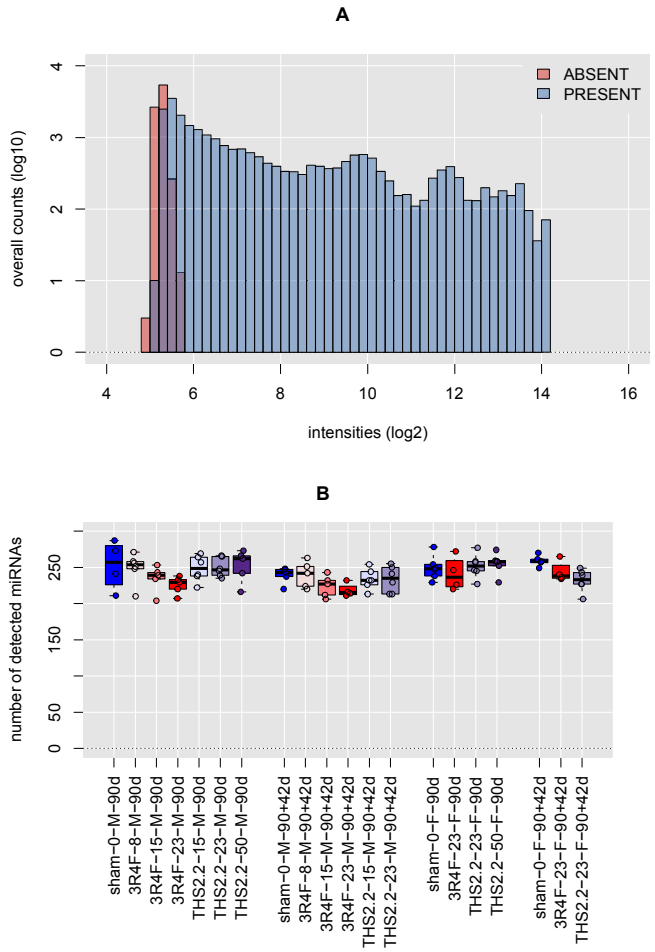

Fig. 1. miRNA detection statistics. A) Histogram displaying the distributions of the miRNA intensities according to their respective detection "present" or "absent" status. The 105 samples and the 321 "present" or "detected" miRNAs were used to generate the figure (see the Materials and Methods section on miRNA data analysis). B) Box plot of the number of "present" miRNAs detected in single samples grouped according to the 20 experimental sample groups included in the design of the study. The box plots follow the standard convention with the bold black horizontal bar representing the distribution median and the surrounding colored rectangle representing its inter-quartile range (i.e. the distance from the first quartile to the third one).

Green-based) was performed. miScript miRNA PCR Arrays are mature miRNA-specific forward primers spotted on a custom 384-well array including controls [SNORD61, SNORD95, positive PCR control (PPC), miRNA reverse transcription control (miRTC)]. The cDNA was prepared by following the manual of the miScript II RT Kit (Qiagen). The qPCR was run in a real-time PCR cycler (Viia7 384-well block). Cq values were then imported into the R environment and processed using the Bioconductor *ReadqPCR* and *NormqPCR* packages (Perkins et al., 2012). δCq values were obtained after subtraction of the mean of the Cq values of two housekeeping genes, SNORD61 and SNORD95. The differential expressions δδCq were calculated using the standard built-in *t*-test function.

Strictly speaking, the selection criterion for the quantitative RT-PCR measurements consisting of a statistically significant difference in expression in at least one of the 16 pairwise comparisons was not met for miR-134 and miR-494. They were nevertheless included in the quantitative RT-PCR measurements because they were very similar to miR-127, miR-379, and miR-541 (see the Results section on genomic clustering of regulated miRNA genes).

2.8. Inference of the changes in the activities of signaling molecules

As described in an accompanying manuscript (Wong et al., 2016), transcriptomic data were generated for the same lung samples as the miRNAs and the corresponding gene differential expression values were calculated using the same statistical models as for the miRNAs. A concise summary of the results obtained for the biological processes relevant for miR-146a/b and miR-182 is provided in Supplementary Fig. 1 in order to further support the conclusions based on these miRNAs. In the present study we used the systems biology approach called Network Perturbation Amplitude (NPA) and more specifically its *Strength* algorithm to infer the changes in the activities of several signaling molecules relevant to this context (Martin et al., 2012). This approach is based on backward causal reasoning, which consists of calculating the changes in the activity of upstream signaling molecules based on the differential expression of the downstream transcripts they causally regulate. For a given protein, the list of its causally regulated transcripts was extracted from Selventa Knowledgebase, which is a comprehensive repository of signed causal relationships between biological entities derived from peer-reviewed scientific literature as well as public and proprietary databases (Catlett et al., 2013). For the sake of clarity, we replaced the abstract openBEL syntax with the corresponding protein names and merged the entities related to the same protein, such as abundances and transcriptional activities. Given the set of signed relationships with downstream transcripts, the changes in the activity of a specific protein inferred by the NPA approach can be quantitatively contrasted across multiple pairwise comparisons, very much like transcript or miRNA differential expression. The obtained NPA values are also accompanied by two statistics that allow quantification of their uncertainty regarding biological variability and their specificity with respect to the choice of the downstream transcripts (Martin et al., 2012).

3. Results

3.1. miRNA detection statistics in lung tissue of rats exposed to CC smoke or THS2.2 aerosol

We first examined the miRNA detection statistics on the Affymetrix GeneChip miRNA-3.0 Microarray. Fig. 1A shows the overall distribution of the single miRNA intensities grouped according to their corresponding "present" or "absent" detection values. This figure confirms that the detection statistics correctly separated the low-intensity values, which cannot be distinguished from the background noise and are not informative, from the higher-intensity signals, for use in drawing conclusions in our study.

Fig. 1B displays the numbers of detected miRNAs across the experimental sample groups. First, CC smoke exposure induced a significant dose-dependent decrease in the number of miRNAs detected in lung tissue, as seen by the median values of 260, 255, 240, and 230 for the male rats exposed to *sham*, *low*, *medium*, and *high* doses of CC smoke, respectively. Second, these differences were still observed 42 days after the cessation of CC smoke exposure with approximately the same magnitude. Third, THS2.2 exposure did not lead to a decrease in the number of detected miRNAs. The distributions found for the lung tissue of the female rats displayed a tendency similar to that found in the male rats, although the fact that not all doses were available made it more difficult to draw firm conclusions (see the Materials and Methods section on experimental design).

3.2. miRNome-wide response in lung tissue of rats exposed to CC smoke or THS2.2 aerosol

We display the miRNome-wide response of the exposed lung tissues using volcano and Q-Q plots (see Fig. 2 for males and Supplementary Fig. 2 for females). They provide a useful overview of the magnitude and statistical significance of the responses that occurred in lung tissue. Volcano plots are standard representations of differential gene expression, while Q-Q plots are normally used in statistical genetics and essentially reveal how different the obtained results are from an undetectable signal. More details about the Q-Q plots are given in the Materials and Methods section on miRNA data analysis.

For the rats exposed to three doses of 3R4F, the volcano plots show that the magnitude of the effect (x-axis) increased with concentration together with the associated statistical significance (first row of the figure, left-hand side). We also observed that only a limited number of miRNAs reached the 0.05 false discovery rate (FDR) threshold for statistically significant regulation (miR-150, miR-146b, miR-182, miR-652). This rather weak signal was also visible in the Q-Q plots with the corresponding points situated above the Benjamini–Hochberg line (second row, left-hand side). However, the clear deviation of the curve of raw p-values from the diagonal toward the upper confidence interval boundary indicates that the measured responses were not random. The Q-Q plots of the comparisons of the 3R4F recovery samples presented similar results for the medium and high 3R4F concentrations, exemplified by a few miRNAs situated immediately below the FDR threshold (fourth row, left-hand side). On the other side, the effects on rats exposed to low 3R4F concentration had disappeared after 42 days of postexposure recovery, as indicated by the raw p-value curve closely following the diagonal, as well as a flat volcano plot. Regarding the global effects of the THS2.2 aerosol after 90 days of exposure, we found no statistically significant differences in miRNA

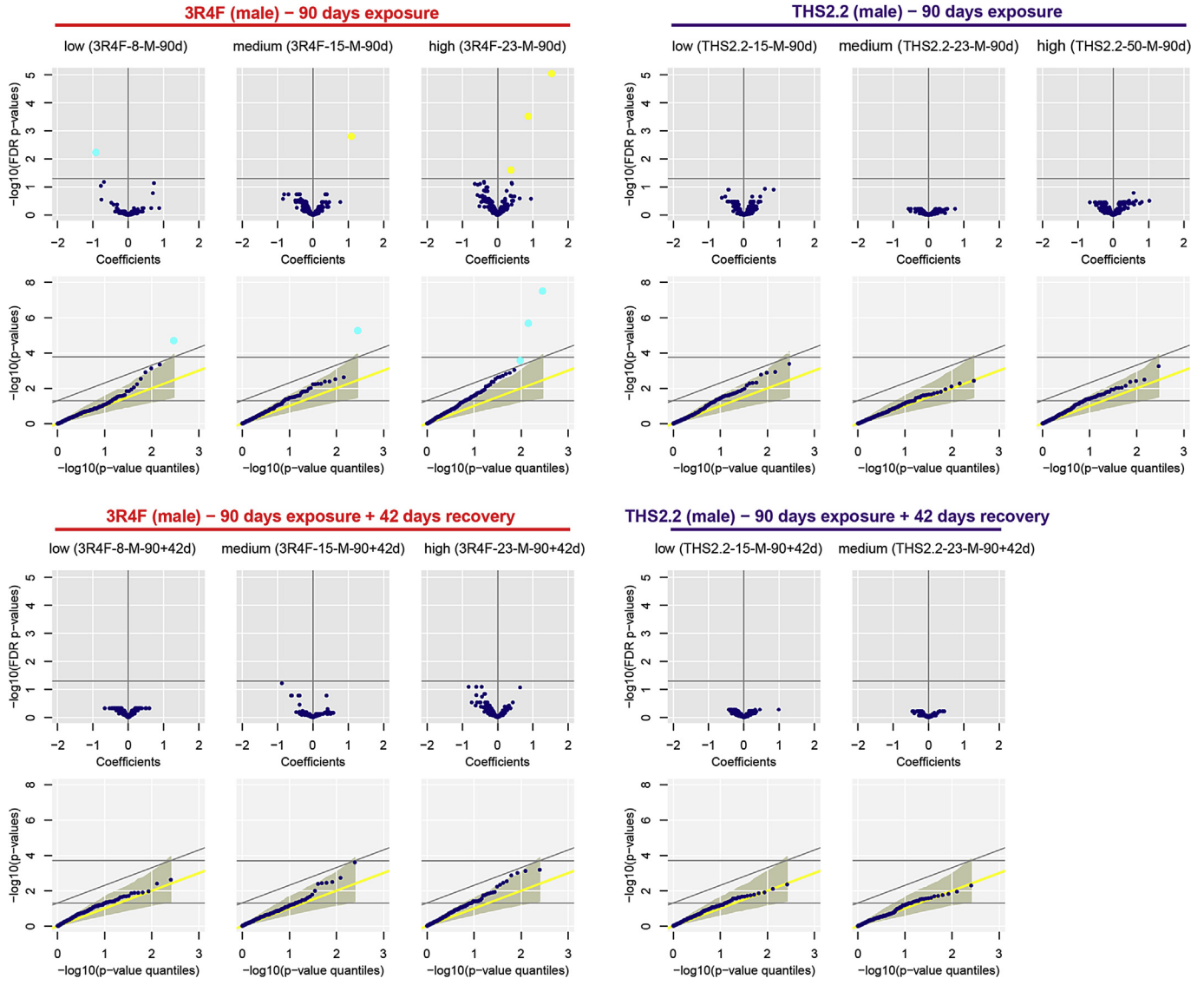

Fig. 2. Global miRNA regulation in male rats. Volcano and Q-Q plots are shown for the 11 pairwise comparisons between CS or THS2.2-exposed male rats and sham-exposed male rats. Volcano plots display the global relationships between the treatment-induced effects (differential miRNA expression, horizontal x-axis) and their statistical significance (log10 FDR, y-axis). Blue (yellow) dots indicate statistically significant negative (positive) regulation (FDR < 0.05). Q-Q plots indicate how distant the global statistical significance of differential miRNA expression (all of the bold-faced points) is from the random case containing no signal (diagonal line). The construction of a Q-Q plot is described in the Materials and Methods section on miRNA data analysis. Blue dots indicate statistically significant regulation of either sign (FDR < 0.05).

expression (first and second rows, right-hand side). Although the corresponding raw p-value curves did not strictly follow the diagonals of the Q-Q plots, the amplitudes of their deviations did not display monotonic dose dependence, which suggests that these effects were too noisy to be correctly interpreted. Finally, very similarly to the results seen after exposure to a low concentration of 3R4F, no effects of THS2.2 aerosol exposure were detected in the recovery group (90 + 42d) (third and fourth rows, right-hand side).

3.3. *miRNAs with a statistically significant difference in expression in lung tissue of rats exposed to CC smoke or THS2.2 aerosol*

All miRNAs that showed a statistically significant (i.e., FDR <0.05) difference in abundance in at least one exposure group compared with the sham group are shown in Fig. 3A (miR−150, miR−146a/b, miR−182, miR−652, miR−224, miR−181c, miR−127, miR−379, miR−541, miR−30b, miR−125a, miR−139). These data are from microarrays in an exploratory phase, which allowed identification of the key responders to the exposures. For confirmation, the levels of a subset of them were reexamined using quantitative RT-PCR (Pritchard et al., 2012). We selected 10 key miRNAs, the responses of which displayed appropriate dose dependences that were similar in male and female rats. We focused on miR-146a/b, miR-182, miR-127, miR-134, miR-379, miR-494, and miR-541 because they showed, to a certain degree, concentration-dependent regulation that was independent of sex. miR-139 was included as a potential recovery marker, while miR-150 seemed to capture low-dose effects. Supplementary Fig. 4 (intensity distributions) and 3B (differential expression) show the results of confirmatory phase by quantitative RT-PCR.

Quantitative RT-PCR results confirmed that the two paralogous miR-146a/b were upregulated both in response to 3R4F smoke exposure and after the recovery period, albeit at a lower intensity (Fig. 3B). In the lungs of female rats, miR-146b displayed a stronger response, which was also manifested by weak but statistically significant upregulation in female rat lungs upon THS2.2 exposure. miR-182 was upregulated in the lungs of both male and female rats exposed to 3R4F smoke, but not in the recovery groups. miR-127, miR-134, miR-379, miR-494, and miR-541 collectively displayed clear downregulation in both the 3R4F smoke exposure and recovery groups, as well as upregulation in the THS2.2 aerosol exposure groups. This upregulation was not observed in the recovery group of THS2.2-exposed rats. miR-139 and miR-150 displayed almost no signal in the quantitative RT-PCR results, so we considered them to be false positives in the microarray analysis. Except for these two miRNAs, the quantitative RT-PCR results accurately confirmed the microarray observations (Supplementary Fig. 5).

3.4. *Mechanistic insight into miRNA regulation using transcriptomic data*

We next aimed to obtain further insight into the mechanisms leading to regulation of the miRNAs in the exposed rat lung tissue. In the literature, it is indicated that miR-146a/b function as negative regulators involved in downregulation of Interleukin 1 (IL-1) receptor-associated kinase 1 (IRAK1) and tumor necrosis factor (TNF) receptor-associated factor 6 protein levels (TRAF6) and that miR-146a/b induction is NFkB-dependent (Taganov et al., 2006). As an alternative pathway, miRNA-146a was described to be induced by IL-1β in alveolar epithelial cells, where the upregulation of miR-146a/b resulted in the suppression of RANTES and IL-8 (Perry et al., 2008). It was further shown that miR-146a and miR-146b were regulated via divergent intracellular pathways. Upon stimulation with IL-1β, miR-146a induction was regulated via an NFkB- and JNK-1/2-dependent mechanism, and miR-146b was regulated via a JNK-1/2- and MEK-1/2-dependent mechanism (Perry et al., 2009).

In the absence of protein activity data, we used a previously reported approach to infer the activities of these signaling molecules based on the transcriptomic data (Fig. 4A and the section

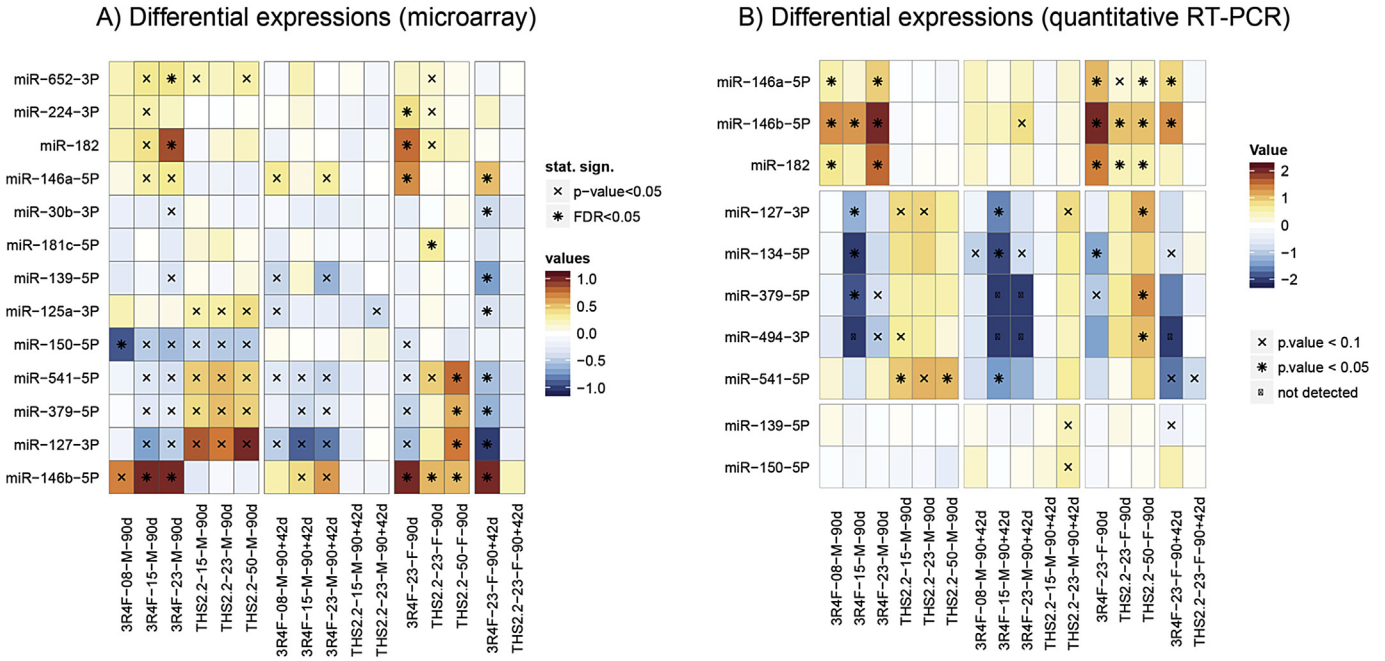

Fig. 3. Regulation of individual miRNAs (all pairwise comparisons). Heat maps display the regulation and the associated statistical significance for the relevant miRNAs. A) Results from the microarray exploratory measurements; only the miRNAs that have an FDR value below 0.05 in at least one of the 16 pairwise comparisons are shown. The miRNAs were ordered by standard clustering. B) Results from the confirmatory quantitative RT-PCR measurements for 10 selected miRNAs. The miRNAs have been grouped according to the considerations explained in the text.

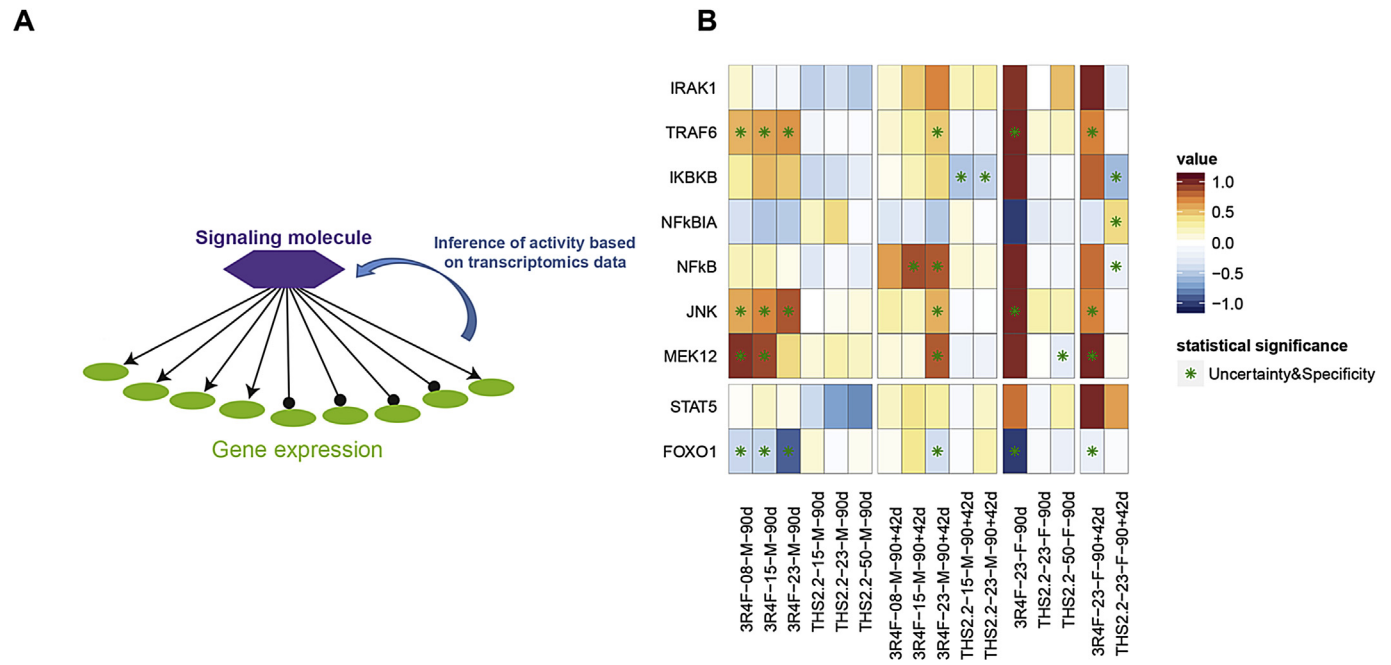

Fig. 4. Mechanistic insight into miRNA regulation using transcriptomic data. A) The principle of inference of the regulation of different signaling components based on transcriptomic data. The differential gene expression in the dataset was used for backward reasoning to infer the regulation of signaling molecules (purple polygon) known to regulate gene expression (green balls). The inference algorithm provides two statistics. Uncertainty measures the experimental variability and specificity requires that the correct genes are regulated in the dataset and that the downstream genes cannot be replaced with a random set of regulated genes. The method inferring the displayed values is described in Materials and Methods. B) The heat map shows the inferred regulation of signaling components known to be causally upstream or downstream of miR-146a/b and miR-182. The transcriptomic data from rat lung were used to infer the activity of the chosen molecules. The information on the gene regulation downstream of these signaling molecules is derived from experimental evidence stored in the Selventa knowledgebase.

about the inference of changes in the activities of signaling molecules in Materials and Methods). Fig. 4B shows the inferred activation or inhibition of the components involved in miR-146a/b signaling based on transcriptomic data. NFkB was inferred to be significantly upregulated only in the male recovery group, but the strong inferred upregulation of NFkB, observed in both exposure and recovery groups in females, did not reach statistical significance. By contrast, NFkB was significantly downregulated in the recovery group of females exposed to THS2.2. The kinase (IKBKB) that targets the inhibitor of NFkB (NFkBIA) to be degraded was predicted to be downregulated in the recovery groups of both sexes after exposure to THS2.2. Accordingly, NFkBIA was inferred to be upregulated in the recovery group of female rats exposed to THS2.2, consistent with the observation that the activity of NFkB was inferred to be downregulated in this group. The miR-146 target TRAF6 was inferred to be strongly upregulated and IRAK1 was only impacted in females with even stronger upregulation in the recovery groups for both sexes. The impact of THS2.2 exposure was significantly reduced compared with that of 3R4F exposure.

The inferred activation of JNK-1/2 was concentration-dependent, present in both sexes, and displayed a statistically significant effect at 90 days, with a smaller impact on the lungs of rats in the recovery group. The impact of THS2.2 exposure was significantly reduced compared with that of 3R4F exposure. MEK-1/2 was inferred to be less activated when the CC smoke concentration increased in the male rat lungs in response to 3R4F exposure at 90 days and in the recovery group exposed to the highest dose of 3R4F. In female rat lungs, it was inferred to be downregulated in the THS2.2-exposed group at 90 days and upregulated in the recovery group after 3R4F exposure (Fig. 4B).

miRNA-182 has been shown to be induced by STAT5, which is activated via the IL-2 pathway, in the context of the transition of naïve helper T cells to clonal expansion (O'Neill, 2010). To determine whether this could also be true in lung tissue, we inferred the activities of STAT5 and FOXO1 based on transcriptomic data. STAT5 was not inferred to be activated in CC smoke-exposed rat lungs, or even in the recovery groups. However, FOXO1 was predicted to be significantly downregulated in response to 3R4F exposure in both male and female rat lungs compared with that in the sham rats. This downregulation was also present, albeit at a lower level, in the recovery groups (Fig. 4B). In the lungs of rats exposed to THS2.2 aerosol, no consistent trends were observed for the inferred regulation of the signaling components.

3.5. Genomic clustering of regulated miRNA genes

When selecting miR-127, miR-134, miR-379, miR-494, and miR-541 for quantitative RT-PCR confirmation (Fig. 3B), we noticed that they are all located within 200 kilobases of each other on chromosome 6, in a region known as the DLK1-DIO3 imprinted domain situated in band 6q32 (da Rocha et al., 2008). Only the maternal copy of chromosome 6 expresses the miRNAs, which are organized into two large clusters regulated by an intergenic differentially methylated region located between Dlk1 and RGD1566401 (or MEG3/GTL2) (Fig. 5A). Since these features are also present in mouse and human on chromosomes 12 and 14, respectively, we decided to investigate in more detail the responses of the detected miRNAs located in this region as captured by the microarray. Fig. 5B shows that, besides the five above-mentioned ones, 19 other mature miRNAs were detected in at least one of the 16 pairwise comparisons in the study. Given that the total number of precursor miRNAs provided by RefSeq for this region is greater than 50 (Pruitt et al., 2014), our results indicate that the transcription of genomically clustered miRNAs was not necessarily as uniform as one might have expected (Baskerville and Bartel, 2005). More specifically, only a fraction of the detected miRNAs displayed a signal that was strong

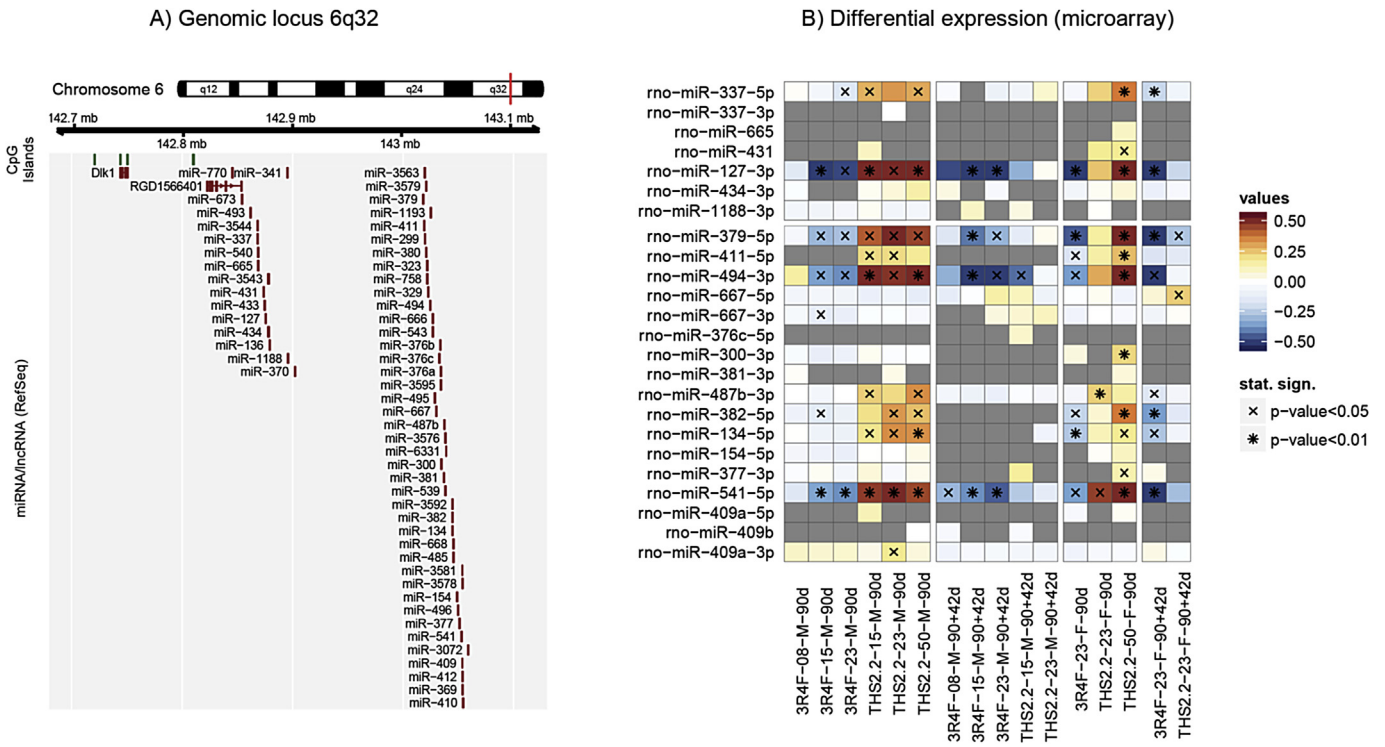

Fig. 5. miRNAs in the DLK1-DIO3 cluster. A) Genomic map of the imprinted DLK1-DIO3 cluster located on rat chromosome 6. CpG islands have been included beside the miRNAs and the long noncoding RNA genes (lncRNAs), as they play an important role in the imprinting mechanism. B) Regulation of all of the detected miRNAs in the DLK1-DIO3 cluster. Note that the criteria for indicating the "statistical significance" on the heat map are different from the ones used on Fig. 3A.

enough to deduce a response profile that could be compared with those of the five already-selected ones. miR-337 and miR-382 approximately displayed both the CC smoke-induced downregulation and the THS2.2-induced upregulation observed in Fig. 3, while miR-411 and miR-487b displayed only the THS2.2-induced upregulation. All of the others displayed a signal that was too weak to draw any definitive conclusions.

4. Discussion

4.1. miRNA detection: global downregulation upon CC smoke exposure

Our observation of a decreased number of detected miRNAs upon CC smoke exposure (Fig. 1B) can be viewed as an indicator of the global downregulation of miRNAs (see the Materials and Methods section on miRNA data analysis). The use of detection statistics has the advantage of being independent of the microarray raw data normalization method, which might reduce such global downregulation effects (Sewer et al., 2014). We also concede that our approach based on detection calls is useful only as long as the global effects between experimental sample groups are larger than the corresponding within-group variabilities. Fortunately, this is predominantly the case in the present study, as can be seen by comparing the within-group interquartile ranges and the between-group median differences in the boxplots of Fig. 1B.

The phenomenon of the global downregulation of miRNAs has already been reported in the literature, initially in disease (mostly cancer) contexts (Izzotti and Pulliero, 2014; Wu et al., 2013), but more recently also in the toxicological context of healthy organisms or systems, particularly after exposure to CC smoke (Graff et al., 2012; Izzotti et al., 2009b; Mathis et al., 2013; Schembri et al., 2009; Sewer et al., 2014). Several mechanisms have been proposed to explain this. Suzuki et al. showed that some toxicants can cause DNA damage and the activation of P53, which interacts with the DROSHA/DGCR8 processing complex and thus modulates the processing of pri-miRNAs to pre-miRNAs (Suzuki and Miyazono, 2010; Suzuki et al., 2009). Another possibility is that several toxicants can form miRNA adducts, which modify the structure of the miRNAs and prevent their access to the catalytic pockets of Dicer, thus arresting their maturation process (Izzotti and Pulliero, 2014). Alternatively, some toxicants can bind to Dicer in the proximity of miRNA catalytic sites and block the maturation of miRNA precursors (Ligorio et al., 2011). This scenario was investigated in detail in the case of alveolar macrophages obtained from healthy smokers and revealed the specific mechanism of Dicer SUMOylation (Gross et al., 2014).

Our observations of a dose-dependent decrease in the number of detected miRNAs upon CC smoke exposure are evidently compatible with all of these explanations. However, more interesting is the fact that (almost) no changes were detected in the recovery groups, which indicates that P53 and/or some CC smoke toxicants were persistently interfering with the miRNA processing machinery. On the other hand, regarding evaluation of the impact of the THS2.2 heat-not-burn product, the absence of any signs of global downregulation of miRNAs constitutes initial evidence of a lower impact of its aerosol in the lung and that the miRNA processing machinery was not affected by the various mechanisms that we described in the case of CC smoke exposure.

4.2. Overall miRNA regulation in response to CC smoke exposure

The global miRNA regulation results revealed several fundamental features of the miRNA response, such as the approximately monotonic dose dependence, the sustained 3R4F effects after exposure cessation, and no (males) or low (females) impact of

THS2.2 (Fig. 2). However, the number of miRNAs that showed a statistically significant difference in their expression level was rather low, even in response to 3R4F exposure. The first reason for this is our choice of separate comparisons for male and female rats. To verify the sensitivity of the study, we tested an alternative statistical model merging both sexes and encoding the animal sex into a discrete covariate. On average, the results contained three to four times more miRNAs that showed a statistically significant difference in their expression levels and confirmed the features enumerated above (Supplementary Fig. 3). In our data processing pipeline described in the Materials and Methods section on miRNA data analysis, we also minimized the effects of multiple testing corrections by restricting the statistical analysis of each comparison to the miRNAs that were detected in the majority of samples in at least one sample group.

To obtain a better understanding of the global miRNA regulation in response to CC smoke or THS2.2 aerosol exposure, we complemented the standard volcano plot of each pairwise comparison with the corresponding Q-Q plot. This has several advantages, the most important of which is the ability of this latter plot to explicitly display the case of a random dataset, which cannot be achieved with a volcano plot. Note that the diagonal corresponds to the random case under the assumption that all miRNAs are independent (uncorrelated), which might be invalid in the case of coexpressed miRNAs (clustered and/or polycistronic). Another advantage is the fact that a Q-Q plot focuses on the raw p-values rather than the FDRs. Raw p-values better reflect the key factors to reach statistical significance: the measured effect size and its variability, as well as the experimental sensitivity resulting from its design (number of replicates).

Regarding the assessment of THS2.2, a better understanding of its reduced impact in lung tissue compared with CC smoke can be obtained by examining the individual miRNAs below.

4.3. Mechanistic insights into miRNA regulation in exposed rat lung

Previous observations showed a relatively poor correlation of miRNA regulation between different studies (Vrijens et al., 2015). Pertinent to our study, miR-146a/b was previously reported to be downregulated in mouse lungs in response to short-term CC smoke exposure (Izzotti et al., 2010; Izzotti and Pulliero, 2014). However, other studies showed the upregulation of miRNA in inflammatory conditions, such as IL-1β-induced alveolar cells (Perry et al., 2008), in a mouse model of ventilator-induced lung injury (Vaporidi et al., 2012) and by proinflammatory cytokines in human airway smooth muscle (Comer et al., 2014). This suggests that, while toxicant exposure is generally thought to induce downregulation of miR-146a/b, the situation may change when tissue homeostasis is compromised. Based on the targets identified for miR-146a/b, they are thought to function as negative regulators of inflammatory responses (Saba et al., 2014). Since we could not infer downregulation of the miR-146a/b targets IRAK1 and TRAF6, one could hypothesize that the inflammatory status of the rat lung had already reached a high level that could not be inhibited by the negative regulation by miR-146a/b, even though it was induced in the lung tissue. The hypothesis on the involvement of the NFkB pathway in miR-146a/b regulation in CC smoke-exposed rat lungs could also not be confirmed. However, the strong inferred upregulation of NFkB in the male recovery group might indicate its involvement in the tissue healing process, independent of the miR-146 pathway. On the other hand, JNK-1/2 and MEK-1/2 upstream of miR-146a/b were inferred to be activated, based on transcriptomic data.

It has been reported that STAT5 is a direct activator of miR-182, which is in turn a robust inhibitor of FOXO1 (O'Neill, 2010), and that oxidative stress may inactivate STAT5 in a JAK2-independent manner (Saba et al., 2014). In CC smoke-exposed rat lungs, we observed that the upregulation of miR-182 was accompanied by strong downregulation of FOXO1. However, STAT5, which has been suggested to be involved upstream of the miR-182 FOXO1 pathway, was not impacted in response to CC smoke exposure in rat lung. This indicates that miR-182 could be regulated via other signaling pathways in the inflamed lung. A potential upstream candidate is STAT3 as a chromatine immunoprecipitation (ChIP) assay revealed that, upon autocrine HGH stimulation, STAT3 and STAT5 directly bind to the promoter region of the miR-96-182-183 cluster (Zhang et al., 2015), and indeed our data suggested that STAT3 was upregulated (data not shown). However, experimental results are needed to confirm this.

After 90 days of THS2.2 exposure, neither miR-146 nor miR-182 was impacted. In line with this, the gene expression-based inference did not predict any significant activations or inhibitions.

Regarding all of the negative findings concerning the hypotheses based on the literature about miR-146 and miR-182 regulatory pathways, it is also possible that, at present, we cannot capture the activation of all components in the signaling pathways. Thus, more controlled experiments are deemed necessary to fully elucidate the function of these miRNA species in the context of pulmonary inflammation.

4.4. miRNAs from the DLK1-DIO3 miRNA cluster

miRNA genes are often clustered in the genome and show similar spatiotemporal regulation, which results from coregulation and even cotranscription (Baskerville and Bartel, 2005). In this study, we saw that several miRNAs from the large DLK1-DIO3 miRNA cluster shared a noteworthy response pattern: they were downregulated upon CC smoke exposure and upregulated upon THS2.2 exposure. The fact that downregulation often corresponded to the absence of detection in both exploratory microarray and confirmatory quantitative RT-PCR measurements indicated that this signal was very weak and unlikely to be present in all of the cellular types constituting the “whole lung” samples. The cells that drive the observed signal might be macrophages. Indeed, it has been shown that CC smoke exposure induces inverse M1 and/or M2 polarization states (Shaykhiev et al., 2009; Titz et al., 2015), and that M2-polarized macrophages exhibit lower levels of miR-127 (Zhang et al., 2013). These two observations agree with the CC smoke part of our findings. Mechanistically, even a role for miR-127 in the context of macrophage polarization was identified (Ying et al., 2015). This suggests that lower miR-127 levels induce an M2-biased response, which fits well with our findings. We observed the clear upregulation of numerous miRNAs belonging to the DLK1-DIO3 miRNA cluster upon THS2.2 exposure. Such a collective effect has already been observed for the human homologous miRNAs and explained in that context by the hypomethylation of upstream CpG islands, which might match the ones shown in Fig. 5A (Aavik et al., 2015).

5. Conclusion

Investigations on the miRNA response to CC smoke exposure have drawn significant interest in recent years, so we wanted to cast our comparative THS2.2 assessment into this context. Systems toxicology tools offered the possibility of inferring upstream and downstream protein activities using our transcriptomic data obtained from the same samples, which provided an additional layer of understanding of the effects of CC smoke and THS2.2. In conclusion, the current study showed that subchronic CC smoke exposure induces global miRNA downregulation in rat lung, which

is probably linked to reactive CC smoke constituents interfering with the miRNA processing machinery. The upregulation of specific miRNA species, such as miR-146a/b and miR-182, indicates that they are causal elements in the inflammatory response in CS-exposed lung. This study also shows that exposure to THS2.2 did not result in effects similar to those observed upon exposure to the reference cigarette.

Conflict of interest statement

The work reported in this publication involved a candidate Modified-Risk Tobacco Product developed by Philip Morris International (PMI) and was solely funded by PMI. All authors are (or were) employees of PMI R&D or worked for PMI R&D under contractual agreements.

Acknowledgements

The authors would like to thank the study team, especially acknowledging the technical assistance and support of the bioresearch and aerosol team at PMI Research Laboratories Singapore particularly Wong Sin Kei, Nigel Tan, Aaron Ong, Woon Ching Qing, Clement Foong, Jenny Ho, Eleena Seow, Subash Krishnan and Shen Yi. We acknowledge the technical assistance for lung slicing, RNA isolation and gene chip preparation provided by Abdelkader Benyagoub, Karine Baumer, Dariusz Peric and Remi Dulize, respectively. We thank Dr. Walter Schlage for his scientific input and critical review of the manuscript.

Transparency document

Transparency document related to this article can be found online at http://dx.doi.org/10.1016/j.yrtph.2016.11.018.

Appendix A. Supplementary data

Supplementary data related to this article can be found at http://dx.doi.org/10.1016/j.yrtph.2016.11.018.

References

Aavik, E., et al., 21 April 2015. Global DNA methylation analysis of human atherosclerotic plaques reveals extensive genomic hypomethylation and reactivation at imprinted locus 14q32 involving induction of a miRNA cluster. Eur. heart J. 36 (16) ehu437.
Affymetrix, 2011. Affymetrix miRNA QCTool User's Guide.
Allison, D.B., et al., 2006. Microarray data analysis: from disarray to consolidation and consensus. Nat. Rev. Genet. 7, 55–65.
Baskerville, S., Bartel, D.P., 2005. Microarray profiling of microRNAs reveals frequent coexpression with neighboring miRNAs and host genes. Rna 11, 241–247.
Benjamini, Y., Hochberg, Y., 1995. Controlling the false discovery rate: a practical and powerful approach to multiple testing. J. R. Stat. Soc. Ser. B Methodol. 289–300.
Bonferroni, C.E., 1935. Il calcolo delle assicurazioni su gruppi di teste. Tipografia del Senato.
Carvalho, B.S., Irizarry, R.A., 2010. A framework for oligonucleotide microarray preprocessing. Bioinformatics 26, 2363–2367.
Catlett, N.L., et al., 2013. Reverse causal reasoning: applying qualitative causal knowledge to the interpretation of high-throughput data. BMC Bioinforma. 14, 1.
Comer, B.S., et al., 2014. MicroRNA-146a and microRNA-146b expression and anti-inflammatory function in human airway smooth muscle. Am. J. Physiol. Lung Cell. Mol. Physiol. 307, L727–L734.
da Rocha, S.T., et al., 2008. Genomic imprinting at the mammalian Dlk1-Dio3 domain. Trends Genet. 24, 306–316.
De Smet, E.G., et al., 2015. Non-coding RNAs in the pathogenesis of COPD. Thorax. thoraxjnl 70 (8), 782–791, 2014–206560.
Family Smoking Prevention and Tobacco Control Act. Public Law No. 111–131 (June 22, 2009).
Gentleman, R.C., et al., 2004. Bioconductor: open software development for computational biology and bioinformatics. Genome Biol. 5, R80.
Graff, J.W., et al., 2012. Cigarette Smoking Decreases Global MicroRNA Expression in Human Alveolar Macrophages.
Gross, T.J., et al., 2014. A microRNA processing defect in smokers' macrophages is linked to SUMOylation of the endonuclease DICER. J. Biol. Chem. 289, 12823–12834.
Haziza, C., 2016. Evaluation of the Tobacco Heating System 2.2. Part 8: 5–Day Randomized Reduced Exposure Clinical Trial in Poland. Regul. Toxicol. Pharmacol. 81 (S2), S139–S150.
Hong, W.Y., Cho, W.C., 2015. The role of microRNAs in toxicology. Arch. Toxicol. 89, 319–325.
Irizarry, R.A., et al., 2003. Summaries of Affymetrix GeneChip probe level data. Nucleic acids Res. 31 e15–e15.
Izzotti, A., et al., 2009a. Downregulation of microRNA expression in the lungs of rats exposed to cigarette smoke. FASEB J. 23 (3), 806–812.
Izzotti, A., et al., 2009b. Relationships of microRNA expression in mouse lung with age and exposure to cigarette smoke and light. FASEB J. 23, 3243–3250.
Izzotti, A., et al., 2010. Modulation of microRNA expression by budesonide, phenethyl isothiocyanate and cigarette smoke in mouse liver and lung. Carcinogenesis 31, 894–901.
Izzotti, A., Pulliero, A., 2014. The effects of environmental chemical carcinogens on the microRNA machinery. Int. J. Hyg. Environ. health 217, 601–627.
Kauffmann, A., et al., 2009. arrayQualityMetrics—a bioconductor package for quality assessment of microarray data. Bioinformatics 25, 415–416.
Kogel, U., et al., 2016. Evaluation of the Tobacco Heating System 2.2. Part 7: Systems Toxicological Assessment of a Mentholated Version Revealed Reduced Cellular and Molecular Exposure Effects Compared with Mentholated and Non-mentholated Cigarette Smoke. Regul. Toxicol. Pharmacol. 81 (S2), S123–S138.
Krol, J., et al., 2010. The widespread regulation of microRNA biogenesis, function and decay. Nat. Rev. Genet. 11, 597.
Lema, C., Cunningham, M.J., 2010. MicroRNAs and their implications in toxicological research. Toxicol. Lett. 198, 100–105.
Ligorio, M., et al., 2011. Mutagens interfere with microRNA maturation by inhibiting DICER. An in silico biology analysis. Mutat. Res. Fundam. Mol. Mech. Mutagen. 717, 116–128.
Liu, X., et al., 2009. Uncovering growth-suppressive MicroRNAs in lung cancer. Clin. Cancer Res. 15, 1177–1183.
Luettich, K., et al., 2014. Systems toxicology approaches enable mechanistic comparison of spontaneous and cigarette smoke-related lung tumor development in the A/J mouse model. Interdiscip. Toxicol. 7, 73–84.
Martin, F., et al., 2014. Quantification of biological network perturbations for mechanistic insight and diagnostics using two-layer causal models. BMC Bioinforma. 15, 1.
Martin, F., et al., 2016. Evaluation of the Tobacco Heating System 2.2. Part 9: Application of Systems Pharmacology to Identify Exposure Response Markers in Periferal Blood of Smokers Switching to THS2.2. Regul. Toxicol. Pharmacol. 81 (S2), S151–S157.
Martin, F., et al., 2012. Assessment of network perturbation amplitudes by applying high-throughput data to causal biological networks. BMC Syst. Biol. 6, 54.
Mathis, C., et al., 2013. Human bronchial epithelial cells exposed in vitro to cigarette smoke at the air-liquid interface resemble bronchial epithelium from human smokers. Am. J. Physiol. Lung Cell. Mol. Physiol. 304, L489–L503.
NACLAR, 2004. (National Advisory Committee for Laboratory Animal Research): guidelines on the Care and Use of Animals for Scientific Purposes.
O'Neill, L.A., 2010. Outfoxing Foxo1 with miR-182. Nat. Immunol. 11, 983–984.
Oviedo, A., et al., 2016. Evaluation of the Tobacco Heating System 2.2. Part 6: 90-day OECD 413 Rat Inhalation Study with Systems Toxicology Endpoints Demonstrates Reduced Exposure Effects of a Mentholated Version Compared with Mentholated and Non-mentholated Cigarette Smoke. Regul. Toxicol. Pharmacol. 81 (S2), S93–S122.
Perkins, J.R., et al., 2012. ReadqPCR and NormqPCR: R packages for the reading, quality checking and normalisation of RT-qPCR quantification cycle (Cq) data. BMC genomics 13, 296.
Perry, M.M., et al., 2008. Rapid changes in microRNA-146a expression negatively regulate the IL-1β-induced inflammatory response in human lung alveolar epithelial cells. J. Immunol. 180, 5689–5698.
Perry, M.M., et al., 2009. Divergent intracellular pathways regulate interleukin-1β-induced miR-146a and miR-146b expression and chemokine release in human alveolar epithelial cells. FEBS Lett. 583, 3349–3355.
Pritchard, C.C., et al., 2012. MicroRNA profiling: approaches and considerations. Nat. Rev. Genet. 13, 358–369.
Pruitt, K.D., et al., 2014. RefSeq: an update on mammalian reference sequences. Nucleic acids Res. 42, D756–D763.
R Core Team, 2012. R: a Language and Environment for Statistical Computing. R Foundation for Statistical Computing, Vienna, Austria. ISBN 3-900051-07-0, 2014.
Ritchie, M.E., et al., 20 April 2015. Limma powers differential expression analyses for RNA-sequencing and microarray studies. Nucleic Acids Res. 43 (7) gkv007.
Saba, R., et al., 2014. MicroRNA-146a: a dominant, negative regulator of the innate immune response. Front. Immunol. 5.
Schaller, J.-P., et al., 2016. Evaluation of the Tobacco Heating System 2.2. Part 2: Chemical Composition, Genotoxicity, Cytotoxicity, and Physical Properties of the Aerosol. Regul. Toxicol. Pharmacol. 81 (S2), S27–S47.
Schaller, J.-P., et al., 2016. Evaluation of the Tobacco Heating System 2.2. Part 3: Influence of the Tobacco Blend on the Formation of Harmful and Potentially Harmful Constituents in the Aerosol. Regul. Toxicol. Pharmacol. 81 (S2), S48–S58.

Schembri, F., et al., 2009. MicroRNAs as modulators of smoking-induced gene expression changes in human airway epithelium. Proc. Natl. Acad. Sci. 106, 2319–2324.
Sewer, A., et al., 2014. Assessment of a novel multi-array normalization method based on spike-in control probes suitable for microRNA datasets with global decreases in expression. BMC Res. notes 7, 302.
Sewer, A., et al., 2016. Evaluation of the Tobacco Heating System 2.2. Part 5: MicroRNA Expression from a 90-day Rat Inhalation Study Indicates Reduced Effects of the Aerosol on Lung Tissue Compared with Cigarette Smoke Exposure. Regul. Toxicol. Pharmacol. 81 (S2), S82–S92.
Shaykhiev, R., et al., 2009. Smoking-dependent reprogramming of alveolar macrophage polarization: implication for pathogenesis of chronic obstructive pulmonary disease. J. Immunol. 183, 2867–2883.
Smith, M., et al., 2016. Evaluation of the Tobacco Heating System 2.2. Part 1: Description of the System and the Scientific Assessment Program. Regul. Toxicol. Pharmacol. 81 (S2), S17–S26.
Suzuki, H.I., Miyazono, K., 2010. Dynamics of microRNA biogenesis: crosstalk between p53 network and microRNA processing pathway. J. Mol. Med. 88, 1085–1094.
Suzuki, H.I., et al., 2009. Modulation of microRNA processing by p53. Nature 460, 529–533.
Taganov, K.D., et al., 2006. NF-κB-dependent induction of microRNA miR-146, an inhibitor targeted to signaling proteins of innate immune responses. Proc. Natl. Acad. Sci. 103, 12481–12486.
Titz, B., et al., 2015. Alterations in the sputum proteome and transcriptome in smokers and early-stage COPD subjects. J. proteom. 128, 306–320.
Vaporidi, K., et al., 2012. Pulmonary microRNA profiling in a mouse model of ventilator-induced lung injury. Am. J. Physiol. Lung Cell. Mol. Physiol. 303, L199–L207.
Vrijens, K., et al., 2015. MicroRNAs as potential signatures of environmental exposure or effect: a systematic review. Environ. health Perspect. 123, 399.
Westra, J.W., et al., 2013. A modular cell-type focused inflammatory process network model for non-diseased pulmonary tissue. Bioinforma. Biol. Insights 7, 167.
Wiesen, J.L., Tomasi, T.B., 2009. Dicer is regulated by cellular stresses and interferons. Mol. Immunol. 46, 1222–1228.
Wong, E.T., et al., 2016. Evaluation of the Tobacco Heating System 2.2. Part 4: 90-day OECD 413 Rat Inhalation Study with Systems Toxicology Endpoints Demonstrates Reduced Exposure Effects Compared with Cigarette Smoke. Regul. Toxicol. Pharmacol. 81 (S2), S59–S81.
Wu, D., et al., 2013. The use of miRNA microarrays for the analysis of cancer samples with global miRNA decrease. RNA 19, 876–888.
Ying, H., et al., 2015. MiR-127 modulates macrophage polarization and promotes lung inflammation and injury by activating the JNK pathway. J. Immunol. 194, 1239–1251.
Zanetti, F., et al., 2016. Systems toxicology assessment of the biological impact of a candidate Modified Risk Tobacco Product on human organotypic oral epithelial cultures. Chem. Res. Toxicol. 29, 1252–1269.
Zhang, W., et al., 2015. Autocrine/Paracrine human growth hormone-stimulated MicroRNA 96-182-183 cluster promotes epithelial-mesenchymal transition and invasion in breast Cancer. J. Biol. Chem. 290, 13812–13829.
Zhang, Y., et al., 2013. Expression profiles of miRNAs in polarized macrophages. Int. J. Mol. Med. 31, 797–802.